JOURNAL OF APPLIED PHYSICS

JOURNAL OF APPLIED

PHYSICS

(Formerly PHYSICS)

OCTOBER, 1938 Vol. 9, No. 10

In This Issue

Page

Fundamental Research in Industry THE EDITOR 611

Filtration of Sound, I R. B. LINDSAY 612

Metallurgical Applications of Electron Diffraction H. R. NELSON 623

Contributed Original Research

Time Lag in Gas-Filled Photoelectric Cells A. M. SKELLETT 631

Currents to Conductors Induced by a Moving Point Charge W. SHOCKLEY 635

On the Electrographic Recording of Fast Electrical Phenomena P. SELÉNYI 637

Plastic Deformation of Lead, Copper and Aluminum Under Static Compression W. JAMES LYONS 641

Drift of Magnetic Permeability at Low Inductions after Demagnetization G. R. PATTERSON 646

Type of Electrical Resonator W. W. HANSEN 654

Electrical Conduction in Quartz, Periclase, and Corundum at Low Field Strength E. G. ROCHOW 664

Effect of Pressure on the Viscosity of Boric Anhydride Glass ERNEST B. DANE, JR. AND FRANCIS BIRCH 669

In Every Issue

Here and There 628

Contributors to This Issue 629

Innovations in Instruments ii

Current Literature of Physics viii

Advertising Index xvi

BOARD OF EDITORS

ELMER HUTCHISSON, *Editor*

Associate Editors

R. M. BOZORTH
D. W. BRONK
W. P. DAVEY
O. S. DUFFENDACK
SAUL DUSHMAN
A. STUART HUNTER
C. H. KUNSMAN
J. T. LITTLETON
L. L. NETTLETON
W. B. NOTTINGHAM
A. R. OLPIN
JOHN T. TATE

Publication of the American Institute of Physics

ADMINISTRATIVE STAFF

HENRY A. BARTON, *Director*

MADELINE M. MITCHELL, *Publications Manager*

WILLIAM C. COPP, *Advertising Manager*

GOVERNING BOARD

JOHN T. TATE, *Chairman*
KARL T. COMPTON
E. C. CRITTENDEN
WHEELER P. DAVEY
HOMER L. DODGE
HARVEY FLETCHER
ARTHUR C. HARDY
VERN O. KNUDSEN
MELVIN MOONEY
FREDERIC PALMER, JR.
R. L. PEEK, JR.
GEORGE B. PEGRAM
W. B. RAYTON
F. K. RICHTMYER
WALLACE WATERFALL

THE JOURNAL OF APPLIED PHYSICS, published monthly at Prince and Lemon Sts., Lancaster, Pa., is devoted to physics in its role as the science basic to other natural sciences and to the arts and industries. Previous to 1937 this publication was known as PHYSICS. It aims to be of service not only in physical laboratories, but also in the laboratories of industrial, chemical, geological, geophysical, meteorological, radio, and similar concerns. THE JOURNAL OF APPLIED PHYSICS publishes editorials, news of physicists and reviews, as well as technical papers of applied physics.

SUBSCRIPTION PRICE

	U. S., POSS. AND CANADA	FOREIGN
To members of scientific societies	$5.00	$5.70
To all others	7.00	7.70

Manuscripts should be submitted to Elmer Hutchisson, Editor, University of Pittsburgh, Pittsburgh, Pennsylvania.

Changes of address, proofs, and complaints of failure to receive the JOURNAL OF APPLIED PHYSICS should be addressed to the Publications Manager. New copies can be sent free only if notice of nondelivery is received within three months of date of issue.

Subscriptions and orders for back numbers should be addressed to Prince and Lemon Streets, Lancaster, Pa. or to the American Institute of Physics, 175 Fifth Avenue, New York, N. Y.

Advertising rates supplied on request. Orders, advertising copy and cuts should be sent to the American Institute of Physics.

Entered as second class matter at the Post Office at Lancaster, Pennsylvania, under the Act of March 3, 1897.
Accepted for mailing at the special rate of postage provided for in the Act of February 28, 1925, authorized May 2, 1932.

Copyright 1938, by the American Institute of Physics.

Journal of Applied Physics

Volume 9 October, 1938 Number 10

Fundamental Research in Industry

RESEARCH in many industrial laboratories is characterized by a great rush for immediate results. One sees carried on in these laboratories tests, tests and still more tests. A tremendous capital is invested in testing machines and a large force is required to operate them and collect data. Yet, if one inquires "What is the fundamental nature of the property being tested?" or "Why did one sample hold up while an apparently similar one failed?" he is told "This is a practical laboratory; we do not have time for such academic questions."

One wonders whether or not this frenzy for immediate results is as effective as many industrial executives appear to believe. It is, of course, self-evident that industrial research laboratories must pay dividends. Still, are there not many examples of industrial laboratories which prove that the largest dividends come from those laboratories which have theorists to help interpret and guide future research. In the laboratories of the aeronautics industry, for example, we find physicists well trained in higher mechanics who are revising age-old engineering formulas in an effort to increase strength and reduce weight of the structural parts. In the laboratories of the telephone industry, we find physicists searching into the nature of magnetism so that better magnets can be built and hence better telephone service can be given. In fact if one lists those industries or those companies whose record of progress during the past decade stands out in a striking manner he finds that he has a list of organizations with enlightened research programs. On the other hand a list of those industries or companies which have stagnated includes primarily those whose executives believe that fundamental research is impractical or that a mere one percent of the budget of a street railway company spent on research is an outrageous extravagance.

We believe sincerely that if a reasonable fraction of industrial budgets is allocated to employ some of those curious individuals who are always asking "Why?" and who can guide research along intelligent channels, then we will see in the industrial future a picture as bright as that painted in the past decade by the brilliant cooperation between theorists and experimentalists in the field of atomic and nuclear physics. Let us see more industrialists study such questions as "Why is a metal hard?" "What makes a liquid viscous?" or "What is the origin of the discharge in this gas?" Then, if ever, will we have real industrial progress.

—THE EDITOR.

For November

Production and Applications of High Energy Particles:

***(1) Electrostatic Generators, by* W. H. WELLS**

***(2) Cyclotrons, by* F. N. D. KURIE**

Original research papers on the Effect of Pressure on the Viscosity of Boric Anhydride Glass, On the Starting of Hg Vapor Discharge Tubes, On the Symmetry of the Benzene Ring, the Role of Solid Friction in Synthetic Dielectrics, Penetration of Oil Sprays and Vitrification and Crystallization of Organic Cells at Low Temperatures.

The Filtration of Sound, I

BY R. B. LINDSAY

Brown University, Providence, Rhode Island

1. Introduction

ACOUSTIC filtration is only one aspect of the general problem connected with the transmission of energy through a medium possessing periodic nonhomogeneity of structure. Many illustrations come to mind, of which we note only a few. Thus a perfectly flexible homogeneous stretched string when loaded with equally concentrated and equally spaced mass particles constitutes such a medium from the standpoint of the propagation of transverse elastic waves. Similarly an electric transmission line containing an iterated combination of inductances, resistances and capacitances is a periodic nonhomogeneous medium for the passage of long electromagnetic waves. Finally a crystal metal lattice is a medium of similar nature for the transmission of electrons.

The mathematical problem of determining the transmission through the various structures just mentioned is fundamentally the same, and it is found that in each case certain frequency ranges (or energy ranges in the case of the electrons) are transmitted while others do not pass. From the purely mathematical point of view there would be a decided gain in developing the subject of energy filtration from the most general standpoint. Here it becomes, however, simply a problem in mathematics, namely the solution of second order differential equations subject to iterated boundary conditions. In this article on the other hand we are primarily interested in the physical phenomena associated with transmission and filtration.

2. Compressional Waves in a Confined Fluid Medium

Let us first examine the propagation of compressional elastic waves in a fluid medium, e.g., a gas like air, confined in a tube. Such situations are still of more than academic interest, as witness the stethoscope, speaking tubes on shipboard, air-conditioning conduits, etc. A very interesting and significant feature of such transmission is its frequency selectivity with respect to alterations in the mode of confinement of the medium and with respect to side attachments.

As an initial illustration consider sound passing through a tube with a constriction or an expansion. (See Fig. 1 (a), (b).) In each case it is assumed that the sound wave comes in from the left and goes off to the right with no reflection from a terminus at the right (i.e., ideally speaking the tube extends to ∞ on the right). The ratio of the transmitted energy flow (e.g. joules per second or watts) at the right of the constriction or expansion to the incident energy flow at the left of the constriction or expansion is called the *power transmission ratio* and is denoted by P_r. The mathematical treatment of the problem shows that P_r is a function of S_2/S_1, i.e., the ratio of the areas of the main line and constriction or expansion respectively, and $\sin^2 kl$, where l is the length of the constriction or expansion and $k=2\pi\nu/c$, where ν is the frequency and c the velocity of the sound. This means that for a given mode of confinement, P_r is periodic

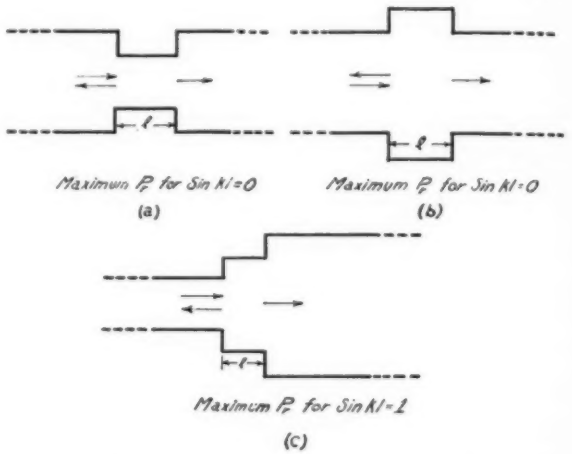

FIG. 1. Constrictions in tubes in which the sound enters from the left and travels to the right.

in frequency with a period equal to $c/2l$. In particular it turns out that when $\sin kl = 0$, P_r is a maximum, falling to a minimum (not zero, of course) for $\sin kl = 1$. This is interesting since $\sin kl = 0$, or $kl = n\pi$ (n integral) is the condition for resonance of a single tube of length l, either open at both ends or closed at both ends. We may look upon the former situation as corresponding to Fig. 1(a), while the latter corresponds to Fig. 1(b). Interestingly enough, Fig. 1(c), where the area of cross section does not revert to its original value, corresponds, as seems quite reasonable, to the case of a tube closed at one end and open at the other, so the condition for maximum P_r is $\sin kl = 1$. Some actual transmission curves for cases (a) and (b) are indicated in Fig. 2.

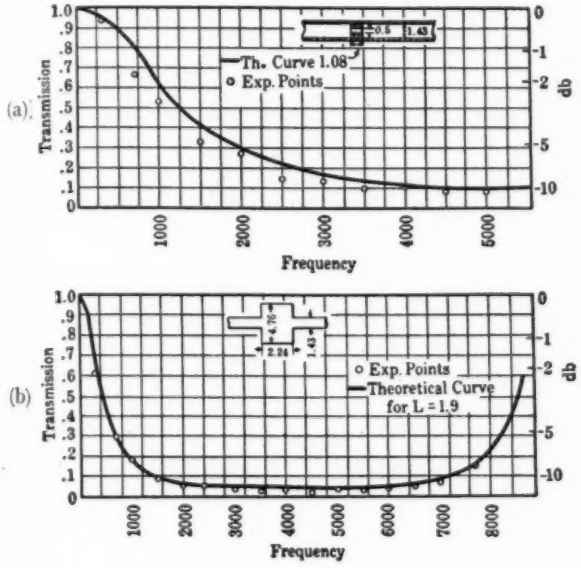

FIG. 2. Transmission curves for two types of tubes.*

A second illustration is provided by a tube with a Helmholtz resonator inserted as a branch. The situation is shown diagrammatically in Fig. 3(a), where the resonator consists of a closed chamber at the side of the tube with a small orifice as the entrance. It now develops, as one might expect, that P_r (i.e., the power transmission ratio across the branch) is no longer periodic in frequency. Rather, as Fig. 4 indicates, P_r has a minimum at the resonance frequency of

* Figs. 2, 4, 5, 6, 10 and 12 are taken with permission from Stewart and Lindsay, *Acoustics* (D. Van Nostrand Co., N. Y.)

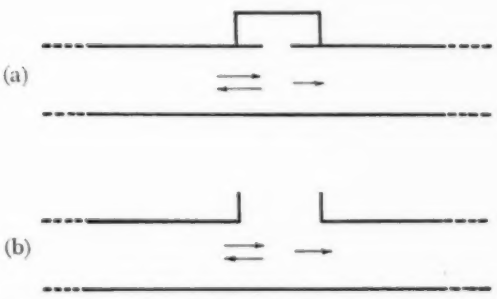

FIG. 3. Further examples of tubes used for transmitting sound.

the resonator and a relatively small value for a considerable frequency range about the resonance point. We should expect this since it is just at the resonance frequency that the resonator will absorb energy most readily from the incident sound wave.

For a third illustration we take the case of sound passing through a tube with a side orifice open to the air (Fig. 3(b)). Here the orifice acts as a branch and P_r measures again the transmission ratio across the branch. The physical description of the behavior of this arrangement is most simply given by noting that the incident sound sets the air in the orifice in motion. Some of the energy of this motion is radiated away into the air. The resultant effect is to reflect some of the incident sound energy and dissipate some of it through radiation. The rest gets by in transmission across the branch. Both absorption effects are most marked at low frequencies. Hence P_r is smaller at low frequencies and rises to nearly unity at high frequencies, as Fig. 5 indicates. This is not really inconsistent with the well-known fact that for given displacement

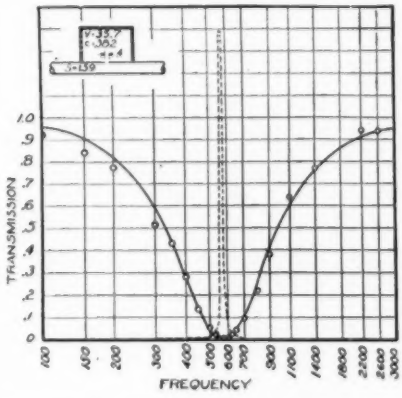

FIG. 4. Transmission curve for tube shown in Fig. 3(a).

velocity of a sound source radiation takes place more efficiently at high frequencies than at low. The point in the present case is that at high frequencies it is harder to get the air in the orifice to vibrate, hence the maximum displacement velocity of the air there is less and there is actually *less* radiation, in spite of the fact that the radiation efficiency is higher. Indeed at sufficiently high frequencies the transmission through the tube behaves as if the orifice were not there at all.

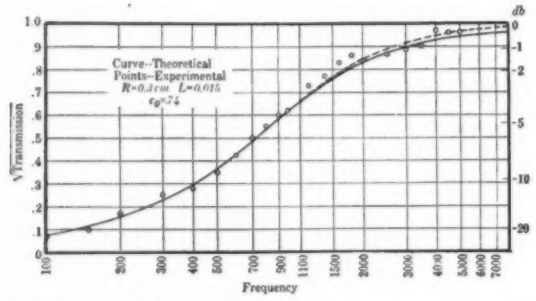

FIG. 5. Transmission curve for tube shown in Fig. 3(b).

3. *Acoustic Filtration in Air. Physical Considerations*

The discussion of the previous section suggests the possibility of using the selectivity of the structures there considered for the purpose of constructing actual acoustic filters. Consider, for example, the tube with a side orifice. The indication is that if a single orifice decreases the transmission at low frequencies, a succession of orifices will cut P_r for this frequency range nearly to zero. This proves to be true experimentally, as the accompanying figure (Fig. 6)

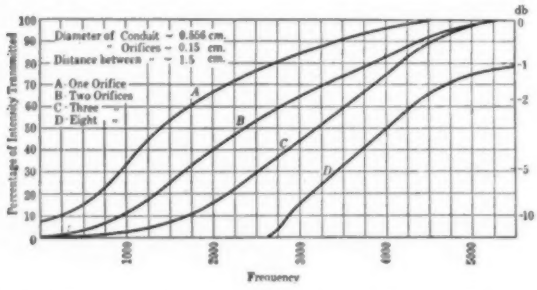

FIG. 6. Transmission curves for a succession of side orifices in a tube.

shows. We should expect that whereas for low frequencies P_r is negligible, when the fundamental frequency of the equivalent open tube between orifices is reached, the transmission will have risen to unity. For higher frequencies the orifice effect will usually have become negligible and large P_r is thus assured independently of tube resonance. This neglects the mathematical refinements we shall presently introduce. However, these purely physical considerations imply that the structure under consideration acts like a *high pass filter* with a transition frequency between the nontransmission or attenuation band and the transmission band which cannot be higher than the first resonance frequency of the main line considered as an open tube. Actually the latter may be considerably above the transition or cut-off frequency.

Continuing the descriptive review of acoustic filtration in air, consider a tube with equally spaced Helmholtz resonators as side branches (Fig. 7). From physical considerations we do not

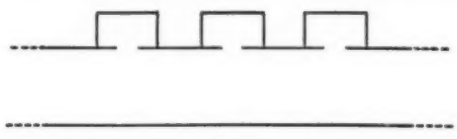

FIG. 7. A tube with equally spaced Helmholtz resonators as side tubes.

expect the resonators to influence P_r for frequencies far away from the resonance frequency of the resonators. Hence we should expect this structure to behave as a low pass filter. As the frequency rises close to the resonance frequency, the resonators go into action, P_r falls and attenuation sets in. However, as the frequency increases still further the effectiveness of the resonators decreases and large P_r again becomes the rule except possibly for $\sin kl = 1$, where l is the distance between resonators. The exact cut-off frequency will depend on the interaction of the main line resonance and the resonator resonance. This can only be found by a closer study of the problem.

4. *Transmission Theory of Acoustic Filtration. Ideal Infinite Case*

There are two principal theories of acoustic filtration. The first, due to G. W. Stewart,[1] is based on the electrical filter analogy and considers the acoustic line as made up of concentrated or "lumped" elements. This is only a first approximation since acoustical elements are

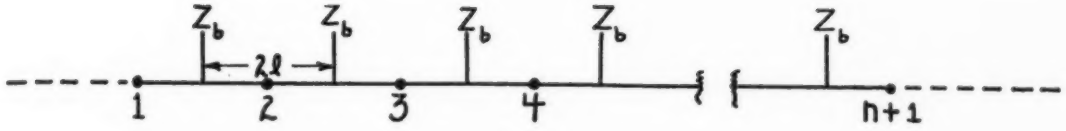

FIG. 8.

rarely lumped in the strict sense. Nevertheless it has been used with considerable success. Since it is very fully described in the book just mentioned we shall not go into it here. Rather we shall confine our attention to the more general transmission theory developed by W. P. Mason.[2] It is somewhat difficult to assign priority since the fundamental idea of the propagation of elastic waves in a medium possessing periodic nonhomogeneity appears to be an old one.[3] Consider the system indicated schematically in Fig. 8. This consists of an infinite acoustic line of cross-sectional area S with equally spaced branches (separation distance $2l$) in which the branch impedance at the junction is Z_b, a pure reactance (i.e., a pure imaginary impedance). Though we shall begin by thinking of the acoustic medium in the line and branches as a gas like air, the method is also applicable to liquid and solid media and to transverse as well as longitudinal waves. For the moment we shall confine the discussion to gases and describe the plane harmonic wave transmission in the line by means of the excess pressure p and the volume current $\dot{X}$ (equal to the product of cross-sectional area and particle velocity). The application of the appropriate boundary conditions satisfied by p and $\dot{X}$ at any branch (in the case of a fluid medium, these are simple hydrodynamical continuity conditions; in the case of solids, the situation is a little more elaborate, as will be seen below) yields the following equations connecting p and $\dot{X}$ for two successive mid-section points j and $j+1$ (e.g., 2, 3, etc. in Fig. 8).

$$p_{j+1}=Ap_j-iBZ\dot{X}_j, \tag{1}$$

$$\dot{X}_{j+1}=A\dot{X}_j-iC/Z\cdot p_j, \tag{2}$$

where

$$\begin{aligned} A&=\cos 2kl+iZ/2Z_b\cdot \sin 2kl,\\ B&=\sin 2kl+iZ/Z_b\cdot \sin^2 kl,\\ C&=\sin 2kl-iZ/Z_b\cdot \cos^2 kl. \end{aligned} \tag{3}$$

In these expressions $Z=\rho_0 c/S$ is the acoustical impedance of a plane harmonic progressive wave. The mean density of the fluid is ρ_0 and the velocity of a compressional wave in the fluid is c. As usual $k=2\pi\nu/c$, where ν is the frequency. Examination of (3) discloses that

$$A^2+BC=1. \tag{4}$$

If we introduce the angle W with

$$A=\cos W, \tag{5}$$

we can write $B=(B/C)^{\frac{1}{2}}\cdot \sin W$ and $C=(C/B)^{\frac{1}{2}}\cdot \sin W$. Eqs. (1) and (2) may now be written

$$p_{j+1}=p_j\cos W-iZ\dot{X}_j(B/C)^{\frac{1}{2}}\cdot \sin W, \tag{6}$$

$$\dot{X}_{j+1}=\dot{X}_j\cos W-i/Z\cdot p_j(C/B)^{\frac{1}{2}}\cdot \sin W. \tag{7}$$

Now $p_j/\dot{X}_j$ is by definition[4] the acoustic impedance at the point j. Its value for given frequency depends entirely on the structure of the acoustic line to the right (or left) of j. But since the line is, by definition, infinite in extent, the impedance must be the same at all mid-section points. Let us call this the *characteristic impedance* of the line and denote it by Z_0. We have then

$$p_j/\dot{X}_j=p_{j+1}/\dot{X}_{j+1}=\cdots=Z_0. \tag{8}$$

The evaluation of Z_0 follows at once by combining (6), (7) and (8). We find

$$Z_0=Z(B/C)^{\frac{1}{2}}. \tag{9}$$

But by resubstituting into (6) and (7) this yields

$$p_{j+1}/p_j=\dot{X}_{j+1}/\dot{X}_j=e^{-iW}. \tag{10}$$

Now when W is *real*, p_{j+1} and p_j can differ only in phase but not in magnitude and the same is of course true of $\dot{X}_{j+1}$ and $\dot{X}_j$. Therefore the structure transmits those frequencies for which W is real. On the other hand when W is complex, p_{j+1} and p_j differ in magnitude and so do $\dot{X}_{j+1}$ and $\dot{X}_j$. Hence for frequencies for which W is complex, a given excess pressure maintained at j will correspond to a smaller one at $j+1$ and so on along the line, so that effectively there is no

transmission. Now cos W is real if Z_b is a pure reactance. Hence the condition for transmission through the infinite structure is

$$|\cos W| \leq 1 \tag{11}$$

while the condition for attenuation is

$$|\cos W| > 1. \tag{12}$$

Reference to the characteristic impedance (9) shows that when $|\cos W| \leq 1$, sin W is real and hence Z_0 is real. However when $|\cos W| > 1$, sin W is pure imaginary and the same is therefore true of $(B/C)^{\frac{1}{2}}$. Hence in this case, Z_0 is pure imaginary. We may therefore characterize the properties of the structure in terms of Z_0: for frequencies such that the characteristic impedance is real, one gets transmission; for frequencies such that Z_0 is imaginary, attenuation results.

If Z_b contains both real and imaginary components, cos W is complex and conditions (11) and (12) no longer possess meaning. In this case, as might be expected, there is no complete transmission for any frequency range. For then W is always complex and p_{j+1} and p_j will always differ in magnitude as well as in phase. We shall not deal with this case in the present paper.

5. *Illustrations of the Application of the Transmission Theory to Air Filters*

Consider first the low pass filter mentioned in Section 3, consisting of a tube with equally spaced Helmholtz resonators as branches. The relevant data follow:

ρ_0 = equilibrium density of air at 20°C, 76 cm pressure = 12.05×10^{-4} gram/cm^3,
c = velocity of sound in air (20°C) = 3.44×10^4 cm/sec.,
S = area of main line = $9\pi/16$ cm^2,
$2l$ = 1.67 cm,
$Z_b = i(\omega M - 1/\omega C')$, where $M = \rho_0/c_0$, $C' = V/\rho_0 c^2$, and c_0 = acoustic conductivity of orifice into resonator[5] = 2.26 cm,
V = volume of resonator chamber = 4.36 cm^3,
n = number of sections = 4.

The transmission characteristics of this structure are indicated in the accompanying plot (Fig. 9) of cos $W = \cos 2kl + Z \sin 2kl/2(\omega M - 1/\omega C')$ as a function of frequency. We see that there is a transmission band extending from $\nu = 0$ to $\nu = 3100$ cycles. The cut-off frequency is the first nonvanishing root of the equation

$$\cos W = -1. \tag{13}$$

The attenuation band extends from $\nu = 3100$ cycles to the frequency corresponding to the first nonvanishing root of

$$\cos W = +1 \tag{14}$$

which in this case is 5600 cycles. Thereafter transmission again sets in and except for very narrow attenuation bands where sin $2kl = 0$, is the rule for all higher frequencies. The transmission through this filter has been measured experimentally[6] and the results are indicated in Fig. 10, which also indicates the appearance of the filter. The sharpness of the cut-off is to be noted as well as the approximate agreement with the theoretically calculated value. Considering the nature of the measurement and the fact that the filter is by no means "infinite," consisting as it does of only 4 sections, the agreement must be considered very good. Of course the value of P_r is by no means unity in the transmission region as the above idealized theory predicts. This is due partly to the neglect to take account of dissipation and partly to the finiteness of the structure. (Cf. Section 6 for the treatment of the finite case.) The method of measurement was hardly sensitive enough to do more than just indicate the presence of the second transmission band at 5600 cycles.

Inspection of the expression for cos W in this case reveals that the following general statements may be made concerning the low pass type of filter just discussed: (1) lowering the resonance

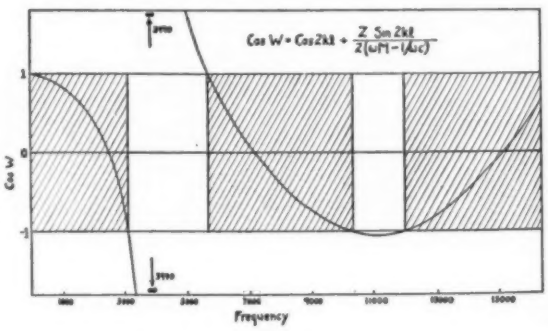

FIG. 9. Variation of cos W with frequency.

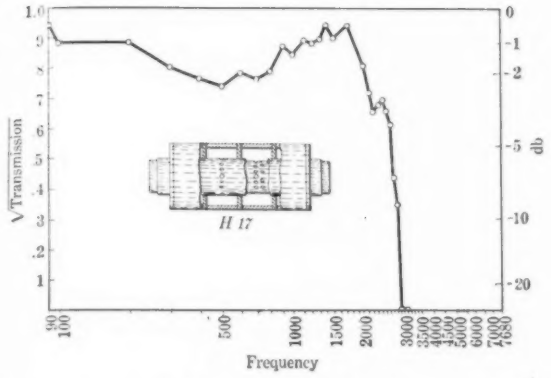

FIG. 10. Low pass filter with equally spaced Helmholtz resonators as branches

frequency of the resonators lowers the cut-off frequency; (2) lowering the cut-off frequency makes the first attenuation region narrower, while raising the cut-off frequency widens this attenuation band; (3) other things remaining the same, increase in the cross sectional area S decreases the cut-off frequency.

As a second illustration of an acoustic filter in air, consider a tube with equally spaced side orifices. The dimensions and other data follow:

$2l = 5$ cm; $n = 12$,
$Z = 56.09$ gram/cm^4 sec.,
$Z_b = i\rho_0\omega/c_0 = 0.0896i\nu$ (c_0 = conductivity of orifices = 0.085 cm),
$Z/2Z_b = 313/i\nu$.

The plot of $\cos W = \cos 2kl + (c_0 Z/2\rho_0\omega) \sin 2kl$ in Fig. 11 shows the transmission characteristics

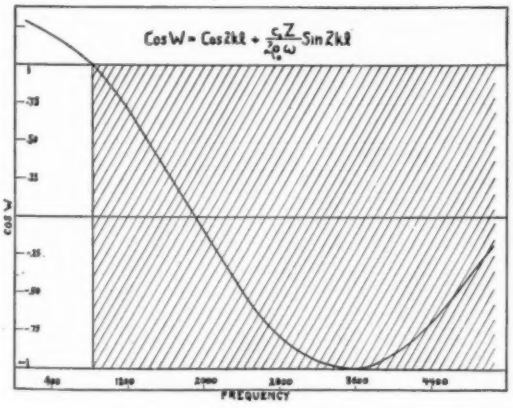

FIG. 11.

of the structure. It is a high pass filter with a theoretical transition frequency at $\nu = 800$ cycles, the first root of $\cos W = +1$. The transmission band which begins there continues indefinitely. The curve of the experimentally measured transmission is shown in Fig. 12. The agreement between theory and experiment is seen to be of the same order as that observed in the low pass type filter. We can make the additional statements that other things remaining the same, increase in the acoustical conductivity, c_0, of the orifices increases the transition frequency. Other things being equal, on the other hand, increase in the cross-sectional area decreases the transition frequency.

6. *Finite Filters*

The theory presented in Section 4 takes no account of the finite length of the filter structure.

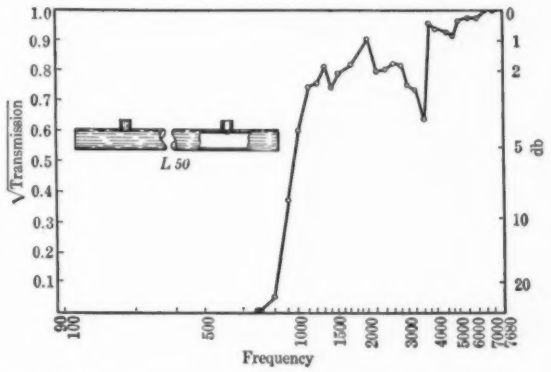

FIG. 12. An acoustic filter having equally spaced side orifices.

In this section we shall introduce the appropriate modification of the theory for this purpose. Referring once more to Fig. 8, we now suppose that the system there indicated consists of n sections beginning at 1 and ending at $n+1$. The whole structure is considered to be inserted in an infinite homogeneous acoustic line with cross-sectional area S_i to the left and S_t to the right of the filter. The main line of the filter itself is assumed to have cross-sectional area S. Acoustic radiation in the form of a plane harmonic wave proceeding from the left is incident on the system at 1 and leaves it at $n+1$ in the form of a plane wave moving solely to the right, the infinite line ruling out the possibility of a wave to the left in the region beyond $n+1$. Eqs. (1) to (7) inclusive still apply. But now from (6) and (7) we can

show by mathematical induction that we also have

$$p_{n+1}=p_1\cos nW-iZ\dot{X}_1(B/C)^{\frac{1}{2}}\cdot\sin nW, \quad (15)$$

$$\dot{X}_{n+1}=\dot{X}_1\cos nW-i/Z\cdot p_1(C/B)^{\frac{1}{2}}\cdot\sin nW. \quad (16)$$

From the boundary conditions at $n+1$ and from what has just been said about that point, it follows that $\dot{X}_{n+1}$ and p_{n+1} are the volume current and excess pressure respectively in the wave traveling out of the filter at its terminus. We shall denote the pressure and volume current in the main line to the left of the filter by

$$p=p_0e^{-ikx}+p_0'e^{ikx}, \quad (17)$$

$$\dot{X}=S_i/\rho_0c\cdot(p_0e^{-ikx}-p_0'e^{ikx}). \quad (18)$$

Here p_0 is the excess pressure in the incident wave at the point 1 (taken as $x=0$) while p_0' is the excess pressure in the reflected wave at the same point. In (17) and (18) we are leaving out the common harmonic time factor $e^{i\omega t}$ for the sake of convenience. The power transmission ratio of the filter is now defined to be

$$P_r=Z_i|p_{n+1}|^2/Z_t|p_0|^2, \quad (19)$$

where $Z_i=\rho_0c/S_i$ and $Z_t=\rho_0c/S_t$. This is the ratio of the average flow of energy per second out of the filter to the average flow of energy per second into the filter. Utilizing the boundary conditions at 1, *viz.*

$$p_1=p_0+p_0'; \quad \dot{X}_1=S_i/\rho_0c\cdot(p_0-p_0'), \quad (20)$$

we are finally led to

$$P_r=\frac{4Z_i/Z_t}{(1+Z_i/Z_t)^2\cos^2 nW+[Z_i/Z\cdot(C/B)^{\frac{1}{2}}+Z/Z_t\cdot(B/C)^{\frac{1}{2}}]^2\sin^2 nW}. \quad (21)$$

The simplest experimental arrangement is that in which $Z_i=Z=Z_t$ by the choice of a common cross-sectional area. In this case (21) reduces to the form

$$P_r=\frac{1}{1+Z^2/|Z_b|^2\cdot(\sin^2 nW)/4\sin^2 W}. \quad (22)$$

The connection between P_r for the finite filter and the transmission characteristics of the corresponding infinite filter given by $\cos W$ in (11) and (12) is now very readily seen. When $|\cos W|>1$, i.e., when the infinite structure has an attenuation band, $W=W_r+iW_i$, where due to the real character of $\cos W$, $W_r=n'\pi$ (n' integral). Hence in this case $\sin W=\pm i\sinh W_i$ and $\sin nW=\pm i\sinh nW_i$. Consequently as n increases, $\sin^2 nW/\sin^2 W$ will increase monotonically and therefore P_r will become negligibly small: this corresponds to attenuation. On the other hand, when $|\cos W|\leq 1$, W is real and both $|\sin nW|$ and $|\sin W|$ are less than or equal to unity. Moreover in this case (cf. Eq. (3)) $|Z_b|$ cannot be very small compared with Z unless $\sin 2kl$ is also very small. The indications therefore are that for $|\cos W|\leq 1$, P_r *can* become of the order of magnitude of unity and will not become zero even if n is very large. This corresponds to the transmission band.

We are now ready to consider some examples. Here it will be interesting for comparison purposes to investigate the low and high pass filters already discussed in Section 5.

Figure 13 shows the plot of P_r for the low pass filter described in Section 5 together with the measured values as taken from Fig. 10. It is of interest to note that the general trend of the two curves is the same, though the theoretical P_r is in every case higher than that measured, as we should expect from the neglect of irreversible dissipation. The agreement of the cut-off is particularly good. We have already mentioned that the second transmission band could hardly be more than just barely detected by the experimental arrangement employed. It is interesting to note that the resonance frequency of the Helmholtz resonator used as a side branch is about 4000 cycles and thus comes at about the center of the attenuation band.

The three peaks in the theoretical curve are readily attributed to the values of W between 0 and π (i.e., in the transmission band, cf. Fig. 9) for which $\sin nW$ (*viz.* $\sin 4W$ in this case) vanishes. These are, of course, $W=\pi/4$, $\pi/2$ and $3\pi/4$. Note that the frequency is plotted on a logarithmic scale. The last peak does not appear

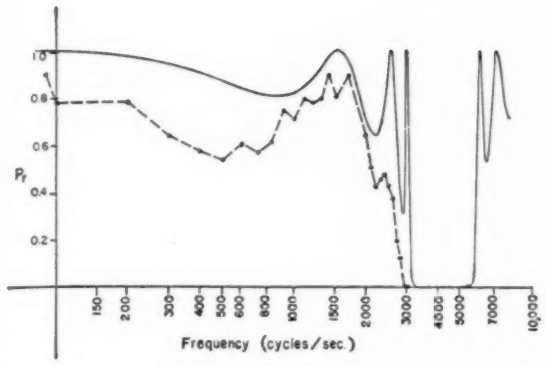

FIG. 13. Transmission curve for a finite low pass filter.

to have been detected experimentally. This is hardly surprising since it is a very sharp one.

The P_r curves calculated and observed for the finite high pass filter of Section 5 are shown in Fig. 14. The general remarks concerning the low pass filter also apply here. We note, however, in addition, the following interesting points.[7] The noticeable dip in the experimental P_r curve at about 3500 cycles is faithfully mirrored in the theoretical curve. This received no explanation at the time when the measurements were originally made. The ripples in the theoretical curve, which are also roughly followed by the experimental results, are due to the $n-1$ (i.e., in this case 11) zeroes of $\sin nW$ as W goes from 0 to π in the transmission region. Another similar series occurs as W goes from π to 2π, etc. The dip comes at the frequency for which $W=\pi$, since here the indeterminate form $\sin^2 nW/\sin^2 W$ has the limiting value n^2. It will be noted that there is but one attenuation band and after the transition frequency, transmission occurs for all higher frequencies. This is in agreement with all experimental results so far obtained.

7. *Alternative Definition of Transmission Ratio for Finite Filters*

While the definition of the power transmission ratio P_r in Eq. (19) is the one commonly meant by this term in acoustics it is well to point out that it is not always the one most simply realized in experimental measurement. To check it experimentally it is necessary to measure the sound intensity in the line directly after the filter and, replacing the filter by a section of the original acoustical line equal in length to the filter, to repeat the measurement at the same place. The ratio of the former to the latter measurement is P_r. Obviously it would be simpler from an experimental point of view to place detecting devices in the line *before* and *after* the filter and make the measurements simultaneously. The ratio in this case, however, will not be P_r. If we assume that the device measures something proportional to the square of the displacement velocity, we can define the new ratio as

$$P_r' = |\xi_{n+1}|^2/|\xi_1|^2. \tag{23}$$

The principal difference between this and P_r given in Eq. (19) lies in the fact that the denominator refers to the *resultant* displacement velocity at the beginning of the filter rather than that in the wave incident on the filter from the left. P_r' follows from Eqs. (15) and (16) by eliminating p_1 between them and replacing p_{n+1} by $Z_t\dot{X}_{n+1}$. We then get

$$P_r' = S_t^2/S_i^2 \cdot \frac{1}{\cos^2 nW + Z_t^2/Z^2 \cdot C^2 \cdot \sin^2 nW/\sin^2 W}. \tag{24}$$

And if we take the conventional situation where $S_i=S_t$, $Z_t=Z$, this reduces to

$$P_r' = \frac{1}{1 - iZ/Z_b \cdot C \cdot \sin^2 nW/\sin^2 W}. \tag{25}$$

It must be emphasized that P_r' is not a genuine transmission coefficient. In particular it can exceed unity. Nevertheless it can be used as a measure of transmission, since by inspection we see that for $|\cos W| \leq 1$, P_r' will in general be large, while for $|\cos W| > 1$, the circular functions become hyperbolic and for n large, P_r'

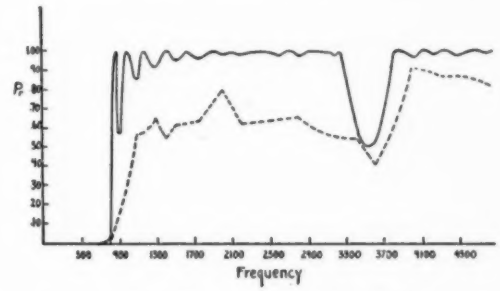

FIG. 14. Transmission curve for a finite high pass filter.

becomes vanishingly small. It is worth pointing out that although P_r' can greatly exceed unity, it cannot become infinite for any frequency. The analytical reason for this is clear from inspection of (24), since infinite P_r' would involve the simultaneous vanishing of both $\cos nW$ and $Z_t/Z\cdot C\cdot\sin nW/\sin W$. This contradicts the restrictions placed on these quantities. Physically, we see that $P_r'=\infty$ would imply a vanishing $\dot{X}_1$ for nonvanishing $\dot{X}_{n+1}$, i.e., complete reflection of the wave incident on the filter with simultaneous nonvanishing wave disturbance in the line beyond the filter. Since the latter is assumed to be infinite, this situation is self-contradictory. Moreover, if P_r' is measured experimentally, P_r can be estimated as

$$P_r=P_r'\left(\frac{1-iZ/Z_b\cdot C\cdot\sin^2 nW/\sin^2 W}{1+Z^2/|Z_b|^2\cdot\sin^2 nW/4\sin^2 W}\right). \quad (26)$$

Since a graphical comparison of P_r and P_r' may be of some interest, Figs. 15 and 16 present

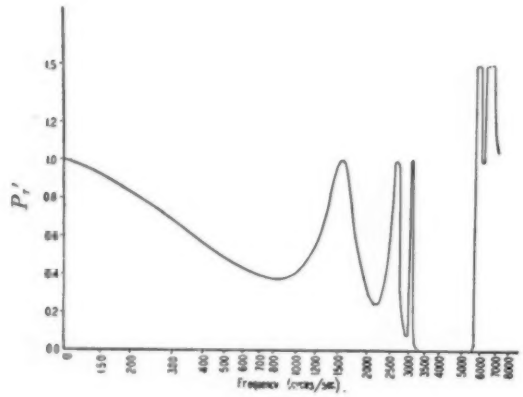

FIG. 15.

the plot of P_r' for the low pass and high pass filters discussed in the last section and for which the P_r curves are shown in Figs. 13 and 14. It will be noted that both P_r and P_r' follow the same general trend. It follows that P_r' can serve as a very useful measure of the transmission through the filter structure.

8. *Finite Filter with a Finite Termination*

In our discussion of finite filters so far we have supposed the acoustic line in which the filter is inserted to be infinite to the right. In any actual filter arrangement this part of the line will be

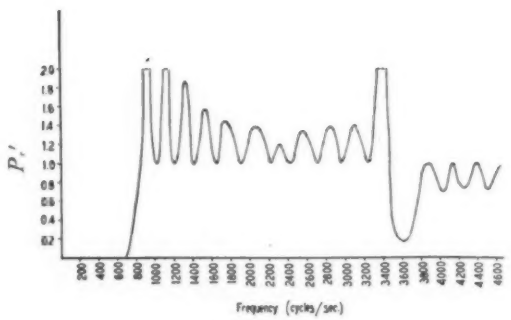

FIG. 16.

finite. It may be made very long and appropriately treated (e.g. lined with felt) so as to cut down the reflected wave toward the left, but the latter will always be present to some extent. We can get some indication of its effect by considering the general case of a finite filter terminated by a finite line. Let its length be l' and the impedance of a plane progressive wave in it be Z'. Since we are still discussing air filters it will be simplest to consider it a cylindrical tube. If its area of cross section is S', we have $Z'=\rho_0 c/S'$. The impedance at the far end of the terminal tube, $Z_{l'}$ is given in terms of the terminal impedance of the filter Z_t, by means of the relation[8]

$$Z_{l'}=\frac{Z_t\cos kl'-iZ'\sin kl'}{\cos kl'-iZ_t/Z'\cdot\sin kl'}. \quad (27)$$

When this is solved for Z_t we get

$$Z_t=p_{n+1}/\dot{X}_{n+1}=\frac{Z_{l'}\cdot\cos kl'+iZ'\cdot\sin kl'}{\cos kl'+iZ_{l'}/Z'\cdot\sin kl'}. \quad (28)$$

Ideally, if the far end of the terminal tube is open we shall have (neglecting the motion of the air in the opening and the radiation) $Z_{l'}=0$ and thus Z_t becomes

$$Z_{t_0}=iZ'\tan kl'. \quad (29)$$

On the other hand if the far end of the tube is rigidly closed, $Z_{l'}=\infty$ and Z_t becomes

$$Z_{t_c}=-iZ'\cot kl'. \quad (30)$$

Going back to (15) and (16) we recall that

$$\dot{\xi}_{n+1}/\dot{\xi}_1=S_i/S'\cdot\frac{1}{\cos nW+iZ_t/Z\cdot C\cdot\sin nW/\sin W}. \quad (31)$$

Hence the P_r' expressions for the cases of the open end and closed end respectively are

$$P_r' = S_i^2/S'^2 \cdot \frac{1}{(\cos nW - Z'/Z \cdot \tan kl' \cdot C \sin nW/\sin W)^2} \quad (32)$$

$$P_r' = S_i^2/S'^2 \cdot \frac{1}{(\cos nW + Z'/Z \cdot \cot kl' \cdot C \cdot \sin nW/\sin W)^2}. \quad (33)$$

Inspection of (32) and (33) indicates that for $|\cos W| \leq 1$, they can become rather small, leading to large P_r' and therefore a transmission band. For $|\cos W| > 1$ the circular functions become hyperbolic and for n large, the denominators become very small, leading to negligible P_r'. Hence we have again the succession of transmission and attenuation bands as before. The situation in the transmission bands is indeed rather complicated due to the resonance effects of the terminating tube. The resultant P_r' values are due to the interaction of the tube resonance and that of the finite filter structure itself. Hence relative dimensions play an important role. We can at any rate make general statements about two limiting cases. Thus if: (1) the length l' of the terminating tube is so small that its fundamental frequency is above the frequency range of the transmission band being considered, the plot of P_r' in this band as W goes from 0 to π will show a definite series of n infinite peaks, corresponding to the n changes of sign of $\cos nW$ in the band. The position of the peaks does not depend markedly on the terminating tube. The infinite value of P_r' at the peak frequencies *is*, of course, an effect of the finite termination and the confinement of the sound energy in a finite system with neglect of dissipation through friction and radiation. On the other hand, if: (2) l' is so large that there are many harmonics of the terminating tube in the frequency range of the transmission band, one will expect subsidiary peaks due to tube resonance. Of course, at the anti-resonance tube frequencies, e.g. those for which $\tan kl' \to \infty$, P_r' will drop to zero even in a transmission band.

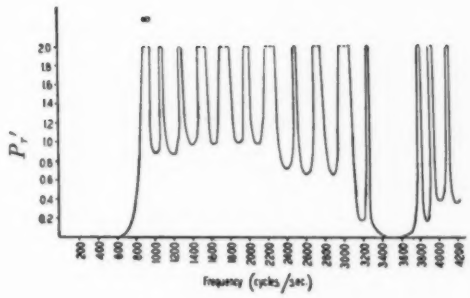

FIG. 17.

By way of illustration we present in Fig. 17 the plot of P_r' for the case of the high pass filter already discussed terminated by a closed tube 5 cm long. For convenience the infinite peaks are terminated at $P_r' = 2$. This situation corresponds more or less to limiting case (1) above. However, certain modifications are to be noticed. In the first place, due to the fact that the first anti-resonance frequency of the terminating tube falls at about 3500 cycles, the transmission there is cut to zero and the dip in the P_r' curve shown in Fig. 15 now becomes effectively a small attenuation band in what is really the transmission band of the equivalent infinite filter. This band extends approximately from 3350 to 3750 cycles. As the anti-resonance frequency is passed the succession of transmission peaks again recurs. It will also be noticed that in the transmission region from 800 cycles to 3350 cycles there are 11 peaks instead of the 12 which would properly correspond to the actual number of sections. The 12th change of sign of $\cos nW$ is masked completely by the large values of $\cot kl'$ and hence the corresponding peak does not appear. It is interesting to observe that the terminating tube has no influence on the transition frequency from the low frequency attenuation band to the transmission band.

We can readily handle the case in which the impedance at the open end of the terminal tube is not taken to be zero but given its actual value in terms of the inertance of the opening as an orifice and the radiation resistance. Thus for

$$Z_{l'} = (\rho_0 \omega k/2\pi) + i\rho_0 \omega/c_0, \quad (34)$$

where c_0 is the acoustic conductivity of the opening[9] we get

$$Z_{i0}' = \frac{\rho_0 \omega k/2\pi + i(\rho_0 \omega/c_0 + Z' \tan kl')}{1 - \rho_0 \omega/c_0 Z' \cdot \tan kl' + i(\rho_0 \omega k/2\pi Z') \cdot \tan kl'}. \tag{35}$$

We shall not trouble to substitute this into (31) but merely note than in doing so we are led to a complex denominator for ξ_{n+1}/ξ_1. This means that P_r' can never become infinite: there is now a definite loss of energy from the system through radiation in addition to the usual frictional dissipation.

Bibliography

1. Stewart and Lindsay, *Acoustics* (New York, 1930) p. 159 ff.
2. W. P. Mason, Bell System Tech. J. **6**, 258 (1927). Phys. Rev. **31**, 283 (1928).
3. Cf. Horace Lamb, Mem. and Proc. Manchester Lit. and Phil. Soc. **42**, 1 (1897–98). Also cf. N. Kasterin, Amst. Ak. Versl. **6**, 460 (1898) and Arch. Néerland. **5**, 506 (1900).
4. Cf. reference 1, p. 50, 55.
5. For the physical meaning of the symbols M, C', c_0 the reader may consult reference 1, p. 47 ff. We are using C' instead of the conventional C to avoid confusion with (3).
6. For the method of measurement, cf. reference 1, p. 197.
7. The rather poor agreement between theory and experiment noted in the paper "Finite Acoustic Filters" (J. Acous. Soc. Am. **8**, 211 (1937)) appears to have been due to an erroneous assignment of dimensions. The experimental curve shown in Fig. 3 of that paper appears actually to correspond to $2l = 5$ cm and $n = 12$. This was kindly called to the author's attention by A. Belov of Leningrad. Figures 11, 12 and 14 of the present paper are based on the revised assignment.
8. Cf. reference 1, p. 138.
9. Reference 1, p. 125.

In educational institutions, science has no limitations in search for truth except those imposed by availability of ideas, workers, facilities and funds. Such institutions have always been the places where the great bulk of new discoveries are made and ideas born, and this will continue to be so, since there exist no other organizations where such studies can be similarly pursued. The practical aims of educational institutions in science are well described by Dr. Isaiah Bowman: "The trade school exists for the admirable purpose of putting practically trained men into jobs; the university exists, among other things, to create and expand the sciences that provide the jobs. It is in engineering that these two points of view are effectively joined."

KARL T. COMPTON—"Science in an American Program for Social Progress."—*Science Monthly*

Metallurgical Applications of Electron Diffraction*

BY H. R. NELSON

Battelle Memorial Institute, Columbus, Ohio

Introduction

THE experimental demonstration of the wave nature of electrons a little over ten years ago was a matter of far-reaching importance in modern physics. Unlike so many of the current developments or discoveries in physics, however, the possibility of using this discovery as a practical research tool was realized almost immediately. The similarity between electron and x-ray diffraction suggested that electrons might be as useful as x-rays in studying crystalline solids.

During the past eight years electron diffraction methods have been applied to a wide variety of problems by investigators in this country, Europe and Japan.[1] Of the several hundred papers which have appeared during this period, nearly half have treated rather fundamental if not altogether practical problems of metallurgical interest. Most of this work has been done in university laboratories often, however, with the assistance and cooperation of interested metallurgists. At present there are at least three metallurgical laboratories in this country in which electron diffraction is in continual use as a research tool.

It is my purpose to discuss some of the more successful metallurgical applications of the present technique, to discuss its limitations as well as its potentialities.

The Experimental Method

I have already mentioned that there is a similarity between electron and x-ray diffraction effects. They are alike in that both involve the interaction of trains of waves in the regular array of atoms of a crystal lattice. The same diffraction laws apply to both effects and similar methods are used for interpreting the diffraction patterns. There is, however, one very important difference. Whereas a beam of x-rays is relatively little affected by solid matter which lies in its path, a beam of electrons is greatly affected by very small amounts of matter. In other words, x-rays penetrate rather deeply into solids while electrons having the energies ordinarily used are stopped by thicknesses of a few millionths of an inch. From the practical point of view this means

FIG. 1. Electron diffraction camera—Battelle Memorial Institute. This camera is similar to one originally described by Thomson and Fraser.[2] The high voltage is supplied by a transformer-rectifier-filter system which is not shown. Near the center of the camera are the controls for manipulating the test sample in the vacuum. The rectangular box at the top is a plate magazine holding up to ten plates, which may be exposed successively without breaking vacuum.

* Presented at the Colloquium on Physical Tools Used in Metallurgy, University of Pittsburgh, July 8, 1938.

that we can shoot electrons at a metal surface with the assurance that any resulting diffraction pattern must be due to material lying within about 100 angstroms of the surface. This low penetrating power accounts for the usefulness of electrons in studying surfaces. Moreover, electrons are so efficiently scattered by matter that very little material is necessary to give a good diffraction pattern and exposure times are very short—a matter of seconds, whereas x-ray exposures are of the order of hours.

Almost every electron diffraction camera has been designed by its user. Consequently no two look much alike. Reduced to essentials, however, every camera consists of a hot filament or a gas discharge tube for a source of electrons, a series of pin holes to give a fine beam of electrons after they have been accelerated by an electric field, a movable sample holder to hold the sample in the proper position in the beam and a photographic plate or film to record the diffraction pattern—all enclosed in a vacuum tight chamber. (See Figs. 1 and 2.) Since the effective wavelength of the electrons depends upon their speed which in turn depends upon the accelerating voltage a constant d.c. voltage, usually between 20 and 70 kv must be applied to the electron tube. A transformer, rectifier and filter system is the most satisfactory source of such power.

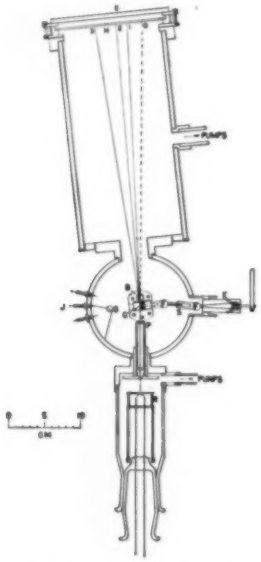

FIG. 2. Schematic diagram of the diffraction camera in Fig. 1. Electrons come from a hot filament in the box *R* and are accelerated by a high voltage field to the anode just above *R*. They then pass through a series of fine holes *P* and are "reflected" at grazing incidence from the surface of the sample *C* in various beams which strike the photographic plate *H* at points 1, 2, 3, etc. By means of a control at the back with actuates the pinion *B*, the sample may be moved out of the beam and the undeflected electrons (dotted line) permitted to locate the center of the ring pattern at *O*. Insulated leads *J* permit heating of the sample by means of a heater *G* or the formation of films in the evacuated camera by vaporization. *K* is a fluorescent screen on which the diffraction pattern may be observed when the plate is withdrawn to the top part of the plate magazine.

There are two different methods of studying surfaces of metals. The simpler, easier and more widely applicable is the "reflection" method in which the electrons fall upon the test surface at grazing incidence, penetrate submicroscopic projections and are diffracted out. Obviously diffraction patterns so obtained are characteristic of the true surface. The transmission method is sometimes used when thin surface films, such as oxide films or a thin electrodeposit of another metal can be removed by dissolving away the basis metal. If such a film is sufficiently thin, and it must not be thicker than a few hundred angstroms, i.e., 2/1,000,000 inch, it can be mounted in the camera so that the electrons pass through it. Aside from involving rather difficult technique in removing and mounting the films, the transmission method is often subject to the objection that the film may have undergone some change during the process of removal.

Applications

Surface chemistry.—The most extensive metallurgical use of electron diffraction has been in the broad field of surface chemistry. Diffraction patterns are used to identify reaction products formed on a metal surface when a few metal atoms combine with the constituents of a gas, a solution or another solid. As examples of such uses we immediately think of the identification of oxide, tarnish or corrosion films on metals.

Many investigations have been carried out on the nature of oxide films formed by oxidizing atmospheres on metals. Long before an oxide film is thick enough to be visible it can usually be detected and identified from a diffraction pattern. The protective air-formed oxide film on aluminum has been found to be amorphous. On exposure to air at room temperature, clean surfaces of copper and iron quickly become covered with thin invisible films of oxide, Cu_2O and γ-Fe_2O_3, respectively.

(a) (b)

FIG. 3. Electron diffraction patterns from an iron film formed by electrodeposits. (a) Immediately after electroplating; (b) after cleaning.

In order to illustrate some of the things which can be done, I should like to discuss some work on iron which has been done at Battelle Memorial Institute. Fig. 3a shows a typical electron diffraction picture made by the reflection method. The specimen was the surface of an iron electrodeposit. The ring pattern is not due to iron, however, but is due to a thin, invisible film of γ-FeOOH, ordinary rust, which formed on the surface even though it was rapidly washed and dried. After this specimen was given a cathodic treatment in NaCN solution the pattern of Fig. 3b was obtained. The short arcs in this picture are due to iron and show that the electrodeposited Fe crystals are standing on their cube corners. The fact that the rust pattern of Fig. 3a consists of continuous rings means that the crystals of the thin rust film are randomly oriented and hence bear no orientation relationship with the underlying iron. Fig. 4 shows the pattern obtained from a film in which the iron crystals are similarly oriented. Here, however, in addition to the iron pattern, there are short arcs due to γ-Fe_2O_3, the oxide which forms when iron is exposed to ordinary air at room temperature. The arced oxide pattern is conclusive evidence that the crystals of the invisible oxide film are oriented and that their orientation is related to that of the underlying iron crystals. By measurements on such plates it has been possible to determine just how the oxide crystals are fastened to the iron.

When iron is oxidized at red heat in air the scale forms in layers which can be dissected and the various surfaces studied separately. Fig. 5a is the pattern due to ordinary ferric oxide, α-Fe_2O_3, from iron heated for a few minutes at 1600°F. At this stage the oxide film has just gone through the interference color stage and has turned black. Slight traces of preferred orientation are apparent. If iron is heated for about an hour at 1600°F the outer surface of the scale has a smooth velvety appearance and gives the pattern of Fig. 5b. This is also α-Fe_2O_3 and shows more pronounced preferred orientation and much larger crystal sizes as indicated by the spotty appearance. If the outer layer of scale is chipped off, turned over and a picture taken of the under side we obtain the pattern of Fig. 5c, which is due to magnetite, Fe_3O_4, with no traces of preferred orientation.

Lower layers of oxide can be studied by the same method and it is found that the oxides of some alloying elements tend to be concentrated in the lower oxide layers.

The work on the identification of tarnish and corrosion films has been done chiefly on surfaces tarnished or corroded in service or under other rather uncertain conditions. Consequently, very little about this important application has appeared in the literature. A metal surface may become mysteriously tarnished; another may show an unusual type of corrosion; still another may resist corrosion better than an apparently similar one. In any case, the first step in the solution of the problem is to find out what is on the surface. We find our diffraction camera of considerable use for such purposes and it takes its place as a service tool along with such well-known tools as the tensile tester or the spectrograph.

It should be mentioned, however, that the diffraction method does not always work. Sometimes the patterns are too weak or there is no pattern at all. Even when a good pattern is obtained we may not be able to identify the unknown. The normal procedure is to guess what the unknown film is. Our guess is then tested by comparing the observed pattern with

the pattern calculated from known crystal structure data on the guessed compound. If we get a match the job is done, if not, we continue guessing and checking until we do get a match, or until it is no longer worth while to continue. Usually many guesses can be eliminated without much time spent on calculations. Even if we fail in completely identifying the film we have learned certain things about it which may be important. We know something about the size of the crystals composing the film and their orientation. Sometimes we can be sure that there are two different compounds present without knowing what either one is. In any case when we get through we always know a number of things which the film is not.

Thin metallic films. — Electron diffraction methods have thrown some light on the structure of very thin metal layers formed by sputtering, by electrodeposition, or by the condensation of metal vapors in a vacuum. When one metal is deposited on another it is found that the first few atoms often tend to arrange themselves in accordance with the crystal lattice of the basic material. In other words the bond layer between the two metals is a crystallographic hybrid in which a transformation from one lattice type to the other takes place. Preferred orientation of the crystals composing these thin films is the rule rather than the exception. Usually the crystals are oriented with a certain crystallographic axis perpendicular to the surface. It has been found, however, that in films formed by the condensation of metallic vapors, there is often a tendency for a crystal axis to point in the direction along which the vapor atoms move as they approach the substrate.

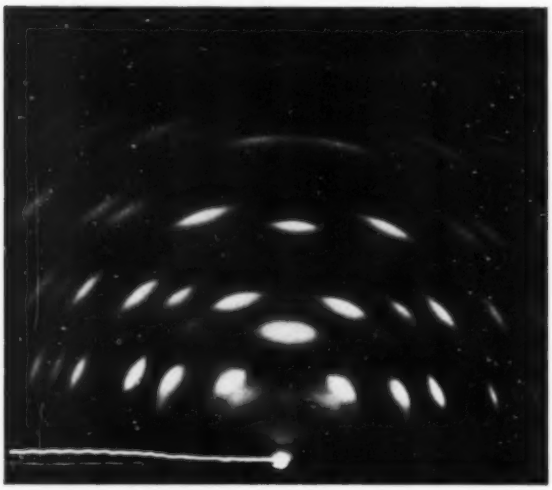

FIG. 4. Pattern from an oriented iron film which had been exposed to ordinary air for a short time. All the reflections due to iron fall on equally spaced horizontal lines. The others are due to the air-formed oxide.

Mechanically worked surfaces.—A large amount of work has been done on the nature of polished metal surfaces. There is not time to discuss this interesting subject in detail. Suffice it to say, however, that electron diffraction studies give evidence of a highly disorganized layer on polished or buffed metal surfaces. Some investigators believe that such surfaces are covered with a layer of amorphous metal. Others believe that the evidence for truly amorphous metal is not conclusive. In my opinion, the patterns obtained from polished surfaces are more likely to be due to a thin amorphous layer of metallic oxide than to truly amorphous metal, and it seems that other possibilities must be tested before we really know the nature of a polished surface. In any case, more work will be done before complete agreement on the interpretation is reached.

Very little has been done on the preferred orientation in rolled metal surfaces. Electrons should be useful, however, in studying deformation structures in the thin surface layer of rolled sheets.

Bearing surfaces and lubrication.—In the field of lubrication and bearing surfaces, electron diffraction methods have already given interesting and useful information and much more is to be expected in the future. The molecular orientation in thin films of various oils and greases has been studied. The effect of graphite additions to oils has been investigated and it has been shown that the graphite in a cast iron engine block forms a lubricating layer on the surface of the cylinders after a period of running in. Of considerable interest also is the possibility of learning something about the nature of the oil-metal bond in the case of the new extreme pressure lubricants and other oils of high film strength. Work along this line is now in progress at Battelle.

Limitations of the method.—I have mentioned rather briefly some of the more important of the

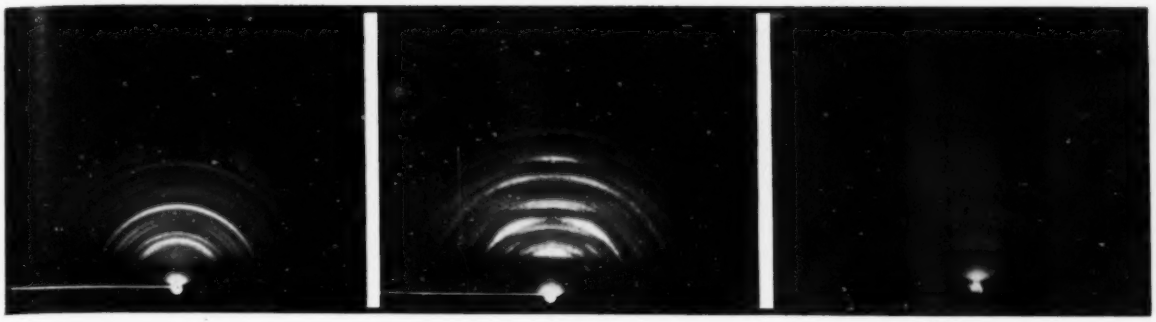

(a) (b) (c)

FIG. 5. Electron diffraction patterns from iron scale formed at high temperatures. (a) α-Fe_2O_3 pattern from the surface of a very thin layer of scale; (b) α-Fe_2O_3 pattern from the top surface of thick scale; (c) Fe_3O_4 pattern from the underside of the same thick scale.

metallurgical applications of electron diffraction. I should like now to point out some of its limitations.

It must be remembered that this method of surface analysis depends upon diffraction in crystalline or pseudo-crystalline films. The atoms composing the surface must, therefore, be arranged with some degree of regularity and this regularity must be continued through a small number of atoms. A single molecular layer of a straight chain hydrocarbon will give a well-defined pattern due to the regular spacing of as little as 10 carbon atoms along the chain. On the other hand, an adsorbed layer of gas or water molecules will escape detection by present techniques because there is no sufficiently extended regularity in such films.

Since the effective wave-length of the electrons is very small most of the diffracted beams are deviated from the incident beam by less than 4°. This means that the grazing angle on the sample must be small—a few minutes of arc. Also it is apparent that the test surface must be flat or convex—never concave. There seems to be no good way of getting at the film at the bottom of a corrosion pit.

Because the camera must be highly evacuated it is obvious that volatile layers cannot be readily studied.

The operations involved in taking the diffraction pictures do not require much skill. A large number of pictures can be taken in a day with almost routine procedure. The interpretation of the patterns, however, requires some skill and experience, and considerable care must be taken in preparing samples. The very sensitivity which makes this method so useful also makes it susceptible to extremely small amounts of contaminating material. The investigator must constantly guard against attaching significance to patterns due to extraneous material which may be present accidentally.

In conclusion, we can say that electron diffraction is already a metallurgical research tool. It is not yet an instrument for routine analysis, although in some laboratories it is called upon to do almost that. Besides, the rather obvious applications which have been discussed, the technique will undoubtedly be applied to other types of problems some of which will not be directly concerned with surface films. As an illustration of such an application, I might mention the possibility of identifying submicroscopic inclusions in metals or studying grain boundary material. To do this successfully it is only necessary to find suitable solvents which will attack the metal more rapidly than the inclusions or grain boundaries. With grazing incidence electrons the diffraction pattern will be characteristic of the minute amount of material left in relief by the solvent. A beginning has already been made in this type of work.

Reference

1. For reviews of the field and extensive bibliographies see: "A General Discussion on the Structure of Metallic Coatings, Films and Surfaces, Part I," Trans. Faraday Soc. **31**, 1043 (1935); G. L. Clark and E. Wolthuis, J. Chem. Ed. **15**, 64 (1938); T. Schoon, Metallwirtschaft **17**, 203 (1938).
2. Thomson and Fraser, Proc. Roy. Soc. **A128**, 641 (1930).

Here and There

New Appointments and Promotions

Elevation of Eugene W. Ritter, as General Manager of the RCA Manufacturing Company's Harrison Plant, replacing J. C. Warner, deceased; and of D. F. Schmit, to succeed Mr. Ritter as Manager of Research and Engineering at the company's tube making plant, was announced by Robert Shannon, Vice President and General Manager.

★

At Cornell University, Dr. Lyman G. Parratt has been promoted from an instructorship to an assistant professorship in physics.

★

Dr. Edward B. Doll, for the past two years teaching assistant in electrical engineering at the California Institute of Technology, and Dr. Lester Tarnopol, for the past year assistant in metallurgy in charge of the x-ray laboratory of metallurgy at Harvard University, have been appointed Assistant Professors in the College of Engineering of the University of Kentucky.

Science, August 12, 1938

★

Dr. Karl F. Oerlein, General Chairman of the Pennsylvania Junior Academy of Science and Professor of Physics at the State Teachers College, Indiana, Pa., has been appointed Head of the Department of Science at the State Teachers College, California, Pa.

★

Dr. Ralph Howard Fowler, fellow of Trinity College, has been reelected to the John Humphrey Plummer professorship of mathematical physics at the University of Cambridge. The London *Times* writes that Professor Fowler resigned from this chair on his acceptance of the directorship of the National Physical Laboratory on the resignation of Professor W. L. Bragg, but that he had been advised to withdraw his acceptance of this post for reasons of health, and signified willingness to be reelected as professor of mathematical physics.

Science, August 19, 1938

★

Dr. Russell H. Lyddane has received a temporary appointment as Assistant Professor of Physics at the University of North Carolina to take the place of Professor Otto Stuhlman, Jr., while the latter is on sabbatical leave. Dr. J. B. Fisk has been appointed Associate Professor of Physics at the same University.

Professor T. H. Morgan, Sir William Bragg, and Professor T. Levi-Civita, Emeritus Professor of Mechanics in the University of Padua, have been elected as foreign associates of the Paris Academy of Sciences.

★

Conference on Engineering and Industrial Statistics

The Massachusetts Institute of Technology held a two-day conference, September 8 and 9, under the direction of the Department of Mathematics and the Department of Economics and Social Science, on the application of statistical methods to industrial and engineering problems. Addresses and discussions by visiting industrial statisticians and Technology staff statisticians included a resumé of certain statistical technique needed for effective handling of industrial data, successful applications of statistical methods in the fields of engineering and quality control, contemporary developments in industrial and engineering statistics. The practical applications of statistical methods in engineering and industrial work have developed steadily in the last ten years, and it was the purpose of this conference to explain to American engineers and executives the nature and possibilities of certain of these cost-saving statistical devices.

★

British Association

Americans on the program of the meeting of the British Association for the Advancement of Science held recently at Cambridge were: Dr. Harlow Shapley, Paine Professor of Practical Astronomy and Director of the Harvard College Observatory, "Metagalactic Gradients and the Expanding Universe Hypothesis;" Dr. R. W. Wood, Professor of Experimental Physics at the Johns Hopkins University, "Diffraction Gratings for Astrophysical Purposes;" Dr. J. H. Van Vleck, Professor of Physics at Harvard University, "The Molecular Field and the Determination of Very Low Temperatures;" Dr. George D. Birkhoff, Perkins Professor of Mathematics and Dean of the Faculty of Arts and Sciences of Harvard University, "Analytic Deformations," and Dr. W. H. Furry of Harvard University, "New Heavy Particles."

★

Optical Society of America

The twenty-third annual meeting of the Optical Society of America will be held on October 27, 28 and 29 at the General Brock Hotel, Niagara Falls, Canada. In addition to the usual program of papers the meeting will include a

symposium on the "Optics of Illumination," in which it is planned to include invited papers on terminology and standards, basic principles of illumination, widely used light sources and recent developments in light sources; a popular lecture by Robert McMath, director of the McMath-Hulbert Observatory of the University of Michigan, illustrated with astronomical motion pictures, including spectroheliographs of solar prominences; visits to the University of Buffalo, the Spencer Lens Company, the Cyanamid Plant, the Queenstown Power House, the Whirlpool, the Welland Ship Canal and the Locks at Thorold. The meeting will be open to non-members as well as members of the society. Non-members who desire to receive the advance program, final notices or other information in regard to the meeting should address their requests to the secretary not later than October 10.

★

From October 12 to 15, 1938, the 74th Meeting of the Electrochemical Society will be held at Rochester, New York, in the Hotel Seneca. Two main symposia are planned in connection with the fall meeting: *The Metallurgy of Silver*, and *Plastics in the Electrochemical Industry*.

★

Instrumentation Contest

An instrumentation contest with a first prize of $200 in cash is announced by the Industrial Instrument Section of Scientific Apparatus Makers of America. Twelve prizes totaling $500 will be awarded by the Apparatus Makers. The contest is open to any engineer or operating man, not employed by an instrument manufacturer. Each contestant is to write about an *unusual* application of a *standard* instrument or control device, telling briefly what conditions or need impelled the application. By instrument or control device is meant any device used for measurement or control in a plant or laboratory, or any accessory used with a device for measurement and control.

The contest will be judged by the following Jury of Award—*Chairman*, Lyman J. Briggs (Director, National Bureau of Standards); *Members:* M. F. Behar (Editor, *Instruments*), W. E. Forsythe (Physicist, Nela Park Research Dept., General Electric Co.), John J. Grebe (Director of Physical Research Laboratory, Dow Chemical Co.), R. J. S. Pigott (Head of Engineering Dept., Gulf Research and Development Co.) and *ex-officio* Phil T. Sprague (Chairman, Industrial Instrument Section S.A.M.A., and President of the Hays Corp.). The contest closes November 15, 1938, and the judging will be held during the week of December 5, 1938. Copies of the contest rules and official entry form can be obtained from Scientific Apparatus Makers of America, 20 North Wacker Drive, R. 3014, Chicago, Illinois.

★

Necrology

Dr. G. M. Johnstone MacKay, director of research of the American Cyanamid Company at Stamford, Connecticut, died on July 29 at the age of fifty-five years.

★

Guy N. Collins, principal botanist in charge of the Division of Genetics and Biophysics of the Bureau of Plant Industry of the U. S. Department of Agriculture, died on August 14 at the age of sixty-six years.

Contributors to This Issue

Dr. Eugene G. Rochow received his B.Chem. and Ph.D. from Cornell University in 1931 and 1935 respectively. In 1933 he was assistant to Professor Alfred Stock, Kaiser-Wilhelm Institut of Dahlem, during his lectures in this country. He was the recipient of Heckscher Foundation Grants in 1934 and 1935 for investigations in metallo-organic compounds. Since 1935 he has been employed at the Research Laboratory of General Electric Company.

Dr. E. B. Dane, Jr., received his A.B., A.M. and Sc.D. from Harvard in 1927, '28, and '36, respectively. The intervening years were spent mining in California. Since returning to Cambridge, he has been working on mineral veins, the Graton precision microscope, a microcolorimeter, and geophysical problems.

Dr. R. B. Lindsay received his A.B. and M.S. degrees from Brown University in 1920 and the Ph.D. degree from M. I. T. in 1924. In 1922–1923 he was fellow of the American-Scandinavian Foundation in Copenhagen. From 1923–1927 he served as instructor in physics at Yale and from 1927–1930 was assistant professor of physics there. From 1930–1936 he was associate professor of theoretical physics at Brown University and since 1936 has been professor of physics and chairman of the department there.

Dr. H. R. Nelson received the A.B. degree from Amherst College in 1926 and the Ph.D. degree from Cornell University in 1934. He was instructor in physics at Cornell from 1928 to 1934. Since 1934 he has been with the Battelle Memorial Institute where much of his work has been devoted to the application of electron diffraction to metallurgical problems.

Dr. A. M. Skellett holds the A.B. and M.S. degrees from Washington University and the Ph.D. from Princeton. In 1929 he resigned his post as Assistant Professor of Physics at the University of Florida to join the research department of the Bell Telephone Laboratories where he has been since that time.

Dr. Paul Selényi, a Hungarian physicist, received his Ph.D. in 1910 from the University of Budapest, where he was assistant from 1907 to 1919. In 1921 he entered the newly organized Tungsram Research Laboratory of the United Incandescent Lamp and Electrical Company, Ltd., Budapest-Ujpest. He worked on diffraction and total reflection of light; stationary light-waves and wide-angle interferences, electronic phenomena of vacuum lamps, glass-electrolysis, photo-cells and photo-elements, photo-electric photometry, cathode-ray tubes and recently in connection with electrography on picture telegraphy and television.

Dr. W. Shockley received his B.Sc. at the California Institute of Technology in 1932 and his Ph.D. at the Massachusetts Institute of Technology in 1936. Since 1936 he has been with the Bell Telephone Laboratories engaged in research in electronics and alloy physics.

Dr. W. James Lyons is an Instructor at Loyola University, New Orleans. Prior to this appointment he spent two years in an industrial laboratory, specializing in ballistic research. Born in Duluth, Minnesota, in 1904, he holds a Ph.B. from the University of Chicago and Ph.D. from St. Louis University.

Mr. G. R. Patterson was born at Barnesville, Ohio, in 1892. He received his B.S. in E.E. in 1916 and M.S. in 1937 from the University of Pittsburgh. He was chief draftsman at the Pittsburgh Transformer Company, Instructor in Mathematics, Instructor in Electrical Engineering, and since 1930 has been Assistant Professor of Electrical Engineering at Carnegie Institute of Technology, where he is conducting research in magnetic materials.

Picture and biography of Professor W. W. Hansen appeared in the April, 1937, issue of the *Journal of Applied Physics* on p. 273.

P. Selényi

W. J. Lyons

G. R. Patterson

R. B. Lindsay

H. R. Nelson

A. M. Skellett

W. Shockley

Contributed Original Research

The Time Lag in Gas-Filled Photoelectric Cells

A. M. Skellett
Bell Telephone Laboratories, Inc., New York, N. Y.
(Received May 14, 1938)

Time lag measurements are described which were made with a light chopper on a gas-filled cell of special design. The resulting response *vs.* frequency characteristic exhibits the resonance oscillations predicted from theory and calculation of the lag from the positive ion mobility agrees with that determined from this curve. The construction of the cell is such that secondary emission and disintegration of the cathode by ion bombardment are eliminated even at high values of gas amplification.

Introduction

THE mechanism which causes the current through a gas-filled photoelectric cell to lag behind the illumination has been the subject of a number of investigations but its nature has not been definitely established. In one method of studying this phenomenon, the intensity of the light falling on the cell is made to vary sinusoidally at various frequencies and the alternating component of the current through the cell is measured. If an appreciable portion of the current were subject to a process for which the time interval is fairly constant, maxima and minima should be observed at frequencies for which the periods equal integral multiples and half-integral multiples of this time interval, respectively. For example, if the process is one in which the time delay is caused by the transits of carriers to the electrodes, then a maximum would be observed when these carriers reached the electrodes in phase with the primary current and a minimum when it was 180° out of phase. Such maxima and minima have been predicted from theoretical considerations,[1, 2] but none of the experimental curves has shown them. They were obtained in the investigation described herein.

The Photoelectric Cell

In this investigation a photoelectric cell was used which had certain features particularly

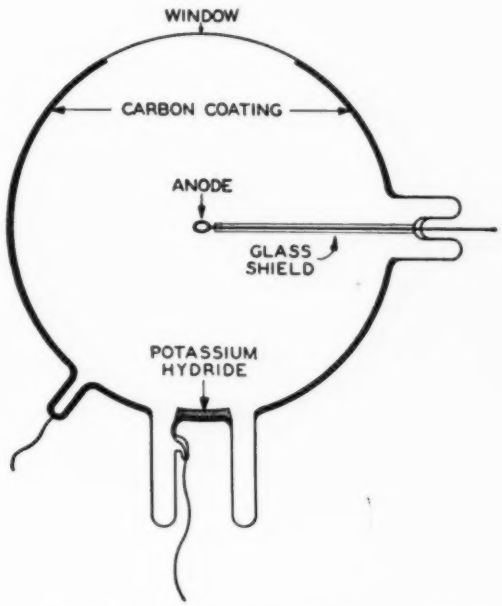

Fig. 1. Section through the photoelectric cell.

[1] Ollendorf, Zeits. f. Physik **13**, 606 (1932).
[2] Kvartskhava and Timofeev, Tech. Phys. U.S.S.R. Part 4 (1935).

suitable for maintaining the constancy of the inertia phenomena. In the first place, the cell was spherical in shape with the anode at the center and practically the whole inside surface served as a cathode so that the electric field was fairly symmetrical throughout. As will be shown later, ionizing collisions involving the photoelectrons will be more numerous near the anode end of their path so that the products of such collisions will travel over nearly equal paths no matter what the direction may be in which they start out.

Figure 1 shows a section through the cell. The photosensitive surface (about $\frac{1}{2}''$ in diameter) forms a very small part of the cathode surface so that very few of the products of the primary collisions would reach it. This isolation of the photosensitive cathode is further enhanced by making it $1\frac{1}{2}$ volts positive with respect to the rest of the cathode or "collector."

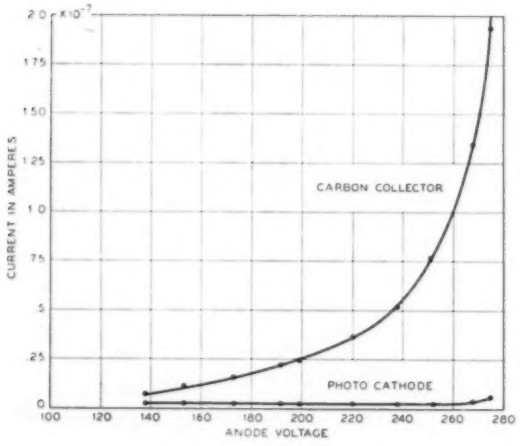

FIG. 2. Voltage-current characteristics of the photoelectric cathode and the collector.

The photosensitive surface was potassium hydride and the collector was a film of Aquadag. The cell was constructed in this special form for other reasons, and from the discussion which follows it is evident that as far as the time lag characteristics are concerned, this particular construction was not important. The cell was filled with argon at a pressure of 0.2 mm of Hg. The radius of the bulb and of the cathode was 6.3 cm and the anode was in the form of a ring of flat wire 1.65 mm wide and 6.3 mm in diameter.

How well this design separates the primary photoelectric current from the currents due to the gas amplification may be seen from the curves of Fig. 2. These are voltage-current characteristics of the currents to the photo-cathode and to the collector. The current to the photo-cathode has the characteristic of a vacuum photo-cell whereas the collector current has the characteristic of a gas-filled cell.

TIME LAG MEASUREMENTS

The response *vs.* frequency measurements were made with a light chopper built on the principle of the ultracentrifuge. On the face of the rotating member a circle of white disks on a black background reflected light through an optical system which focused an image of this pattern on a series of straight-edged openings. The resultant modulation of the light intensity was approximately sinusoidal.

Curve No. 1 of Fig. 3 shows the response *vs.*

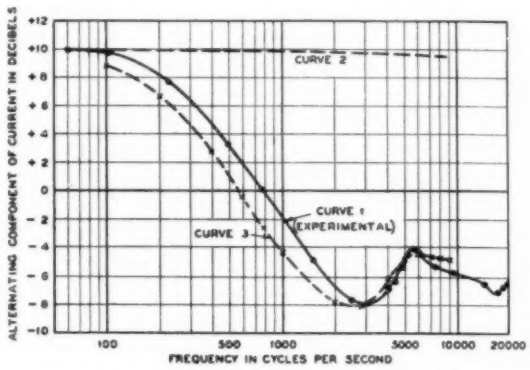

FIG. 3. Experimental and theoretical response *vs.* frequency characteristics.

frequency curve of the cell at an anode voltage of 232 volts. The first maximum falls at approximately twice the frequency of the first minimum as would be expected if a constant time interval is involved in the lag. The value of the time lag on this basis is 1.72×10^{-4} second which is the reciprocal of the frequency of the first maximum.

CALCULATION OF THE TRANSIT TIME

Within the scope of these measurements, effects due to the transit time of the electrons and to space charge are negligible.

Accordingly, the first determination should be

that of the transit time of the positive ions in the cell. For this we need to know their velocities in the various regions of the cell and hence the potential distribution in it. It may be shown from electrostatic theory that the field, E, in volts per centimeter is given by

$$E=\frac{V}{r^2(1/R_1-1/R_2)}, \tag{1}$$

where V is the voltage across the cell, r the distance measured radially from the center of the sphere, R_1 the radius of the inner sphere (anode) and R_2 the radius of the outer sphere (cathode). The velocity of an ion is

$$v=\mu E, \tag{2}$$

where μ is the mobility. The distance traveled, dr, in a time dt may be expressed by

$$dr=vdt \tag{3}$$

so that

$$dt=\frac{(1/R_1-1/R_2)r^2}{V\mu}dr,$$

from which we may obtain the transit time T taken by an ion in traveling from the vicinity of the anode to the cathode.

$$T=\int_{r=R_1}^{r=R_2}\frac{(1/R_1-1/R_2)r^2}{V\mu}dr$$

$$=\frac{(1/R_1-1/R_2)(R_2^3-R_1^3)}{3V\mu}. \tag{4}$$

The value of μ, for argon,[3] at the pressure used is 6.3×10^3. If the assumption is made that the anode ring approximates a sphere of the same diameter, $R_1=0.315$ cm. Putting these values in (4) the transit time is

$$T=1.71\times10^{-4} \text{ second}$$

in agreement with the value of 1.72×10^{-4} second obtained from the frequency characteristic of Fig. 3.

The exactness of this agreement is probably not of as much significance as the fact that such exact agreement may be obtained with the data available and the reasonable assumption that was made concerning the value of R_1 the radius of the equivalent sphere at the anode. However, R_1 can scarcely be greatly different from the value assumed and small variations of R_1 from this value will not change the order of magnitude of T.

To justify the assumption that all the ions are formed near the anode, the potential distribution in the cell must be known. This may be obtained by integration of Eq. (1) with respect to r.

$$P=\int\frac{Vdr}{(1/R_1-1/R_2)r^2}, \tag{5}$$

where P is the potential in volts. The potential distribution thus calculated is given in Table I.

TABLE I.

$r(cm)$	$P(volts)$
6.3	0
5	3.2
4	7.0
3	13.4
2	26.2
1	64.7
0.5	141.5
0.315	232.0

The bunching of the field at the anode is apparent. If the integration of Eq. (4) were carried from $r=2$ cm instead of $r=R_1$ the value of T would be altered by less than 2 percent, and there can be no ionization whatever until the electrons have crossed more than half the distance to the anode.

Thus the assumptions are valid and the agreement between the observed and calculated values of T must be real. The time lag in this cell must have been due for the most part to the transit time of positive ions across it.

Discussion of Mechanism of Current Flow

The flow of current in the external circuit due to the transportation of charges by the ions has been investigated by W. Shockley.[4] His results as applied to this structure show that the greater part of the current, resulting from the transit of an ion, flows when the ion is in the vicinity of the

[3] *International Critical Tables*, Vol. 6, p. 111.

[4] Shockley, companion paper in this issue.

anode and is moving swiftly. When it reaches the collector or cathode this current drops to zero. Thus the current due to the ions does not lag appreciably behind that which is due to the electrons that produced them and if no new electrons were released by the ions on their arrival at the collector the response of the cell would be that shown by curve No. 2 of Fig. 3.

Since the experimental curve so definitely shows a time lag that is equal to the transit time of the ions, the conclusion that the ions do release new electrons when they reach this electrode seems inescapable.[5] Granting this, the current due to an instantaneous flash of light will flow in a series of pulses of decreasing amplitude following one another at intervals equal to the transit time of the ions. The transit times of individual ions will vary considerably from the average and as a consequence these pulses will not be sharp but will be spread over appreciable periods of time.

An expression for the total response of the cell has been worked out by W. Shockley on the following assumptions: The charge carried by each pulse is ρ times that of the previous pulse; the instantaneous value of current of each pulse (except the pulse initiated by the flash of light) is proportional to the rate of arrival at the cathode of the ions of the previous pulse; the probability that an ion generated at $t=0$ will arrive at the cathode between t and $t+dt$ is given by the error function distribution

$$\tfrac{1}{2}(\pi)^{\frac{1}{2}}T\exp-\frac{(T-t)^2}{4x^2T^2}dt.$$

In this, T is the average time of transit of an ion and $\sqrt{2}\times T$ is the root mean square deviation of this time. Thus the response due to the instantaneous flash of light consists of a series of weaker and weaker pulses spread over wider and wider times. The response due to unit photoelectric current of frequency ω, i.e., $\exp i\omega t$, is represented by

$$J(t)=k\exp(i\omega t)[1+\rho\exp(-i\theta-x^2\theta^2)+(\rho\exp(-i\theta-x^2\theta^2))^2+\cdots]$$
$$=k\exp(i\omega t)/(1-\rho\exp(-i\theta-\theta^2x^2)),$$

where k is the amplification factor due solely to ionizing collisions in the gas.

This function has been fitted to the experimental curve at the points where $\theta=0$, π, and 2π. The resulting curve[6] is shown as No. 3 on Fig. 3. The values for the disposable parameters necessary for this fit were

$$\rho=0.8165,$$
$$x=0.24.$$

That is, the second pulse will have an amplitude 0.8165 times that of the first and will be "spread" over a time equal to $0.24T$.

The amplification at the voltage used (232 volts) was 16 times, so that the sum of the series of pulses must have been equal to 16 times the photoelectric emission. Thus

$$k(1+\rho+\rho^2+\rho^3+\cdots)=16.$$

Putting in the value of ρ found above

$$k=2.94.$$

This means that for each electron starting from the cathode, 2.94 electrons will arrive at the anode. This is a reasonable value since the field strengths near the anode run up to hundreds of volts per cm.

Concluding Discussion

There appears to be no evidence here that (1) there are two kinds of lag operative at low and high frequencies,[7] (2) that metastable atoms play an appreciable part in the time lag process,[8] (3) that the low frequency lag is very complex in nature,[7] and (4) that thermal changes in the cathode,[9] aggregations of positive ions close to it,[10] or ionization by positive ions,[11] are responsible for the lag. Ionization by positive ions may, of course, occur in this cell.

[5] It is of interest to point out that in this case electrons are apparently being liberated by bombarding ions with only a few electron volts of energy.

[6] Several computations were made resulting in curves which fitted the experimental one better in certain regions (notably at low frequencies) than curve No. 3. At the higher frequencies, however, the agreement was not as good.

[7] Campbell, Noble and Stoodley, Proc. Phys. Soc. **48**, 589 (1936).

[8] Schroeter and Lubszynski, Physik Zeits. **31**, 897 (1930).

[9] Kingdon and Thompson, Physics **1**, 343 (1931).

[10] E. L. E. Weatcroft, Phil. Mag. **7**, 162 (1931).

[11] Fourmarier, Comptes Rendus **194**, 86 (1932).

Previous investigators who have concluded that the transit time of positive ions in their cells was too short to account for the lags they observed, have generally neglected to calculate the potential distribution in the cell. Without this knowledge such a conclusion is questionable.

ACKNOWLEDGMENT

I wish to express my appreciation to Dr. J. B. Johnson for his valuable criticism in the preparation of this paper and to Mr. M. W. Baldwin, who made the response *vs.* frequency measurements, for his cooperation.

Currents to Conductors Induced by a Moving Point Charge

W. SHOCKLEY
Bell Telephone Laboratories, Inc., New York, N. Y.
(Received May 14, 1938)

General expressions are derived for the currents which flow in the external circuit connecting a system of conductors when a point charge is moving among the conductors. The results are applied to obtain explicit expressions for several cases of practical interest.

IN the earlier days of vacuum tube technique when the radiofrequencies in use were relatively low compared to those attained at present, it was acceptable to regard the transit of an electron across a vacuum tube as an instantaneous burst of current. At present, however, the time of transit of the electron is of comparable duration with the periods of alternating circuits and it is consequently of interest to know the instantaneous value of the current induced by the moving charge over its entire time of transit.

Before discussing what effect the moving charge has, we must introduce certain conventions as to what part of the total field is to be attributed to the charge and what part to other causes. It proves most convenient to consider that all of the conductors are grounded and to examine the currents to them through the external circuit due to the motion of the charge. If the voltages on the conductors are varying, however, charges will be induced and currents will flow as dictated by the coefficients of capacity. In keeping with the superposition principle,[1] the net current is found by adding the currents induced by the moving charge (or each moving charge if there are several) and the currents due to changing voltages.

[1] Jeans, *Mathematical Theory of Electricity and Magnetism*, fourth edition, p. 90.

We are thus led to consider the charges and currents induced on a system of grounded stationary conductors by the motion of a point charge. If we have a system of grounded conductors, perhaps as illustrated in Fig. 1, num-

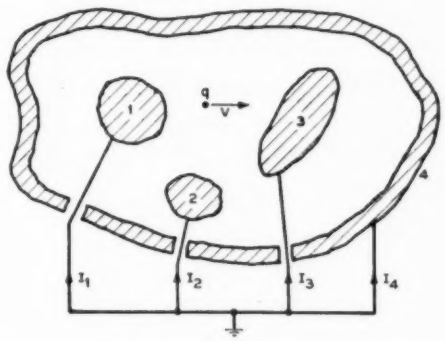

FIG. 1. Schematic representation of conductors and currents.

bered 1, 2, $\cdots$ n, say, then the charge q_1 induced on conductor 1 due to a unit point charge in the space is calculated as follows: Let conductor 1 be at unit potential and the others be grounded and let the space between the conductors be free of charge. The electrostatic potential produced by this situation has the value $V_1(r)$ at the arbitrary point r of space. Then, in terms of this potential distribution, the charge, q_1, induced on 1 by a unit charge at r is

$$q_1 = -V_1(r). \tag{1}$$

Proof: Let us imagine that a vanishingly small conductor is placed at r; let it be number 0 and the other conductors be numbers 1 to n.

Situation 1. Let conductor 0 be uncharged, conductor 1 be at unit potential, $2 \cdots n$ be at zero potential. The charges Q_i' and potentials V_i' accordingly satisfy the equations: $V_0' = V_1(r)$, $V_1' = 1$, $V_2' = \cdots = V_n' = 0$; $Q_0' = 0$. *Situation 2.* Let conductor 0 possess unit charge. Let all other conductors be grounded and denote the charge on 1 by q_1. Then $Q_0'' = 1$, $Q_1'' = q_1$, $V_1 = \cdots = V_n = 0$. According to Green's reciprocation theorem:[2]

$$0 = \Sigma_i (V_i' Q_i'' - V_i'' Q_i') = V_1(r) + q_1$$

and this is Eq. (1).

If the point charge moves with a vector velocity $v = dr/dt$, we find for I_1, the current which flows to conductor 1 through the external circuit,

$$I_1 = dq_1/dt = -\nabla V_1(r) \cdot dr/dt = E_1(r) \cdot v, \quad (2)$$

where $E_1(r)$ is the electric field at point r due to unit potential on 1 with $2 \cdots n$ grounded. By the same argument we find that the current to the ith conductor is

$$I_i = E_i(r) \cdot v. \quad (3)$$

(As was pointed out above, the current just calculated, although it is expressed in terms of fields produced by potentials on the electrodes, is that induced by the motion of the charge and does not include currents produced by changing potentials upon the conductors.) Since we have used a theorem of electrostatics in our theory, the results will not be valid if retardation effects are important within the volume throughout which the charges move; they will be valid, however, if these effects are small, even for large transit angles of the moving charges.

[2] Reference 1, p. 92.

Applications

Infinite plane parallel plates

If conductors 1 and 2 are perpendicular to the X axis and have intercepts $x = 0$ and $x = d$, respectively, then $E_1 = 1/d$ and $E_2 = -1/d$; and for a velocity $v = dx/dt$, we get the data of Table I.

TABLE I. *Currents induced by unit point charge moving with velocity v.*

	I_1	I_2	I_3
Parallel Planes	v/d	$-v/d$	—
Coaxial Cylinders	$v/r \ln b/a$	$-v/r \ln (b/a)$	—
Concentric Spheres	$\frac{vab}{(b-a)r^2}$	$-\frac{vab}{(b-a)r^2}$	—
Cylindrical Triode $a<r<b$	$\frac{v}{r \ln b/a}$	$\frac{-\mu v}{(1+\mu) r \ln (b/a)}$	$\frac{-v}{(1+\mu) r \ln (b/a)}$
$b<r<c$	0	$\frac{\mu v}{(1+\mu) r \ln c/b}$	$\frac{-\mu v}{(1+\mu) r \ln (c/b)}$

Coaxial cylinders and concentric spheres

For these we let 1, the inner conductor, have radius a and 2 have radius b and let $v = dr/dt$.

Cylindrical triode

Let the three electrodes in order of increasing radii be 1, cathode, radius a; 2 grid b; 3 anode c. Denoting the amplification factor by μ and assuming that $\mu \gg 1$, the average potentials at the grid due to unit potential on 1, 2, and 3, respectively, are $V_1(b) = 0$, $V_2(b) = \mu/(1+\mu)$, $V_3(b) = 1/(1+\mu)$.[3] Letting $v = dr/dt$, we get the remaining data of Table I.

[3] For a more accurate treatment suitable for small amplification factors see Dow, *Fundamentals of Engineering Electronics*, p. 49.

On the Electrographic Recording of Fast Electrical Phenomena*

P. SELÉNYI
Tungsram Research Laboratory, Ujpest, near Budapest, Hungary
(Received May 10, 1938)

ALMOST in all branches of science and technique one needs and one applies methods for recording, i.e., for conserving in a permanent and visible form the courses of variable phenomena. The most simple form of recording is a *mechanical* one: the seismical motion of the earth is recorded in a seismograph with a fine point on sooted paper; registering voltmeters draw the fluctuations of the supplied voltage with ink on a uniformly moving paper-ribbon, etc. Fast phenomena, such as the vibration of an oscillograph mirror or the motion of the cathode-ray spot on the fluorescent screen of a Braun tube, are recorded mostly photographically. In the picture and facsimile telegraphy one uses the *chemical* action of the electrical current for reproducing the transmitted signals, and the magnetic sound recorders utilize the *magnetic* action of the current for the production of a record which is, of course, permanent but not visible.

Some years ago I invented an entirely new method of recording which comprises the conservation of electrical signals in form of an *invisible electrical picture* on the surface of an insulating sheet by means of the *electrostatic charges* transported in vacuum by the cathode rays or by those of an ion beam moving in the free atmospheric air and developing the latent image by dusting over with a fine, electrically charged powder, such as minium, talcum, lycopodium powder, etc. Whilst the first and more complicated method—utilizing the cathode or Lenard rays—has not been developed beyond the experimental stage, the second more simple method has reached in a short time a high standard, and I succeeded already in 1935 in applying this method to picture and facsimile telegraphy.[1] Apart from these and other practical applications this method of recording (named by us "Electrography") may be, I think, a valuable tool in many branches of science and technique because of its unique advantages over other existing methods of recording.[2]

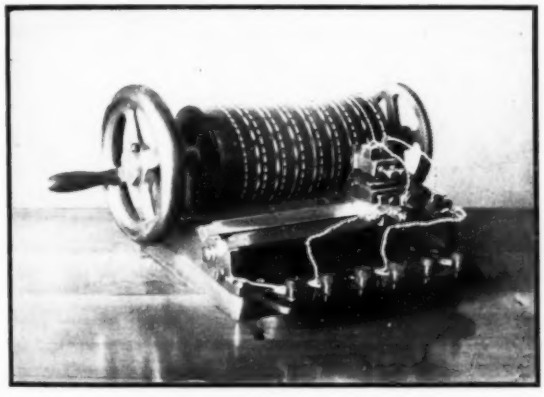

FIG. 1. Electrographic oscillograph with two recording systems (first model).

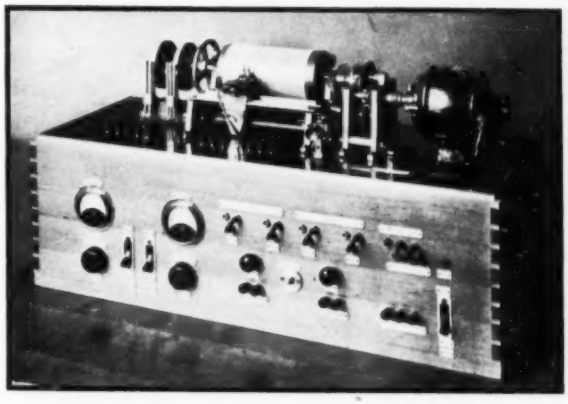

FIG. 2. A more perfect model of the electrographic oscillograph.

Figure 1 shows a simple hand-driven form of such an electrographic recording apparatus ("electrographic oscillograph"), Fig. 2 a motor-

* The electrographic method of recording discussed in our paper should not be confused with the "Electrographic Effect" observed by Elizabeth Schickele and Percy H. Carr, J. App. Phys. **8**, 558 (1937).

[1] See Elektrotechn. Zeits. **56**, 961 (1935) and Wireless Eng. **15**, 303 (1938).

[2] For more detailed accounts see Zeits. f. tech. Physik **16**, 607 (1935), and **17**, 477 (1936).

driven model with many improvements (timing-device, etc.) whilst Fig. 3 which we will use for

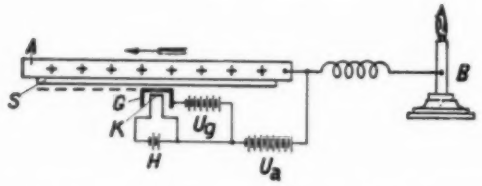

FIG. 3. Diagrammatic arrangement of the electrographic recording system.

explaining the principle of electrography shows diagrammatically the essential parts of the devices. On Fig. 3 K is a hot cathode, e.g., a platinum wire of 0.1–0.2 mm diameter, coated with barium oxide and energized by the battery H, G a control electrode (grid) consisting of a metal cap with a small circular or linear opening and A is a metal plate (anode) covered on its frontal surface with a thin sheet S of insulating material. The distances cathode-grid and grid-sheet must be as small as possible about $\frac{1}{2}$–1 mm. The whole arrangement operates in the following manner. Electrons emerge from the hot cathode, attach themselves to the gas molecules and are driven by the anode voltage Ua of 500 to 1000 volts through the opening in G and are finally deposited on S forming a negatively charged spot on the latter. The anode may be moved with the sheet in the direction of the arrow and the ion beam then traces an invisible electric line on the sheet, which is capable of development similar to the well-known Lichtenberg-figures, i.e., by dusting over with a positively charged fine powder, e.g., with lycopodium powder

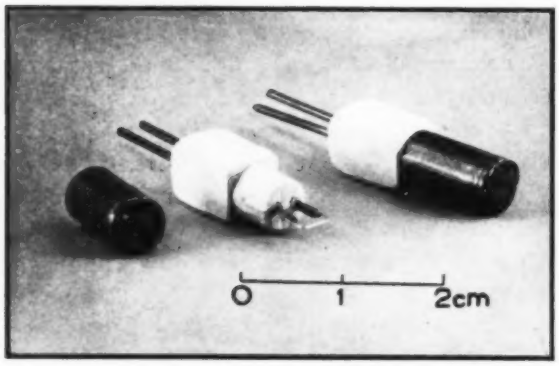

FIG. 4. The "ion gun" of the electrographic recording system.

sprayed out from a container with a current of air. The most remarkable property of this "ion gun" is that the intensity of the beam and hence that of the electric line can be controlled by the grid-potential Ug, a 100 percent modulation being effected with 5–10 volts. If the record is not to be preserved, the powder particles constituting the visible record may be blown away from the insulator sheet with a strong blast of air and its electrical charges neutralized with the Bunsen flame B: the sheet is ready for a new record.

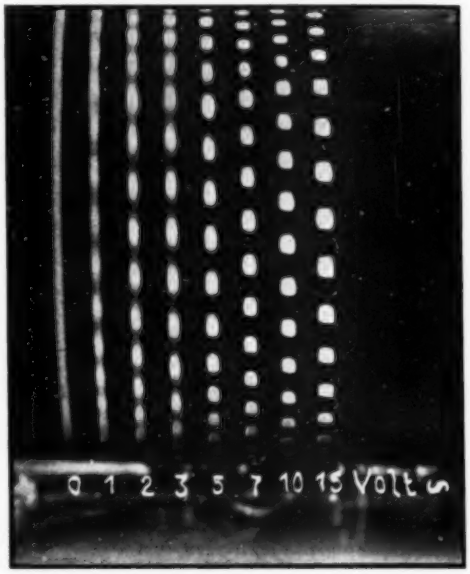

FIG. 5. Records of an alternating current, 50 cycles per second; 1···15 volts.

Arrangement and function of the whole system is comparable with that of a Braun tube, operated in the air instead of in vacuum. But there are many other differences also. Our ion beam is very short (about two millimeters only) whilst the cathode rays in a Braun tube are 30–50 cm long, consequently the ion beam is to be influenced only in respect to its intensity and not in respect to its direction. In a cathode-ray tube we utilized the *energy* of the electrons for exciting the fluorescent screen; in our recording system we utilize the *charge* of the ions to produce the invisible electrical record. In this respect electrography is comparable with photography: first an invisible latent image is produced and this is then made visible by developing. But the

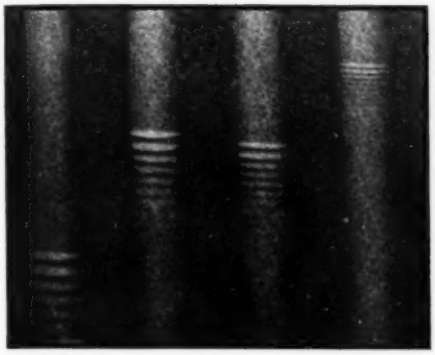

FIG. 6. Records of damped electrical oscillations, magnified 2½ times.

development of the photographic latent image needs many operations while the development of electrographic record is effected instantly by dusting it over. Another advantage of very great importance is the simplicity of the whole arrangement, the absence of any inertia of the recording and the cheapness of the consumed material (paper coated with paraffin, shellac, insulating varnish, etc., or films of artificial plastics).

Figure 4 is a photograph of the ion gun. A U-shaped platinum wire is sealed on two nickel electrodes fixed in a ceramic die; the slotted metal cap, forming the control electrode fits the cylindrical part of the ceramic die. In the devices on Fig. 1 and Fig. 2 the metallic drum forms the anode whilst the ion guns—having

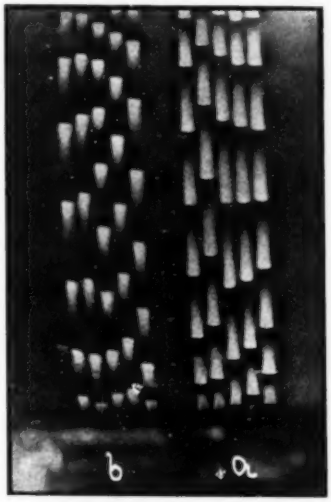

FIG. 7. Voltage (b) and current (a) of a saw toothed electric oscillation.

their slit horizontally—fit the carriage which moves parallel to the axis of the drum. Subsequently if we turn the drum the records are produced on the sheet covering the drum, in the form of spirals. If we disconnect the coupling between the drum and the carriage, the latter remains unmoved and the records are produced continuously on the same circumference of the drum. The device on Fig. 2 is also provided with a momentary coupling: the drum starts, makes one revolution and stops. In the same moment as the drum starts an electric contact starts the occurrence to be recorded.

For making a record the control electrode must be biased with a positive voltage. For example the record marked 0 on Fig. 5 was produced with

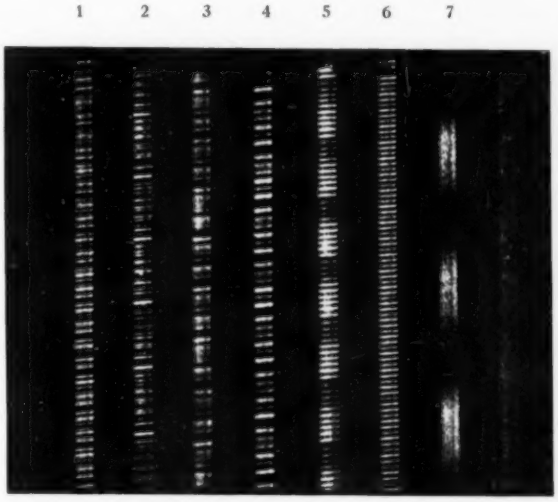

FIG. 8. Sound records of the vowels (as pronounced in the Hungarian language). 1, vowel *i*, 2, vowel *e*, 3, vowel *u*, 4, vowel *o*, 5, vowel *a*, 6, tone of a normal "*a*" pipe, 7, alternating current of 50 cycles per second.

a biasing of +10 volts; the record is under this condition uniform in width and in intensity. The other records on Fig. 5 are produced by superposing an alternating voltage of 50 cycles per second and of 1, 2, 3, 5, 7, 10 and 15 volts on the biasing. The records are—as visible—substantially records of variable intensity; the record of 3 volts has nearly 100 percent modulation and the other records are already overmodulated.

The records on Figs. 6–8 demonstrate the use of our apparatus in manifold applications. It will be especially useful as a time measuring device.

I mention for example the examination of fuse wires under variable overload, carried out by us last year.[3] A record from this investigation is reproduced on Fig. 9. Similar examples are: the

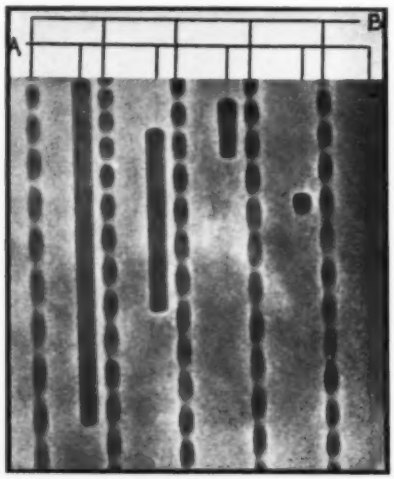

FIG. 9. A, Records of the burn-out of a 0.1 mm nickel wire with increasing current intensity. B, Records of the 50 cycles per second alternating current which serve as time marks.

measuring of the velocity of projectiles or that of the artificial seismic waves in practical geology, etc. Our method is especially useful for the recording of unexpected phenomena such as surge voltages or other disturbances in high voltage distribution systems, etc. By biasing the control electrode negatively corresponding to the cut-off potential of the characteristic, the ion-beam will be suppressed and one can let the drum rotate for any length of time without tracing a record thereon. Thus the recording system will work only at the moment that the unexpected phenomenon occurs and impart to the grid a positive potential.

A similar example of more scientific interest is the recording of radioactive or cosmic rays with the aid of the Geiger counter and amplifier as shown in Fig. 10. These researches are executed mostly with mechanical counting devices, but these have strong limitations in respect to the speed of counting and consequently in resolving power. In Fig. 10 we recorded some hundred kicks per second produced by a weak radio-active preparation, but we could have recorded some thousand per second (see Fig. 11) and the resolving power of our devices seems to reach 1/100,000 sec. or less. This point will be discussed in more detail.

The control by the grid voltage has no inertia, therefore the resolving power depends only upon the following factors: on the fineness of the powder used for developing, on the speed of recording and on the quantity of the static charges delivered by the ion gun. The records on Fig. 11 were produced at a speed of recording of one meter per second and are developed with asphalt powder which is finer than lycopodium powder, but not of homogeneous size. The record of the 6000 per/sec. current contains therefore 6 lines/mm; by using the finest powders (such as talcum, minium, etc.) and recording sheets which have a smoother surface than that of paraffinated paper,[4] we were able to record 10 lines/mm. By increasing the speed of rotation of the recording drum the resolving power will increase in the same proportion. But apart from the mechanical limitation which might be reached at a speed of 100 to 120 meter per second there arises another limitation. In view of the small mobility of the negative ions at atmospheric pressure the intensity of the ion-beam is very small (order of

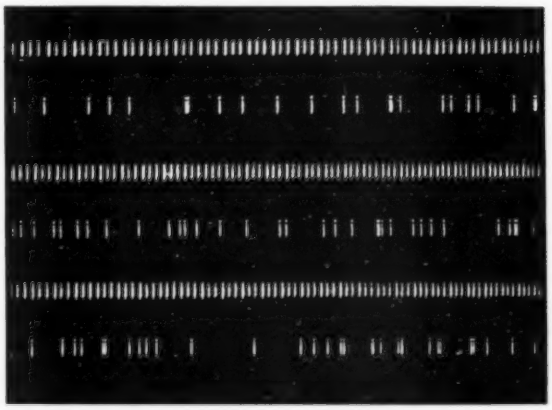

FIG. 10. Records of a Geiger counter; time marks, alternating current of 1300 cycles per second.

[3] See Elektrotechnik u. Maschinenbau (Vienna) **55**, 122 (1937).

[4] Ordinary commercial paraffinated paper cannot be used because the paraffin coating is too thin. We prepare the paper in a simple manner by pulling it through molten paraffin. The surface of such a coating is not completely smooth, under a magnifying glass it exhibits hills and after some days it is finely crystallined.

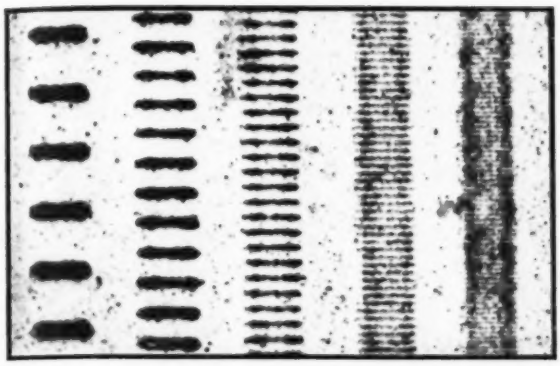

FIG. 11. Records of alternating currents of 500, 1000, 2000, 4000 and 6000 cycles per second; magnified 4.7 times.

magnitude 10^{-7}A) and though the quantity of electricity, which is necessary to charge the recording surface is also small (less than 1/100 micro-coulomb per square decimeter), at very great speeds of recording the charges delivered by the ion gun will not suffice for the production of a record, which is capable of development. The fact that we succeeded without difficulty in recording an alternating current of 20,000 per/sec. at a speed of 10 m/sec. (a higher frequency in the range of 100,000 per/sec. was not at our disposal) proves that this limit lies at still higher speeds and the resolving power may reach the value of 1/100,000 sec. Operating our devices in vacuum instead of in atmospheric air it may even be possible to arrive at a resolving power of one-millionth second.

Plastic Deformation of Lead, Copper and Aluminum Under Static Compression

W. JAMES LYONS
Department of Physics, Loyola University, New Orleans, Louisiana
(Received June 1, 1938)

Creep in metals under constant load indicates that plastic deformation depends on the duration as well as the magnitude of the compressive force. The dependence of deformation on duration is significant in the lead crushers used in measuring pressures. Static compression tests on lead, extending over 30-minute periods, and under various loads up to 109 kg have been conducted. The dependence of deformation on duration is found to be great under the higher loads, and much greater than the dependence in the case of copper and aluminum, on which comparative tests were made. The deformation-compression-time relation is found to be approximately linear under constant pressure. The present data are in agreement with the results of Bogomolov and Kunin on lead for pressures in a higher range. However, the law derived by them does not hold in the pressure-range of the present tests.

INTRODUCTION

THE phenomenon of "creep" in metals in general, and in lead, copper and aluminum in particular, is well known. It has long been recognized that this effect in lead is very pronounced. Not only does lead have a low modulus of plasticity and yield point, but it has also a high rate of deformation under moderate static loads. This latter point has significance in the use of cylinders of ductile metal for the measurement of forces and pressures by compression of the cylinders. Lead and copper are so employed in interior-ballistics research. With a high velocity of deformation, the remaining length of the "crusher" cylinder becomes a function not of the magnitude of the compressive force alone, as current practice implicitly assumes, but also to an appreciable extent, of the duration of that force. Evidently, as was pointed out by Schwinning[1] with reference to copper cylinders, tests conducted under various periods of compression

[1] Schwinning, Zeits. f. das ges. Shiess.-und Springwesen, 5 (1932).

can yield no reliable, or even comparable measures of pressure.

The present investigation was undertaken to obtain accurate numerical data on the rate of deformation of lead cylinders under various static loads. In comparison, tests have been made on copper and aluminum cylinders also. The duration of the compressive forces in the present tests has been on the order of minutes, no observations for intervals within the range of momentary impact (dynamic compression) having been made.

Apparatus and Method

The cylindrical test pieces were compressed between the polished, flat surfaces of a steel piston and anvil, as shown in Fig. 1. Both piston

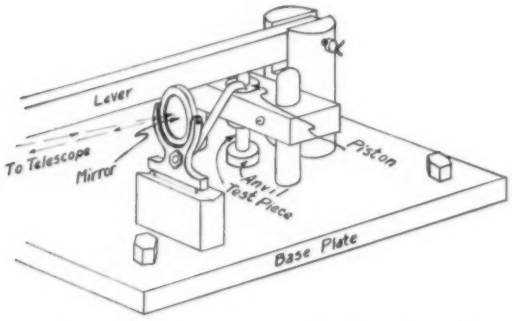

Fig. 1. Detail of compressing mechanism, with mirror of optical lever.

and anvil are 1.90 cm in diameter. The latter, turned from tool steel, rests on a steel plate, 1.3 cm thick, which in turn is securely bolted to a heavy lathe bed. The piston fits and travels in a hole in a stationary cross arm. On the upper surface of the piston, concentric and of one piece with it, is a stud, rounded on top, through which the compressive force is communicated to the piston.

Compression is achieved by means of a lever resting on this stud. The fulcrum, 8.94 cm from the stud, is a pin in a steel upright. At the other end of the bar slotted weights of known mass are hung. The T.M.A. of the system was found from linear measurements to be 22.0.

A feature of the apparatus is the provision for making a continuous observation of the progressive deformation of a single test cylinder. At any instant the deformation may be measured without interrupting, or affecting in any way, the compressive force. This is accomplished by employing an optical lever to indicate the amount of deformation. The third leg of the tilting mirror rests on the compressing piston beside the stud. The moment arm of the mirror is 7.47 cm, while the mirror-to-scale distance was found to be 293.7 cm. The reflected image of the scale was read by telescope. Both telescope and scale are mounted on a stand rigidly fixed to the lathe bed, the complete outfit being set up on a concrete basement floor. In preliminary tests of the stability of the apparatus, one extending up to 120 hours, the extreme displacement of the cross hair on the scale was found to be 0.06 cm. This is less than the least directly-readable division on the scale (1 mm), and equivalent to an apparent displacement at the piston of 7.6×10^{-4} cm. This figure is completely masked by the nonuniformity of the cylinders.

A direct calibration of the optical lever was made by alternately placing between the piston and anvil (with lever raised) two cylinders of different lengths, accurately known, and observing the displacements on the scale. The magnification thus determined was found to differ by one percent from that computed from linear measurements. The average of the two magnifications, 79.0, was used in calculating deformations. With this arrangement it is possible to read directly displacements as small as 1.3×10^{-5} cm at the piston.

The length of each test cylinder was measured with micrometer calipers before and after compression, for a continual check on the calibration of the optical lever. Uniform close contact between the surfaces of piston, cylinder and anvil was assured by viewing and adjusting them against a strong light. Precautions were taken to keep all surfaces free of oils and greases. Every test cylinder was rinsed in ethyl alcohol before being placed on the anvil. Previous workers[2] have shown that lubrication of the contact surfaces significantly affects the compression. That variable was avoided here.

Five individual cylinders were tested at each load. Each curve of Fig. 2 and 4 is, therefore, the average of five curves, each for a single cylinder.

[2] A. Nadai, *Plasticity* (McGraw-Hill, 1931), p. 121.

The points defining the curves are the means of five readings taken at corresponding times after application of the load. Initial readings were taken 5 to 10 sec. after application, and later readings as indicated.

All tests were conducted at room temperature.

Test Specimens

The lead and copper cylinders tested were produced under the specifications of the Sporting Arms and Ammunition Manufacturers' Institute, and were kindly supplied to the writer by Dr. R. L. Womer of the Western Cartridge Company. In accordance with these specifications the lead crushers contain at least 99.7 percent of the pure metal. Of the remaining components not more than 0.2 percent is tin. After being cast, the crushers are swaged to their final cylindrical form. From a series of measurements the mean length was found to be 1.270 cm and the mean diameter 0.826 cm.

The copper specimens are of electrolytic copper, 99.9 percent pure. They are cut from hard-drawn rods, and after annealing at around 540°C, are accurately trimmed to their final dimensions. Copper cylinders of two sizes were tested in the present work, one having a length of 1.270 cm, the other a length of 1.016 cm. Results with the two sizes were in good agreement.

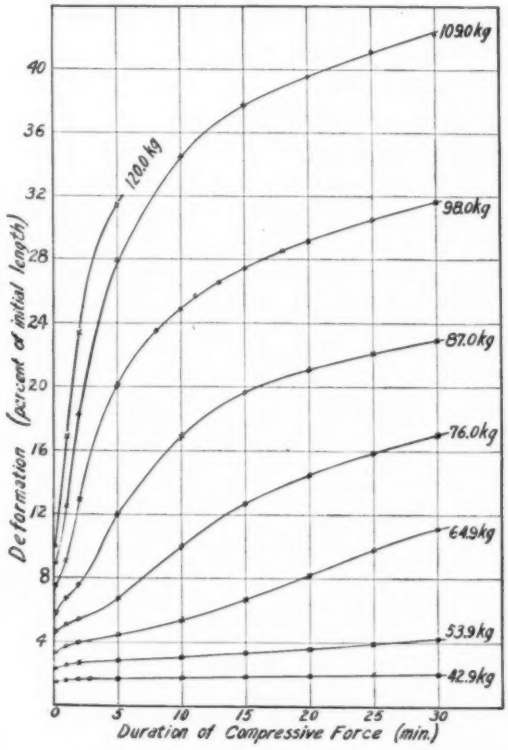

Fig. 2. Deformation of lead cylinders as a function of the duration of various compressive forces.

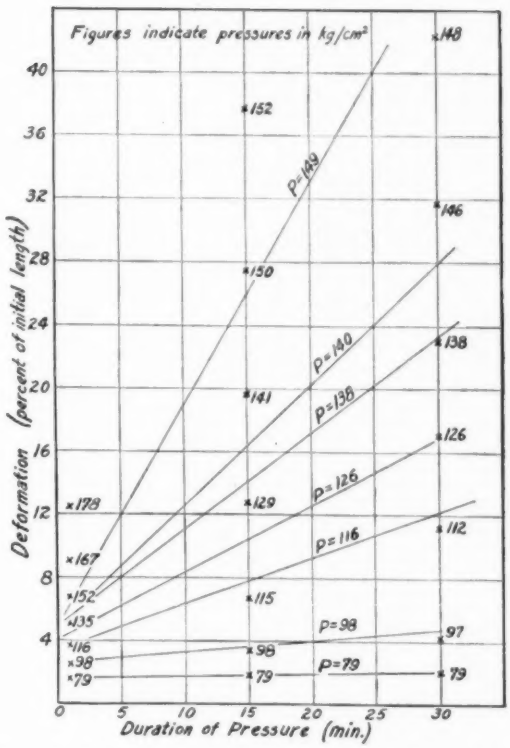

Fig. 3. Approximate curves developed from those of Fig. 2 showing deformation of lead for various constant pressures.

The aluminum cylinders were cut from a rod of commercially pure metal, having a guaranteed minimum aluminum content of 99 percent, and probable content of 99.72 percent. The rod was cold-drawn and unannealed; it was of 0.474 cm diameter.

Discussion of Results

The results of thirty-minute tests on lead for seven different loads are shown in Fig. 2. The compressive forces on the cylinders rather than the equivalent pressures are given, because the latter, of course, did not remain constant during the compression. The pressure at any stage under constant load, can be computed from the expression

$$s=(1-e)s_0, \qquad (1)$$

where s is opposing stress after unit length of the cylinder has been compressed an amount e, and s_0 is initial stress. It is evident from Eq. (1) that the equivalent pressure decreases as the deformation and concomitantly, the cross-sectional area, increase. That the bending over of the curves in Fig. 2 is due largely to this decrease in pressure is shown by Fig. 3. In Fig. 3 have been reproduced from Fig. 2 the deformations at 1, 15 and 30 min. for each load. Beside each point opposite 1 min. is indicated the prevailing pressure in kg/cm², as computed by Eq. (1). Beside the points at 15 and 30 min, are indicated average pressures during the preceding 14 and 29 min., respectively. This plotting gives a rough distribution along the deformation coordinate of the best single pressures to be associated with each deformation. The best isobaric lines through these points appear to be linear; several have been drawn in. Prevailing pressures at 30 min. as computed by Eq. (1), and as computed from average diameters of the barrel-shaped cylinders (measured after the completion of each compression test), are in substantial agreement.

Figure 3 indicates that the time-deformation curves are not asymptotic to some line of permanent deformation, the possibility of which Fig. 2 suggests. The linearity of the curves of Fig. 3 is in agreement with the behavior generally observed in metals in long time tests. A similar linear relationship after the initial deformation and adjustment, observed in copper and unannealed aluminum with the present apparatus, is shown in Fig. 4. The pressures indicated are

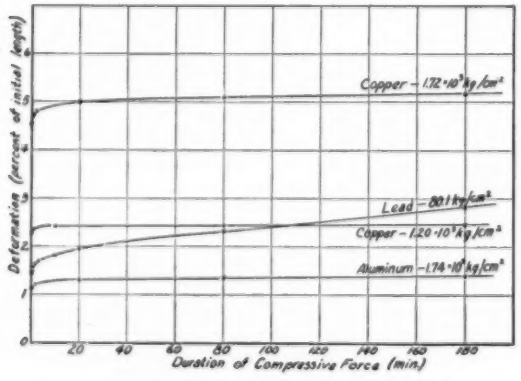

FIG. 4. Comparison of the rates of deformation of metallic cylinders under various initial pressures.

referred to the original cross-sectional areas. Because of the small deformations involved here the compressions may be regarded, with little error, as taking place under constant pressure. Also shown is a curve for lead which is a continuation of that for the minimum load (42.9 kg) in Fig. 2. Attention is called to the relative velocities of deformation; that of lead is significantly different from the others. Thus, under a pressure less than one-twentieth of that on copper, the rate of deformation of lead is five times as great. The relative rates with lead under higher pressures can be judged from Fig. 3. The "creep limit"[3] seems already to have been exceeded with a pressure of 80.1 kg/cm² on the lead. The creep limit, like the elastic limit of lead, may be negligibly small.

The great importance of the velocity in the deformation of lead, as indicated by these data,[4] casts considerable doubt on the significance of compression calibration tests which do not explicitly involve measurements of time or velocity. Certainly for the intervals examined here, no reliable relation identifies a single pressure with a given deformation without involving time in a complicated manner. Qualitatively, the same relations that hold for lead hold for copper and aluminum also. However, the initial deformations in the latter so completely dominate subsequent changes that time may be ignored, with minor or even imperceptible error. For better accuracy, of course, comparisons must be limited to periods of the same order.

Bogomolov and Kunin[5] have recently completed both static and dynamic compression tests on lead cylinders in a pressure range above that of the present tests. Their cylinders were of different size from those used by the writer, being initially 5.00 mm in diameter and 7.50 mm in length. The cylinders were turned from rods which had been drawn. This difference in preparation is probably not significant. They tested twelve specimens under loads up to 500 kg and from their results arrived at a law

$$Fl^m=C, \qquad (2)$$

[3] Nadai, reference 2, p. 287.

[4] Parallel or nearly parallel isobaric lines in Fig. 3 would indicate little importance of velocity of deformation.

[5] U. N. Bogomolov and N. F. Kunin, J. Tech. Phys. (U. S. S. R.), **5**, issue 5 (1935).

where F is load (compressive force), l is remaining length, C and m are constants depending on the material and dimensions of the cylinder. This law was not found to hold for the present results. However, the two sets of data, each limited to the region of experiment, are in excellent agreement, as is shown by Fig. 5.

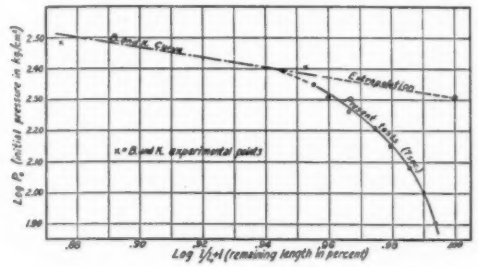
B. and K. Curve
Extrapolation
Present tests (true)
x = B. and K. experimental points
Log P_0 (initial pressure in kg/cm²)
Log $l/_{l_0}$ (remaining length in percent)

FIG. 5. Pressure-deformation relation for lead under static compression, expressed in logarithms of initial pressure and of remaining length.

In Fig. 5 have been plotted the two lowest experimental points and the Bogomolov and Kunin curve for static compression, taken as accurately as possible from the published graph. The curve is linear, in agreement with Eq. (2). Also plotted are results of the initial observations in the present tests. To compare the two sets of data it was necessary to express l for both sizes of cylinders in percent of initial length. Similarly to nullify differences in cross-sectional areas, it was simplest to express F as initial pressure, P_0.

Bogomolov and Kunin extrapolate their curve into the region of lower pressures to obtain a "deformation tension," for which they quote the value 2.04 kg/mm². The quantity thus derived is interpreted as the maximum stress resisting deformation, set up in a metal. Compression under higher pressures takes place against this constant maximum stress, the difference between pressure and opposing stress increasing with the pressure. Consequently, as the deforming force attains the level of the B. and K. curve, the pressure-rate of deformation rapidly increases, as the combined curves of Fig. 5 show. The present tests, clearly, eliminate the interpretation of deformation tension as the minimum limit of pressure sufficient to cause plastic compression.

ACCURACY

The accuracy of the experimental results, summarized in Fig. 2, may be said to depend upon four factors: (a) the refinement of the optical lever system, (b) the accuracy with which the compressive forces were known, (c) the uniformity among identical observations, and (d) displacement in the apparatus itself, under load. Factor (a), the optical lever and its calibration, have been amply described.

(b) There was the possibility of error being introduced by a shift of the point of application of the compressive force, changing the lever-arm ratio, as the lever moved down with deformation of the test cylinder. The rounded end of the stud on the piston, and the relatively small distance of travel of the application point, tend to minimize this shift. Repeated inspections showed it to be imperceptible, except during the last few minutes of the tests under the 98.0 kg load.

Another effect having a bearing on accuracy under (b) is the decrease in the actual compressive force for a given load, when the lever is out of the horizontal position. In this case, the transverse force exerted by the lever on the stud has a horizontal component different from zero. Under the smaller loads this effect could be neglected because the lever did not depart appreciably from a horizontal position. At the higher loads shims were clamped to the lever above the stud, so that the lever came into the horizontal position midway through the deformation process. Thus at no time was the lever out more than 5.5° from the horizontal on either side. A calculation shows that with the lever at this angle the actual compressive force differs by less than one percent from that calculated from the load and T.M.A. of the lever. This error, occurring on the steep part of the curve, rapidly drops toward zero.

(c) As indicated previously, the curves of Fig. 2 are averages of five independent sets of observations. A typical example of the uniformity within each group of curves is afforded by the data for the 76.0 kg load. Here the extreme variation in the initial deformations was 0.014 cm and in the thirty-minute deformations 0.049 cm. The dispersion of a group of curves was less for the smaller loads. Since precautions were taken

to make operations on all cylinders identical, the variations are ascribed to differences in crystal structure and alignment, in the cylinders. The increase in the extreme variation, after the initial deformation, supports this view.

(d) A small, elastic displacement in the apparatus under high loads was detected. In the test for this factor an accurately turned cylinder of hard tool steel, 1.27 cm long and 1.59 cm in diameter was used. The dimensions and material of this proof cylinder permitted its compression being neglected. With repeated applications of a 307 kg compressive force the mean over-all displacement recorded by the mirror was found to be 8.9×10^{-4} cm. Contributing to this displacement could be compression of the anvil and piston, and flexure of the base plate. While this error has no significance when applied to the data for lead, a correction for it was made in obtaining the curves of Fig. 4.

The cooperation and correspondence of the physics laboratory staff at the Western Cartridge Company have been found very helpful in the pursuit of this investigation.

Drift of Magnetic Permeability at Low Inductions after Demagnetization*

G. R. Patterson
Carnegie Institute of Technology, Pittsburgh, Pennsylvania
(Received April 25, 1938)

Attempts at measurement of the magnetic properties of ferromagnetic materials at very low flux densities showed inconsistencies which were attributed either to errors in methods or to some behavior of the material. Check tests, using the same procedure in each case, eliminated the first supposition. The results of this investigation show that, with a steel of medium silicon content tested at 10 gausses over a period of 24 hours, there exists a 5 to 15 percent decrease in permeability. On the average, 50 to 60 percent of this drift occurred within one hour after demagnetization and none after 24 hours.

Introduction

THE measurement of the magnetic properties of ferromagnetic materials has long been a task of the electrical engineer. At first the problem was to measure these properties for materials having medium values of such characteristics as the moderate inductions used in the design and operation of the ordinary electromagnetic machines. This branch of the field of measurements became so developed that by means of any one of the numerous permeameters it was rather easy to determine the magnetic qualities of the various kinds of iron and steel.

With the introduction of magnetic materials into new lines of work and the development of special materials to do this work, the measurement of these magnetic properties became more difficult; and in many cases previously accepted methods were inadequate and new methods had to be devised. According to a previous publication[1] developments of commercial magnetic materials have followed several major directions: (1) new core materials suitable for radiofrequencies; (2) new nickel-iron alloys with high initial and maximum permeabilities; (3) production and study of the properties of sheet with preferred grain orientation; and (4) the discovery of a number of new permanent magnet materials having remarkably high coercive forces. Of all these various new requirements of test, one of particular importance in this investigation is the measurement of permeability at low flux densities, as used in some radio and communication work.

* Submitted to the Graduate School of the University of Pittsburgh in partial fulfillment of the requirements for the degree of Master of Science, June 9, 1937.

[1] Thomas Spooner, Elect. Engineering **54**, 1354 (1935).

The American Society for Testing Materials specifies two alternative methods for the determination of permeability at low densities.[2] These two methods which employ alternating current of either 60 or 1000 cycles per second, are designated as the bridge method and the potentiometer method respectively.

Several tests by different persons have shown that consistent results were not obtained by the two methods, and that check tests by either method seldom agreed with the original results obtained by the same method, the differences sometimes amounting to as much as 10 or 12 percent.[3]

These results would indicate errors in one or both of the methods, or inconsistency in the materials under test. Tests by Sanford showed that the lack of agreement was not due to the method of measurement, for if the same procedure was followed in each case the results by the two methods agreed fairly well; therefore the apparent error must be due to the behavior of the material.

The purpose of this investigation was to test for variation in permeability, using several different samples under various conditions.

Description of Apparatus

The apparatus used in the bridge method is essentially a parallel Owen bridge; that is, one in which the resistance and capacitance forming the variable arm are in parallel. A diagram of connections of the bridge is shown in Fig. 1.

The A. S. T. M. standards specify the requirements for the apparatus as follows:

a. *Power supply.* The supply voltage shall be of approximately sine wave form, having not more than 10 percent of total harmonics present.

b. *Test winding.* The testing winding shall consist of four solenoids surrounding the four sides of the magnetic circuit and connected in series. The solenoids shall be wound on forms of nonmagnetic, nonconducting material. There shall be two windings on each solenoid. The inside winding shall consist of 25 turns wound uniformly on the form; the second winding shall consist of 250 turns wound uniformly over the first.

c. *Voltmeter.* Any voltmeter capable of indicating the voltage supplied to the bridge at the test frequency with an accuracy of at least plus or minus 2 percent may be used.

d. *Fixed capacitor.* The fixed capacitor shall be a high grade mica condenser of 1.0 microfarad plus or minus 0.25 percent capacitance having a power factor of not more than 0.0015 at 1000 cycles per second.

e. *Fixed resistor.* The fixed resistor shall be a nonreactive resistance of 10 ohms plus or minus 0.1 percent with a time constant not to exceed one microsecond.

f. *Adjustable capacitor.* The adjustable capacitor shall be a three-decade mica condenser having steps of $9\times(0.1+0.01+0.001)$ microfarads adjusted to an accuracy of plus or minus (0.25 percent plus 50 micro-microfarads), and having a power factor of not more than 0.0015 at 1000 cycles per second.

g. *Adjustable resistor.* The adjustable resistor shall be a four-decade nonreactive resistance having steps of $10\times(1000+100+10+1)$ ohms adjusted to an accuracy of plus or minus (0.1 percent+0.05 ohm) with a time constant not to exceed one microsecond.

h. *Detector.* For the 1000-cycle-per-second test a telephone receiver is recommended as a detector. A single-stage vacuum tube amplifier preceding the receiver is recommended when it is necessary to increase the sensitivity.

i. *Supply transformer.* The supply transformer shall be a suitable transformer providing efficient and distortionless inductive coupling and substantial electrostatic isolation between the source of supply and the bridge network.

The above requirements were met in the selection of the specified apparatus, and in addition the following pieces of equipment were used:

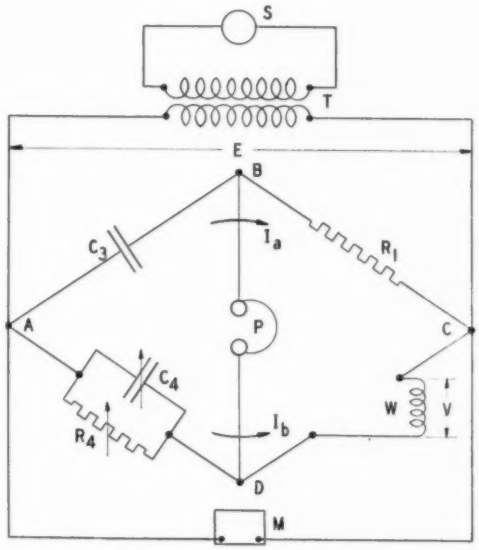

Fig. 1. Schematic diagram of connections.

S, alternating current supply
T, supply transformer
C_3, fixed capacitor
R_1, fixed resistor
C_4, adjustable capacitor
R_4, adjustable resistor
P, detector
W, test winding
M, voltmeter.

[2] *Book of A. S. T. M. Standards*, Part I Metals (1936).
[3] Raymond L. Sanford, Nat. Bur. Stand. J. Research 13, 371 (1934).

A noninductive fractional ohm resistor of high quality was connected in series with the adjustable resistor to give a finer adjustment.

A high quality air condenser was connected in parallel with the adjustable capacitor to give a finer adjustment of the variable capacitance.

In the detecting system, in addition to the amplifier and telephones, an audio transformer and a band pass filter were used to increase the sensitivity and eliminate extraneous sounds from the telephones.

The voltmeter consisted of a microammeter used with a copper-oxide rectifier and a shielded decade resistor to give the proper range as required.

The demagnetizing equipment required the use of a Variac and a stepdown transformer. The same voltmeter was used as in the main bridge setup; a different value of external series resistance being used to give the proper range as required.

Method of Procedure

The apparatus was assembled and connected as shown in the actual diagram of connections in Fig. 2.

One distinguishing feature of this test is the manner of building up the magnetic circuit. The circuit is a square similar to an Epstein square, except that the strips of each leg overlap the strips of both adjacent legs at the corners, as shown in Fig. 3.

This gives a corner joint which has twice the thickness of the rest of the magnetic circuit,

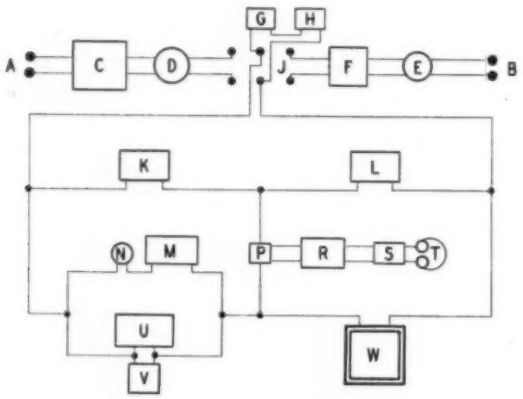

Fig. 2. Actual diagram of connections.

A, B, 110-volt-60-cycle alternating current supply
C, 1000 cycle oscillator
D, transformer
E, variac
F, transformer
G, voltmeter
H, shielded multiplier
J, D.P.D.T. switch
K, fixed mica condenser
L, shielded fixed resistor
M, shielded variable resistor
N, fractional ohm resistor
P, audio-transformer
R, amplifier
S, band pass filter
T, telephones
U, variable mica condenser
V, variable air condenser
W, test coils and specimen

thereby gaining the name of double-lapped joint.[4] The effects of the air gaps in this type of joint are very small, because of their large area and short length. Also, the reluctance of the magnetic material in the joints is low compared to

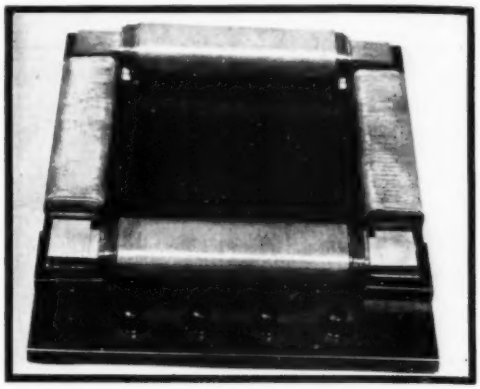

Fig. 3. Test winding and specimen.

the reluctance of the legs because of the double thickness of the joint. There is no clamping at the joints.

The length and width of the strips used were such as to permit the magnetic circuit to be built up in a half-length Epstein frame; that is, 28 centimeters long and 3 centimeters wide.

Before making a test, the material was magnetized to 10,000 gausses and immediately demagnetized, using a 60-cycle-per-second alternating current for the entire process.

All tests for permeability were made using an alternating current of 1000 cycles per second. The permeability of the specimen is calculated in terms of the measured inductance. The core loss may be calculated from the excess of the apparent resistance of the test winding over its ohmic resistance. In balancing the bridge data were obtained from which this core loss could have been calculated; however, it was not done as this item was not of particular concern in this investigation.

After the demagnetization the sample was ready for test and the 1000-cycle-per-second alternating current was applied to the bridge. The maximum flux density is proportional to the voltage applied to the bridge, thus this voltage was adjusted to give the value of induction

[4] S. L. Burgwin, Rev. Sci. Inst. **7**, 272 (1936).

desired for the test. The values of the fixed resistor and the fixed capacitor are specified in the A. S. T. M. standards, with these values properly set, the adjustable resistor and adjustable capacitor were varied until there was a minimum tone heard in the telephones. With all these values, for balance of the bridge, known it was possible to calculate the permeability of the specimen under test.

Induction and Permeability Formulae

Referring to Fig. 1:

$$E = Nd\phi/dt\ 10^{-8} \text{ volt},$$

$$E_{av} = N2\phi/\tfrac{1}{2}f\ (10)^{-8},$$

$$E_{av} = 4\phi fN\ (10)^{-8},$$

$$\frac{E_{eff}}{E_{av}} = \frac{E_m/\sqrt{2}}{2E_m/\pi} = \frac{0.707}{0.636} = 1.11,$$

$$E_{eff} = 4.44\phi fN\ (10)^{-8} \text{ volt},$$

$$E_{eff} = 4.44BAfN\ (10)^{-8},$$

$$V = 4.44BAfN\ (10)^{-8} \text{ volt},$$

V = voltage across test coil,

$$I_a = E/(R_1 - j/\omega C_3) = E\omega C_3/(R_1\omega C_3 - j),$$

at balance $V = I_a R_1$,

$$V = E\omega C_3 R_1/(R_1\omega C_3 - j),$$

$$E/V = (R_1\omega C_3 - j)/\omega C_3 R_1,$$

$$E^2/V^2 = (R_1^2\omega^2 C_3^2 + 1)/\omega^2 C_3^2 R_1^2 = 1/\omega^2 C_3^2 R_1^2 + 1,$$

$$C_3 = 1\times 10^{-6} \text{ farad}$$

at 1000 cycles per second $R_1 = 10$ ohms, $N = 100$ turns; at 60 cycles per second, $R_1 = 100$ ohms, $N = 1000$ turns

$$\frac{1}{\omega^2 C_3^2 R_1^2} + 1 = \frac{1}{10^6\times 10^{-12}\times 10^2} + 1 = \frac{1}{10^{-4}} + 1$$

$$= 10{,}000 + 1$$

1 = 0.01 percent of 10,000 and is negligible.

$$E/V = 1/\omega C_3 R_1,$$

$$E = 4.44BAfN\ (10)^{-8}\times(1/\omega C_3 R_1),$$

$$E = \frac{\sqrt{2}\pi fBAN}{10^8}\times\frac{1}{2\pi fC_3R_1} = \frac{1}{2}\,\frac{\sqrt{2}BNA}{C_3R_1\,10^8}$$

at 1000 cycles per second

$$E = \frac{\sqrt{2}}{2}\,\frac{B\times 100\times A}{1\times 10^{-6}\times 10\times 10^8} = 0.0707BA$$

at 60 cycles per second

$$E = \frac{\sqrt{2}}{2}\,\frac{B\times 1000\times A}{1\times 10^{-6}\times 100\times 10^8} = 0.0707BA$$

E = alternating e.m.f. in volts, applied to the bridge,

B = flux density of the specimen, in gausses,

A = cross-sectional area of the specimen, in square centimeters,

$$\dot{I}_a\dot{Z}_{AB} = \dot{I}_b\dot{Z}_{AD},$$

$$\dot{I}_a\dot{Z}_{BC} = \dot{I}_b\dot{Z}_{DC},$$

$$I_a/j\omega c_3 = I_b R_4,$$

$$I_a R_1 = I_b j\omega L,$$

$$I_a R_1/(I_a/j\omega c_3) = I_b j\omega L/I_b R_4,$$

$$R_1 C_3 = L/R_4,$$

$$L = R_1 R_4 C_3,$$

$$L = 0.4\pi N^2\mu A/(l\times 10^8),$$

$$\mu = L\times l\times 10^8/4\pi N^2 A,$$

$$\mu = R_1 R_4 C_3\times l\times 10^8/0.4\pi N^2 A,$$

$C_3 = 1\times 10^{-6}$ farad, $l = 94$ centimeters, at 1000 cycles per second,

$$\mu = 10\times R_4\times 1\times 10^{-6}\times 94\times 10^8/0.4\pi(100)^2 A,$$

$$\mu = 7.47R_4/A,$$

at 60 cycles per second,

$$\mu = 100\times R_4\times 1\times 10^{-6}\times 94\times 10^8/0.4\pi(1000)^2 A$$

$$\mu = 0.747R_4/A.$$

The demagnetizing process, to which each specimen was subjected before testing at the low densities, was performed with an alternating current of 60 cycles per second, with the same apparatus and connections as shown in Fig. 1. The value of the adjustable resistor R_4 was set at zero.

$R_1 = 10$ ohms, $R_4 = 0$, $C_3 = 1.0$ microfarad,

$X_3 = 10^6/(2\pi fC_3) = 10^6/(2\pi\times 60\times 1) = 2650$ ohms.

For the balanced bridge

$$V = I_a R_1 = 10 I_a;$$

for the unbalanced bridge as used in demagnetization

$$\dot{V} + \dot{I}_b \dot{R}_4 = \dot{I}_a \dot{X}_3 + \dot{I}_a \dot{R}_1,$$

$$\dot{V} = \dot{I}_a \dot{X}_3 + \dot{I}_a \dot{R}_1,$$

or approximately $V = 2650 I_a$.

Also, since $R_4 = 0$, $V = E$,

$$\frac{V(\text{unbalanced})}{V(\text{balanced})} = \frac{2650 I_a}{10 I_a} = \frac{2650}{10},$$

$$V(\text{unbalanced}) = 265\, V(\text{balanced}).$$

B is directly proportional to E.

$$B(\text{unbalanced}) = 265\, B(\text{balanced}).$$

For the balanced bridge:

$$E = 0.0707\, BA \text{ (volt)}.$$

For the unbalanced bridge:

$$E = 0.0707(B/265)\, A \text{ (volts)},$$
$$B = 10{,}000 \text{ gausses},$$
$$E = 2.67\, A \text{ (volts)}.$$

Description of Tests

Tests of four different specimens, ranging in silicon content from 1.0 percent to 4.5 percent, were made as outlined in the procedure. As specified by the A.S.T.M. standards, the total weight of each sample was in excess of one kilogram. These specifications of standard tests also state that for the 1000-cycle per second test, the 25-turn windings and R_1 equal 10 ohms shall be used.

The laminated silicon steel comprising the specimen was weighed, and knowing the density from values given by the A.S.T.M., the cross-sectional area of the sample was calculated.

The sample was magnetized to 10,000 gausses by applying the proper voltage to the terminals of the bridge and then immediately demagnetized by gradually reducing the voltage to zero. The alternating, 60-cycle per second, voltage necessary to be applied to the bridge terminals in order to produce an induction of 10,000 gausses is given by the expression, $E = 2.67\, A$ (volts).

The 1000-cycle per second supply was connected to the bridge and, with the fixed resistor set at 10 ohms and the fixed capacitor at 1.0 microfarad, the supply voltage was adjusted to give an induction of 10 gausses. The voltage required for this magnetization is given by the expression, $E = 0.0707\, BA$ (volts). Adjustments of the variable resistor and variable capacitor were then made as quickly as possible to give a minimum sound in the detector phones. Readings were taken every five minutes for the first half-hour, every ten minutes for the next half-hour, and then at greater intervals until 24 or more hours had elapsed. The magnetizing current was applied only at the time of taking readings. This test was performed for specimens having percent silicon contents of 1.0, 2.75, 3.5, and 4.5, respectively.

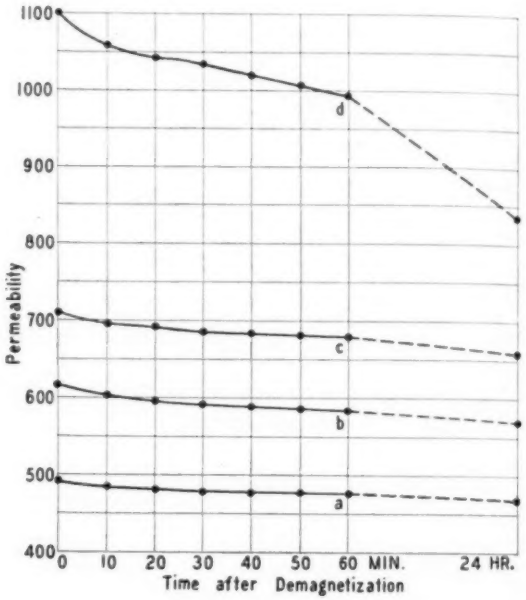

Fig. 4. Relation between permeability and time after demagnetization. a. 1.0 percent silicon steel. b. 2.75 percent silicon steel. c. 3.5 percent silicon steel. d. 4.5 percent silicon steel. Flux density = 10 gausses.

As mentioned above, the adjustments for each reading were made in as short a time as possible, for the values of the variable quantities, and thus the permeability, changed with the length of time of the application of the magnetizing current. As a check on the results produced by this effect, two very similar tests were made of the 3.5 percent silicon steel at a flux density of

10 gausses. One test was similar to those previously made with the current off between readings; in the other, the current was on continuously for the entire duration of the test. Also in order to investigate any results from this effect which might appear in the first group of tests, since the time between readings was different for the first and second half-hours of the test, another test of the 3.5 percent silicon steel was made at 10 gausses, taking readings at five-minute intervals for the entire first hour.

In view of the possibility of a drift in the permeability not existing at different values of a low flux density, the 3.5 percent silicon steel was tested at densities of 5, 10, 15, 20, and 25 gausses. The procedure was the same as in the first tests; readings were taken at 10-minute intervals for one hour, and the current was off between readings.

From general appearances, the major portion of the drift of the permeability was taking place the first hour after demagnetization and very little after twenty-four hours. For this reason another test was made of the 3.5 percent silicon steel at a density of 10 gausses; in which test the specimen was magnetized to 10,000 gausses and then demagnetized as in all previous tests; but in this case, unlike the others, the sample then remained undisturbed for twenty-four hours before any tests were made at 10 gausses. Then, after the twenty-four-hour period after demagnetization had elapsed, readings were taken at a flux density of 10 gausses, in like manner to those of previous tests.

Results of Tests

The permeability, which is the factor of prime importance throughout this entire investigation, may be calculated from the balanced Owen bridge, by the equation $\mu = 7.47 R_4/A$.

1. Drift of permeability in steels of various silicon content

In all cases where the standard test was performed, the measurements for permeability being taken immediately after demagnetization of the sample, there was a decided decrease in the permeability with an increase in time after demagnetization. The significant figures of the results are shown in Table I.

Table I.

Percent silicon content	1.0	2.75	3.5	4.5
Initial permeability	486.6	614	710	1105
Permeability after 1 hour	478.0	588	681	993
Permeability after 24 hours	473.0	573	660	835
Percent drift in 24 hours	2.8	6.7	7.0	24.4
Percent of 24-hour drift in one hour	63.2	63.4	58.0	41.5

For the specimens tested, these results show a maximum drift of the initial permeability of 24.4 percent in 24 hours; and in the extreme case 63.4 percent of this change took place during the first hour. The 4.5 percent silicon steel was a high permeability, low loss steel, and in it a great change in the permeability may be expected. The 1.0 percent silicon steel had a low value of initial permeability and thus a small drift would be anticipated.

For the samples having a medium percentage of silicon content, 2.75 and 3.5, the drift in permeability in 24 hours was approximately 7 percent of the initial value, and about 60 percent of this change took place the first hour after demagnetization. Figs. 4, 5, and 6 are graphs of the complete results of these tests.

2. Drift of permeability at various flux densities

Again, the results of these tests showed that a considerable drift in permeability took place

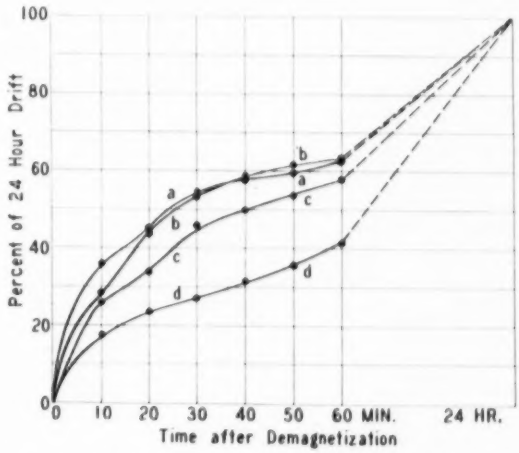

Fig. 5. Relation between drift and time after demagnetization. a. 1.0 percent silicon steel. b. 2.75 percent silicon steel. c. 3.5 percent silicon steel. d. 4.5 percent silicon steel. Flux density = 10 gausses.

during the first hour after demagnetization. The tests were all made using the 3.5 percent silicon steel and values of flux density of 5, 10, 15, 20,

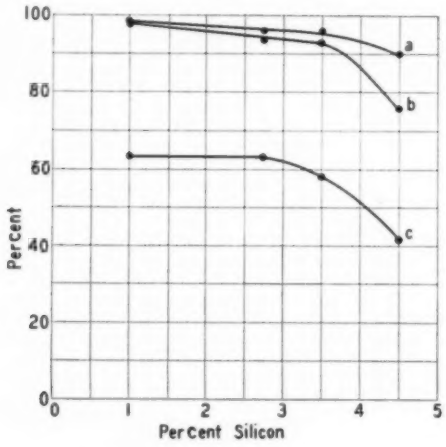

FIG. 6. Variation of permeability and drift with percentage of silicon. a, percent of maximum permeability after one hour; b, percent of maximum permeability after 24 hours; c, percent of the 24-hour drift in the first hour. Flux density = 10 gausses.

and 25 gausses. The greatest drift took place at 5 gausses; the drift gradually decreasing to that at 25 gausses, which was the smallest. A graph of the drift of permeability at various flux densities is shown in Fig. 7.

3. Drift of permeability 24 hours after demagnetization

The results of this test were as might have been predicted from observations of the previous tests. As explained in the Description of Tests, the material was magnetized to 10,000 gausses, demagnetized, and then permitted to stand for twenty-four hours before making any tests of permeability. The results show that during the first hour these readings were being taken there was a very slight drop in the value of the permeability; the change being from 650 to 649. Then, to a time 23 hours later, or 24 hours after the first reading was taken, there was no additional change.

This drift was so small that it may have been within the errors of measurement, although there was a definite indication of a very slight decrease in the value of the permeability. The results of this test are shown in Fig. 8.

DISCUSSION

The results of this investigation furnish conclusive proof that there is a drift of magnetic permeability at low inductions after demagnetization. A conservative statement regarding this phenomenon would be that for steels of medium silicon content, when tested at low flux densities of the order of 10 gausses, the permeability decreases from 5 to 15 percent of its initial value during the first 24 hours after demagnetization; approximately 50 to 60 percent of this change takes place the first hour, and practically none 24 hours after demagnetization.

Although specimens were tested under various conditions, as previously outlined and discussed, the purpose of this investigation was to ascertain whether or not this drift of permeability actually existed in all cases; and no direct attempt was made to eliminate the effect or to discover its cause. However, such a definite trend in the change of the permeability arouses some interest as to the possible causes of this drifting. At first thought it may be attributed to a number of causes; namely, method of testing, influence of the earth's magnetic field, temperature effects, and aging of the steel. A previous investigation[3] regarding the agreement of the bridge and potentiometer methods of measuring permeability at

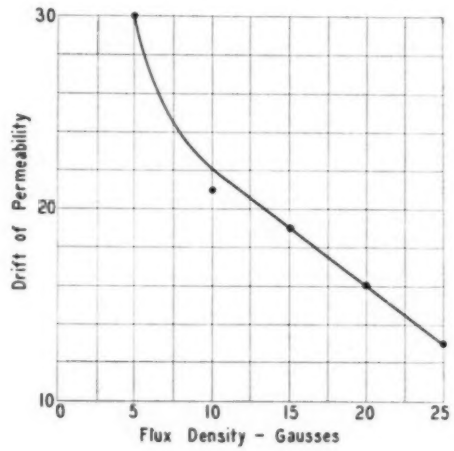

FIG. 7. Drift one hour after demagnetization. 3.5 percent silicon steel.

low inductions demonstrated conclusively that unless the same procedure with respect to time was observed, inconsistent results were obtained

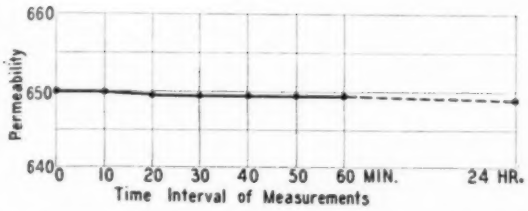

FIG. 8. Permeability 24 hours after demagnetization. Flux density = 10 gausses, .5 percent silicon steel.

in the alternating-current bridge method, alternating-current potentiometer method, and the direct-current ballistic method. Also, in this same investigation,[3] the specimen was oriented so as to bring the earth's field at right angles to that of the magnetizing coils, and the effect still remained. These results should eliminate the first two possibilities. The change could not be caused by temperature effects, as the temperature remained practically constant throughout the tests; and besides, the change was greater than could be accounted for by the temperature coefficient of magnetic permeability. The drift cannot be attributed to aging of the material, for: silicon steel is considered nonaging, the same results can be reproduced time after time, and if these specimens ever had any tendency for aging it should have occurred long before these tests were made, as they were used for some time in the Westinghouse Research Laboratories before being used for these tests.

One plausible explanation may be given by the theory of orientation of domains in the iron crystal, as stated by R. M. Bozorth.[5] The structure of a single crystal of iron may be represented by a cube with an atom at each corner and one at the center, the whole crystal made up of such cubes packed together face to face. Even when the crystal is apparently unmagnetized, or demagnetized, there are small regions, called domains, that are magnetized to saturation in one of the six equivalent directions of the crystal faces. Actually, the domains vary considerably in size and shape, but are represented conveniently as squares. Each of the six directions is equally stable and equally probable when no field is applied. This condition of nonmagnetization exists when the material is free from any strain, such as tension or compression, and any one of the six directions may be considered the direction of easy magnetization. Because of the inherent strains which exist in any piece of material this ideal condition actually does not exist, and the number of directions of easy magnetization is reduced to two. Furthermore, when an external magnetic field is applied this number is reduced to one.

The material in its unmagnetized condition has an orientation of the domains such that magnetic forces within the material, as a whole, are neutralized. When an external magnetizing force is applied and the material becomes magnetized, there is a shifting or rotation of the domains. This movement of the domains is accompanied by physical strains of tension and compression, and thus energy must be supplied from the magnetizing source. Incidentally, this setting up of the strains accounts for the property of reluctance of the material. When the material is demagnetized the domains do not completely return at once to their original status, and some additional energy must be supplied to obtain the original orientation of domains. From the results of this investigation time appears to be an important function of this complete change.

If this explanation of the phenomenon is correct, the drift in permeability after demagnetization may be eliminated or hastened by some external application of energy, possibly in the form of heat or mechanical vibrations. As previously stated, the purpose of these tests was to prove the existence of a drift in magnetic permeability at low inductions after demagnetization, and no attempt was made to verify any of the explanations. The answers to the questions which arose are merely probabilities, and it is hoped that their verification may be the result of a future study of this problem.

[5] R. M. Bozorth, Elect. Engineering **54**, 1251 (1935).

A Type of Electrical Resonator

W. W. Hansen
Stanford University, California
(Received July 17, 1937)*

The theory of the use of certain shapes of "hohlraums" as electrical resonators is developed. In many respects they are equivalent to lumped constant circuits with properly chosen circuit constants. Suitable values for these circuit constants are found. The theory of coupling onto these hohlraum types of resonators is developed approximately.

I. Qualitative Considerations

CONSIDER a closed surface of a (hypothetical) material of infinite conductivity which divides all space into two regions: inside and outside. Such an enclosure is often postulated when developing the theory of black body radiation in which connection it is known as a hohlraum. Now it is known that there exist solutions of Maxwell's equations which are zero outside, finite inside, have a definite frequency, and have a vanishing tangential component of the electrical field at the boundary.

Because of the condition that the tangential electric field must vanish not all frequencies are allowed: only certain discrete frequencies have associated with them fields satisfying this condition. Thus any closed conducting surface has certain allowed or resonance frequencies; the values of these frequencies are determined by the size and shape of the surface. Because the enclosure can contain a periodically repeating electromagnetic field only when the frequency of such a field is properly chosen it is proper to call the enclosure a resonator.[1]

The objects of the present paper are to point out that such a resonator may often be equivalent to a conventional resonant circuit; to calculate in a few cases the constants of this equivalent lumped constant circuit; and to show how actually to use such a resonator to replace an ordinary resonant circuit.

These calculations will presently be done exactly but it is a profitable preliminary to get some of the results approximately by a simple qualitative discussion.

We first decide what constants of the equivalent circuit we will compute. We might think to take these to be the inductance L, the capacity C, and, if we consider losses, a series resistance R. But it is simpler, and for most purposes more useful, to consider instead the three equivalent parameters $(LC)^{\frac{1}{2}}$, $(L/C)^{\frac{1}{2}}$ and $Q=(L/C)^{\frac{1}{2}}/R$. The first of these determines the frequency, the second is of dimensions resistance and is often called the characteristic impedance, and the third is a measure of the losses.

Though any hohlraum has an infinite sequence of allowed frequencies we will for brevity, but without serious loss of understanding, speak for some time only of the lowest frequency. Moreover in our qualitative considerations we will suppose the enclosure to be of some simple, nonreentrant, shape—for example, a sphere.

Considering first the quantity $(LC)^{\frac{1}{2}}$ it is plain that this is just $\lambda/2\pi c$ with λ the wave-length corresponding to the lowest allowed frequency. This wave-length will be determined by the

* The ideas covered in this paper were conceived several years ago in connection with a scheme for producing high voltage electrons. Experimental work along this line did not progress as rapidly as had been hoped, however, and it was finally decided to describe some of the ideas without waiting for the high voltage electrons. Hence this paper was prepared and was received by the *Journal of Applied Physics* in July, 1937. It was accepted for publication soon thereafter. However, just as the article was to appear the Stanford University authorities decided that publication might have an adverse effect on commercial developments of this and related devices and the editor was asked to hold the article back until the present time. This the editor very kindly agreed to. The present note is written by the author to explain the unusual lapse of time between the dates of reception and publication.

[1] The fact that only particular (eigenvalues) of frequency are allowed inside a hollow conductor has of course been known for a long time. Moreover some particular shapes of "hohlraum" have been used as electrical resonators; the ordinary "concentric line" resonator is a case in point. In further connection with this point we may refer to Southworth, Bell System Tech. J. **15**, 284 (1936) and Barrow, Proc. I. R. E. **24**, 1298 (1936), who noted the phenomenon.

linear size of the resonator and if the latter is of simple shape so that all dimensions are of the same order the wave-length will be about equal to one of these dimensions.[2] For example, for a sphere it turns out that $\lambda = 1.14$ times the diameter.

Coming now to the quantity $(L/C)^{\frac{1}{2}}$ we may make two remarks. First, its value depends on the definition of the current which is to a considerable extent arbitrary. This point will be discussed in detail presently. Second, one may predict on dimensional grounds that $(L/C)^{\frac{1}{2}}$ will be given, in order of magnitude, by the velocity of light. This is true because $(L/C)^{\frac{1}{2}}$ has the dimensions of resistance, or, what is equivalent, of velocity and the velocity of light is the only thing available of proper dimensions. For simple shapes such as those here considered, any dimensionless factors can be counted on to be small.

Finally we come to the dimensionless quantity Q, which is a measure of the losses; in fact, Q is just π times the ratio of the energy stored in the circuit to the energy lost per half-cycle.[3] With this in mind we can estimate Q as follows. Consider a hohlraum with an allowed electromagnetic field inside and no field outside. If the hohlraum were made of perfectly conducting material the field would be entirely confined to the inside, there would be no losses and Q would be infinite. If, however, the material is not a perfect conductor the fields will penetrate the inner surface slightly (skin effect). To order of magnitude we can consider that all electromagnetic energy stored in this inner skin will be converted into heat in the ensuing half-cycle or so.[4] If this is true Q will be approximately equal to π (volume of hohlraum)/(surface area of hohlraum times δ), where δ is the skin depth. For a sphere this would make $Q \sim a/\delta$ with a the radius of the sphere.

[2] It might be thought that one-half wave-length would approximate the sphere diameter. But it must be remembered that when the wave fronts are strongly curved the distance between successive nodal surfaces is greater than the distances between nodes for plane waves of the same frequency.

[3] The fields will decrease by a factor e in Q/π cycles.

[4] We may note that if the surface is not completely closed but has a hole in it, energy will leak out the hole as radiation and damp the oscillations in much the same way. See later for an approximate treatment of this.

II. Quantitative Calculations of $(LC)^{\frac{1}{2}}$, $(L/C)^{\frac{1}{2}}$, and Q

The quantities L and C are best defined in terms of the Lagrange function. As is well known, the equation

$$\delta \int \mathfrak{L} dt = \delta \frac{1}{8\pi} \int [\mathbf{B}^2 - \mathbf{E}^2] d\tau dt = 0 \qquad (1)$$

together with certain auxiliary conditions on $\mathbf{E}$ and $\mathbf{B}$ together imply that $\mathbf{E}$ and $\mathbf{B}$ solve Maxwell's equations. This variation problem is conveniently reduced by introducing two functions $\mathbf{A}_2$, $\mathbf{A}_3$ such that

$$\begin{gathered} \nabla \cdot \mathbf{A} = 0, \quad \nabla^2 \mathbf{A} + (\omega^2/c^2)\mathbf{A} = 0, \\ \mathbf{A}_2 = (c/\omega) \nabla x \mathbf{A}_3, \quad \mathbf{A}_3 = (c/\omega) \nabla x \mathbf{A}_2. \end{gathered} \qquad (2)$$

Also the $\mathbf{A}$ satisfy certain boundary conditions: this requirement determines ω. Then we use a generalized coordinate q and set[5]

$$\mathbf{E} = \omega q b \mathbf{A}_3, \quad \mathbf{B} = \dot{q} b \mathbf{A}_2, \qquad (3)$$

with b a normalizing factor, to be chosen presently. With this choice for $\mathbf{E}$ and $\mathbf{B}$ it will be found that Eq. (1) will be satisfied if

$$\frac{b^2}{4\pi} \int \mathbf{A}_2^2 d\tau \ddot{q} + \frac{b^2 \omega^2}{4\pi} \int \mathbf{A}_3^2 d\tau q = 0. \qquad (4)$$

Thus if we define quantities L and C,

$$\begin{aligned} L &= \frac{b^2}{4\pi} \int \mathbf{A}_2^2 d\tau, \\ C &= \frac{4\pi}{b^2 \omega^2} \frac{1}{\int \mathbf{A}_3^2 d\tau}, \end{aligned} \qquad (5)$$

and treat $\dot{q}$ as a current then if the equation

$$L\dot{i} + \frac{1}{C} \int i dt = 0 \qquad (6)$$

is satisfied then (4) and so (1) will be satisfied and our fields will satisfy Maxwell's equations, and we conclude that (5) is a possible self-consistent pair of definitions for L and C. It should be noted, however, that (5) really determines

[5] To be general we should take $\mathbf{E}$ and $\mathbf{B}$ to be built up of all possible functions $\mathbf{A}$. Then we would find an equivalent inductance and capacitance for each of the possible modes of vibration.

only the product $(LC)^{\frac{1}{2}}$, the ratio $(L/C)^{\frac{1}{2}}$ depends on the magnitude of b which is as yet unspecified.

We may now actually make the calculation for a few specific shapes of resonator. This calculation can be performed exactly in only a few cases; those computable with a reasonable expenditure of labor and also likely to be of practical use include the sphere, right circular cylinder and the rectangular prism. We have also made approximate calculations of the wave-length for a regular n-sided prism with plane ends.

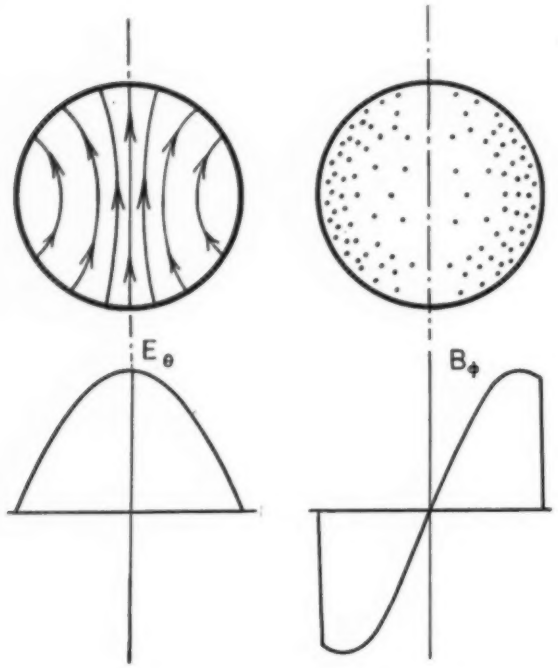

FIG. 1. The left-hand pair of drawings represent a possible field inside a spherical conducting shell at a time when $\mathbf{B}=0$. The upper picture is a cross section of the sphere, the lower is a graph showing the variation with r of the electric field in the equatorial plane. The right-hand drawings show the situation 1/4 cycle later when the electric field has disappeared and the magnetic field has taken up the energy. The vector $\mathbf{B}$ is entirely in the ϕ direction and its variation with r is shown in the graph below.

We may take, for example, a spherical resonator. Suitable wave functions are fairly well known.[6] Using the notation of the last article cited we may take

$$\mathbf{E}=\omega q b\mathbf{A}_{3ls}, \quad \mathbf{B}=\dot{q}b\mathbf{A}_{2ls} \tag{7}$$

inside the sphere, and

$$\mathbf{E}=0=\mathbf{B}$$

outside the sphere. This makes $\mathbf{E}$ and $\mathbf{B}$ solutions of Maxwell's equations and makes them zero outside; it remains only to make the tangential component of $\mathbf{E}$ on the sphere zero. This is done by properly choosing the relation between $\omega/c=k$ and the radius of the sphere a. It will be found that ka must be a root of

$$\frac{1}{k}\frac{d}{dr}((kr)^{\frac{1}{2}}J_{l+\frac{1}{2}}(kr))=0. \tag{8}$$

The lowest root of this equation, and the only one we will consider, is $ka=2.76$ which corresponds to $\lambda=2.28a$ and $(LC)^{\frac{1}{2}}=0.363a/c$.

This determines $\mathbf{E}$, $\mathbf{B}$, and $(LC)^{\frac{1}{2}}$ for this case. Graphs of the fields will be found in Fig. 1. It will be observed that the current flow is always in the θ direction, that is along the meridian lines of the sphere.

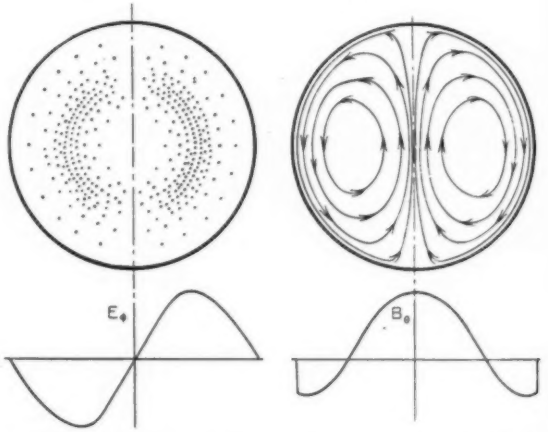

FIG. 2. Another possible electromagnetic field inside a sphere. Dots in the upper left-hand picture represent ends of lines of $\mathbf{E}$ which is entirely in the ϕ direction.

To determine $(L/C)^{\frac{1}{2}}$ we must choose the constant b, or what comes to the same thing, we must decide exactly what we are going to mean by $\dot{q}$, the current. We arbitrarily take $\dot{q}$ to be the total current crossing the equator. Then it is obvious that

$$b=\frac{4\pi}{\int \mathbf{A}_2\cdot d\mathbf{s}}, \tag{9}$$

[6] G. Mie, Ann. d. Physik **25**, 377 (1908); H. Bateman, *Electrical and Optical Wave Motion;* M. Born, *Optik*, p. 274 *et seq.;* G. Wolfsohn, *Handbuch der Physik*, Vol. 20, p. 307 *et seq.;* W. W. Hansen, Phys. Rev. **47**, 129 (1935); W. W. Hansen and J. G. Beckerley, Proc. I. R. E. **24**, 1594 (1936).

where the line integral is taken around the equator. It follows that[7]

$$\left(\frac{L}{C}\right)^{\frac{1}{2}} = 4\pi k c \frac{\int \mathbf{A}_2^2 d\tau}{[\int \mathbf{A}_2 \cdot d\mathbf{s}]^2} = 2.66c. \qquad (10)$$

It remains only to calculate Q. The energy stored is computed[8] in terms of integral $\mathbf{B}^2 d\tau$ while the energy lost depends on the current on the surface of the sphere and so on $\mathbf{B}$ at the surface, and also on the resistivity ρ of the hohlraum material. It is readily found that

$$Q = \sqrt{2} \frac{\int \mathbf{A}_2^2 d\tau}{\delta \int \mathbf{A}_2^2 |d\sigma|} = 1.024 a/\delta \qquad (11)$$

with $\delta = (\rho/\pi\omega)^{\frac{1}{2}}$.

We may mention in passing that there is another type of oscillations inside a sphere which is derivable from that of Fig. 1 by interchanging **E** and **B**. No calculations will be made for this field but an illustration of it will be found in Fig. 2.[9]

Calculations for a cylindrical resonator of radius a and height $2z_0$ can be made in exactly the same way as for a spherical resonator. Suitable functions may be found in the last paper of reference 1. The fields occurring are represented in Fig. 3. In this case, as in the spherical case, there is another set of modes of oscillation of a different type, the one of these of lowest frequency is depicted in Fig. 4.

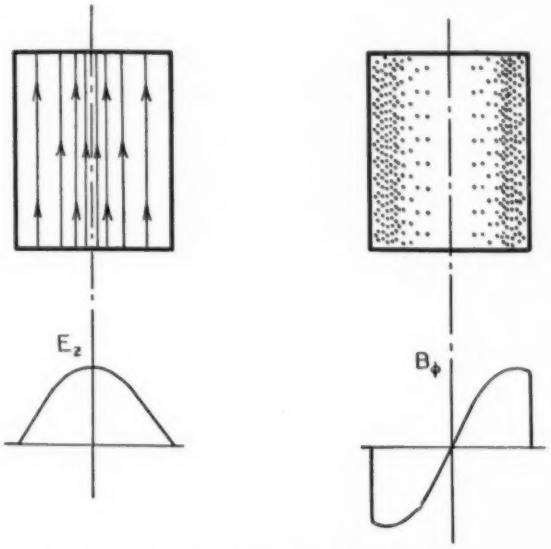

FIG. 3. Fields inside a circular cylinder.

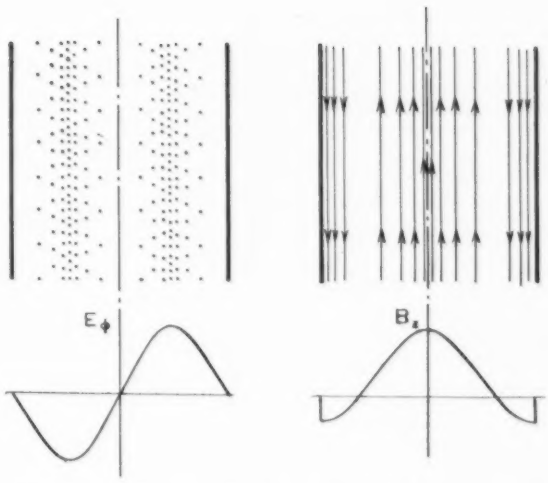

FIG. 4. Another possible field inside a cylinder. To facilitate comparison with Fig. 3 the length of the cylinder, $2z_0$, has been considered as very large compared to the radius a as this makes the wave-length depend on a only and otherwise simplifies the pictures. Near the ends, which are not shown, the lines of **B** in the central bundle spread out, go radially, and finally turn completely around to form the outer lines of **B**.

Finally we have made calculations for a square prism[10] of sides $2a$, $2a$, $2z_0$ with the electric field running in the z direction. The functions **A** for this purpose are easily built up out of trigonometric functions.

The results of these calculations are collected in Table I.

A number of points in connection with Table I are perhaps worth further discussion.

First of all it should be noted that all quantities have been worked out in terms of a and other dimensions and ρ and δ. This is the most useful formulation for determining the characteristics of a specific resonator but for comparison between resonators of different types the formulae should be rewritten in terms of λ. When this is done it will be found, for example, that a cylinder gives about 8 percent higher Q than a

[7] Use has been made of the easily proved fact that integral $\mathbf{A}_2^2 d\tau$ = integral $\mathbf{A}_3^2 d\tau$.

[8] In doing this we use the original functions which assumed no losses. In so doing we make an error but one that is negligible if $\delta \ll \lambda$. For $\lambda = 100$ cm, $\delta/\lambda \sim 5 \times 10^{-6}$.

[9] It is perhaps worth pointing out that no free charge ever appears on the conductor so there is nothing analogous to the condenser of the conventional resonant circuit.

[10] Exact calculations can easily be made for a rectangular prism.

TABLE I. *Values of "equivalent" inductance, capacity, series and shunt resistance, Q, M/L and the coupled impedance are given for various types of resonator working, in each case, on the lowest frequency. The symbol a denotes the radius of cylinder or sphere or the semi-side of the square prism, z_0 is half the height of the cylinder or prism, δ is the skin depth $(\rho/\pi\omega)^{\frac{1}{2}}$ with ρ resistivity and ω radian frequency, and c is the velocity of light. Any consistent set of electromagnetic units can be used, for example with ρ in abohm cm lengths should be in cm and L, C, R will come out in absolute e.m.u. and λ in cm. To convert abohms to ohms multiply by 10^{-9}.*

	Cylinder	Prism (square)	Sphere
$2\pi c(LC)^{\frac{1}{2}}=\lambda$	$2.61a$	$2.83a$	$2.28a$
$\left(\frac{L}{C}\right)^{\frac{1}{2}}$	$4.81\frac{z_0}{a}c$	$4.29\frac{z_0}{a}c$	$2.66c$
Q	$1.414\frac{a}{\delta}\frac{1}{1+\frac{1}{2}(a/z_0)}$	$1.414\frac{a}{\delta}\frac{1}{1+\frac{1}{2}(a/z_0)}$	$1.024\frac{a}{\delta}$
L	$4\pi.159z_0$	$4\pi.154z_0$	$4\pi.0768a$
C	$\frac{1}{4\pi c^2}1.09\frac{a^2}{z_0}$	$\frac{1}{4\pi c^2}1.32\frac{a^2}{z_0}$	$\frac{1}{4\pi c^2}1.72a$
Series $R=\frac{1}{Q}\left(\frac{L}{C}\right)^{\frac{1}{2}}$	$.450\frac{z_0\rho}{a\delta}\left(1+\frac{1}{2}\frac{a}{z_0}\right)$	$.435\frac{z_0\rho}{a\delta}\left(1+\frac{1}{2}\frac{a}{z_0}\right)$	$0.300\frac{\rho}{\delta}$
Shunt $R=Q\left(\frac{L}{C}\right)^{\frac{1}{2}}$	$6.80\frac{z_0}{\delta}\frac{1}{1+\frac{1}{2}(a/z_0)}c$	$6.07\frac{z_0}{\delta}\frac{1}{1+\frac{1}{2}(a/z_0)}c$	$2.72\frac{a}{\delta}c$
$\frac{M}{L}$	$\frac{\Sigma}{az_0}$	$1.272\frac{\Sigma}{az_0}$	$2.08\frac{\Sigma}{a^2}$
Coupled impedance $=\left(\frac{M}{L}\right)^2Q\left(\frac{L}{C}\right)^{\frac{1}{2}}$	$6.80\left(\frac{\Sigma}{az_0}\right)^2z_0\frac{1}{\delta}\frac{1}{1+\frac{1}{2}(a/z_0)}c$	$9.87\left(\frac{\Sigma}{az_0}\right)^2z_0\frac{1}{\delta}\frac{1}{1+\frac{1}{2}(a/z_0)}c$	$11.8\frac{\Sigma^2}{a^3\delta}c$

square prism working at the same wave-length. It is also interesting to note that a cylinder with height equal to its diameter gives a slightly lower Q than a sphere, but that a very long cylinder is better than a sphere. It should also be noted that δ is proportional to $\lambda^{\frac{1}{2}}$ so that for similar shape[11] Q varies as $\lambda^{\frac{1}{2}}$.

This raises the question, what is the most efficient[11a] shape of resonator possible? It is not possible to answer the question completely at present but some useful remarks can be made. Suppose we start from a very long circular cylinder with the idea of making other shapes by continuous deformation. First of all any change to a noncircular cylinder decreases Q because it makes the current distribution nonuniform and so increases the losses while on the other hand the field inside, and so the energy stored, is not greatly changed. A special case of this statement is the square prism above and the proposition is easily proved in general. Next we may consider a deformation that would convert the cylinder into a surface of revolution like an hourglass. It is difficult to prove rigorously but it seems highly likely that this would lower the efficiency because of increased current density at the small part of the hourglass. Another possibility would be to indent one end so making a reentrant figure that would, in the limit, become a section of concentric transmission line. To keep the wavelength constant it would be necessary to reduce greatly the diameter (and moreover the length could not exceed $\lambda/4$) and this would reduce Q because the volume/surface ratio would be reduced. All the above modifications reduce the Q value. However, if we recall that a sphere is more efficient than a cylinder of roughly comparable size, we see that it may be a good idea to round the ends of the cylinder. Qualitative arguments endorse this suggestion. Thus one is led to expect that some shape like that of a long prolate spheroid is the most efficient possible shape, being in the above special case 1.2 times better than a cylinder of the same length and

[11] This is an extremely general proposition. If the losses in any electromagnetic resonator, including, of course, the conventional coil and condenser, are due entirely to resistance losses and the skin depth is small compared to the smallest linear dimension then if all dimensions are altered by a factor n the value of Q will be changed by $n^{\frac{1}{2}}$.

[11a] In what follows "most efficient" is to be interpreted as "having the highest Q."

resonant frequency. But the superiority of the ellipsoid will decrease as z_0 becomes large compared to a and in the limit $z_0 \to \infty$ there may be no difference. The above guess is practically impossible to prove; nevertheless we believe it to be a good one. But whatever the most efficient shape may be it can be regarded as certain that given material of a specified conductivity and also required a fixed λ, no electrical resonator can be devised that will operate at its lowest frequency with a Q value greatly in excess of λ/δ.

On the other hand if operation on higher modes of vibration is allowed it is easily shown that arbitrarily high values of Q may be obtained.

Having concluded that oscillators of the above type are the most efficient possible it may be of interest to compute some numerical values. Such values are given in Fig. 5. Here Q is plotted against λ for various shapes of resonator, the material in all cases being copper. The cylinder and prism have been assumed to have $z_0 \gg a$. To get other cases the Q value given should be divided by $1+\frac{1}{2}(a/z_0)$.

Since the above results will no doubt be compared with those for concentric lines as given by Terman[12] it seems advisable to explain various points that will arise when this comparison is made.

Terman gives the formula $Q=0.0839(f)^{\frac{1}{2}}bH$ where f is the frequency in cycles per second, b is the inside diameter of the outer conductor, and H is a dimensionless factor which is unity if, as we will assume for simplicity, the two radii of the concentric cylinders stand in the ratio e. Also he says, "As may be seen, Q is proportional to $(f)^{\frac{1}{2}}$, is proportional to the diameter b of the outer conductor, is a function of the line proportions (b/a), and is independent of the number of quarter wave-lengths involved in the line. It is particularly interesting to note that, unlike ordinary circuits, the selectivity factor Q, tends to become larger the greater the frequency."

This last statement seems to be in conflict with footnote 11 and various other statements above which assert that Q varies as $1/(f)^{\frac{1}{2}}$, for similar shapes. This disagreement is only apparent for different things are held constant. Terman holds the diameter constant and then on increasing f the Q rises; it might be said that in increasing f one tends to decrease Q but that this tendency is more than balanced by a change to a more efficient shape. In our arguments above, on the other hand, the resonators compared have been geometrically similar, only the absolute scale has been varied.

Another apparent discrepancy occurs if one allows b in the above quoted formula to become very large and compares the resulting arbitrarily high Q with the assertion of the present paper that there is an upper limit to the Q obtainable with a resonator working at its lowest frequency and that that limit is given to order of magnitude by the ratio λ/δ.

But in deriving this formula it was assumed that the concentric line was of conventional shape, i.e. long compared to the diameter b and so the losses in the ends were neglected by comparison with the losses in the tubes. So if one uses a line say $\lambda/2$ long then if b is made large the quoted formula must be modified; if this is done it will be found that there is no contradiction. On the other hand, one might take a very long line (working on a high harmonic) in which case b and so Q may become quite large before the formula ceases to hold. In this case, however, one is working on a high mode of vibration and as stated above, it is possible in this way to get Q to exceed λ/δ.

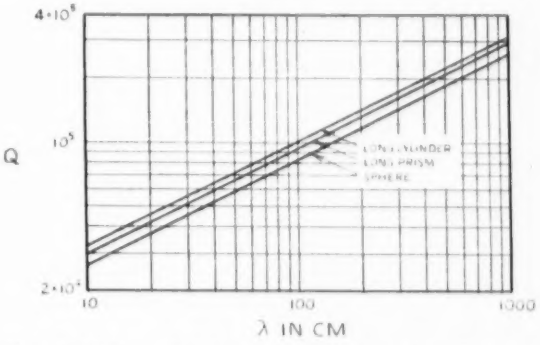

FIG. 5. Values of Q for various shapes of resonator are plotted against λ. The resonator material is taken to be copper, $\rho=1.72\times10^3$ abohm cm.

III. Definition and Computation of Mutual Inductances

Although some cases can be devised in which resonators of the above type can be used without

[12] F. E. Terman, Trans. A. I. E. E. **53**, 1046 (1934).

auxiliary coupling apparatus this is not the usual case and the question arises, how can we make use of such resonators in conventional circuits? One way of doing this is illustrated in Fig. 6 (a) where a loop is inserted into the resonator in such a way as to encircle magnetic flux if the resonator is excited in the desired mode of oscillation. Then a voltage will appear across the ends of the loop and, by analogy with lumped constant circuits, we may expect the arrangement to act more or less like the equivalent circuit shown in 6 (b).

The appropriate constants can be defined just as before. Then we defined a Lagrange function as the integral of $(\mathbf{B}^2-\mathbf{E}^2)/8\pi$ and wrote this as a quadratic function of q and $\dot{q}$ and called the coefficient of the $\dot{q}^2$ term $L/2$. Now, however, we need two quantities $\dot{q}$, one, say $\dot{q}_1$ for the resonator current, the other, $\dot{q}_2$, for the current in the loop. Then if we again reduce $\mathfrak{L}$ to a quadratic function of the q and $\dot{q}$ and if we define the coefficient of $\dot{q}_1\dot{q}_2$ to be M then the ordinary equations used with circuits like 6b will be identical with the Lagrange equations that insure that Maxwell's equations will hold.

In certain cases the above outlined calculations can be performed approximately. This we proceed to do.

It will be assumed that the loop is small compared to the wave-length, that the current distribution in the loop is uniform, that the field and current distribution of the resonator are unaffected by the presence of the loop, and *vice versa*. These assumptions are not independent; in fact they are all satisfied if the loop is very small compared to both the resonator and the wave-length. For notation, let all quantities with subscript 1 refer to the resonator, those with 2 to the loop.

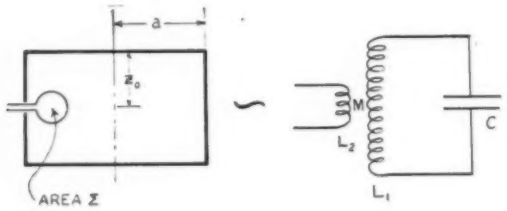

(a) (b)

FIG. 6. Resonator with coupling loop and lumped constant circuit which is equivalent.

Then

$$\frac{1}{8\pi}\int \mathbf{B}^2 d\tau = \frac{1}{8\pi}\left[\int \mathbf{B}_1^2 d\tau + 2\int \mathbf{B}_1\cdot\mathbf{B}_2 d\tau + \int \mathbf{B}_2^2 d\tau\right]. \quad (12)$$

We are interested only in the center term. In fact

$$M = \frac{1}{4\pi i_1 i_2}\int \mathbf{B}_1\cdot\mathbf{B}_2 d\tau. \quad (13)$$

Write $\mathbf{B}_1$ as derivable from a vector potential $\mathbf{A}_1$. Then after reductions using various vector identities and the fact that $\mathbf{B}_2$ satisfies Maxwell's equations we find

$$\int \mathbf{B}_1\cdot\mathbf{B}_2 d\tau = \int \mathbf{A}_1\times\mathbf{B}_2\cdot d\boldsymbol{\sigma} - \int \mathbf{E}_2\cdot\mathbf{E}_1 d\tau. \quad (14)$$

The last term is of the nature of an electrostatic coupling and can be neglected when the loop is in the region of weak electric field.[13] We assume this to be so. The remaining surface integral is to be taken over a surface which includes all the space inside the resonator except that occupied by the wire of the loop. It is readily verified that the integral comes to zero over the surface of the resonator because $\mathbf{A}_1$ has no tangential component there. The integration over the surface just outside the loop is done in two stages. See Fig. 7 for notation. First we integrate around a small closed path just surrounding the wire of the loop, this gives $4\pi i_2$; then the remaining line integral around the loop is transformed by Stokes' theorem. Thus

$$\int \mathbf{A}_1\times\mathbf{B}_2\cdot d\boldsymbol{\sigma} = \int \mathbf{A}_1\cdot d\mathbf{s}' \int \mathbf{B}_2\cdot d\mathbf{s}$$

$$= 4\pi i_2 \int \mathbf{A}_1\cdot d\mathbf{s}' = 4\pi i_2 \int \mathbf{B}_1\cdot d\boldsymbol{\sigma}' = 4\pi i_1 i_2 \alpha. \quad (15)$$

$$M = \alpha, \quad (16)$$

where αi_1 is the total flux due to the resonator that passes through the loop.

If the loop is sufficiently small the flux through

[13] This reminds us that it will also be possible electrostatically to couple an external circuit to the resonator.

it can be approximated by its area, say Σ, times the field at the center of the loop. If so

$$M=4\pi\frac{\mathbf{A}_1\cdot\Sigma}{\int\mathbf{A}_1\cdot d\mathbf{s}}, \tag{17}$$

where the $\mathbf{A}_1$ in the numerator is taken at the center of the loop.

For many purposes a more useful quantity than M is M/L. This is easily found to be

$$\frac{M\omega}{L\omega}=\frac{\Sigma\cdot\mathbf{A}_1\int\mathbf{A}_1\cdot d\mathbf{s}}{\int\mathbf{A}_1^2 d\tau}. \tag{18}$$

To order of magnitude this quantity is the ratio to the area of the loop to half the (vertical) sectional area of the resonator. Its exact value is given in Table I. Computable with the aid of this quantity is the impedance coupled into the loop circuit. Values of this, at resonance, are also given in Table I.

IV. Miscellaneous Results

In addition to the above we have accumulated a number of results not easily classified but which may well be of use to some one. These we present in this section.

It has been found that, for mechanical reasons, the square prism type of resonator is very convenient. In some cases a regular n-sided prism would be convenient and formulae for use with such a shape would be of use. The losses are not different enough to be worth worrying about but one often wants to know λ fairly closely so we have attempted an approximate calculation. For a wave function we took

$$\mathbf{A}=\mathbf{k}_z(J_0(kr)+\beta\cos n\phi J_n(kr)), \tag{19}$$

which is an exact solution of the wave equation and then adjusted β in such a way that the surface on which $\mathbf{A}=0$ was flat at the center of the sides of the prism. Thus the boundary conditions are approximately fulfilled. The resulting value of λ is

$$\lambda=2.61a(1+1/n^2) \tag{20}$$

with a the distance from the center of the prism to the center of any of the n sides. This formula will give a value of λ that is slightly low and some other approximate fit of the boundary conditions would give a different and perhaps better coefficient for the term in $1/n^2$. On the other hand the result is undoubtedly of the right form

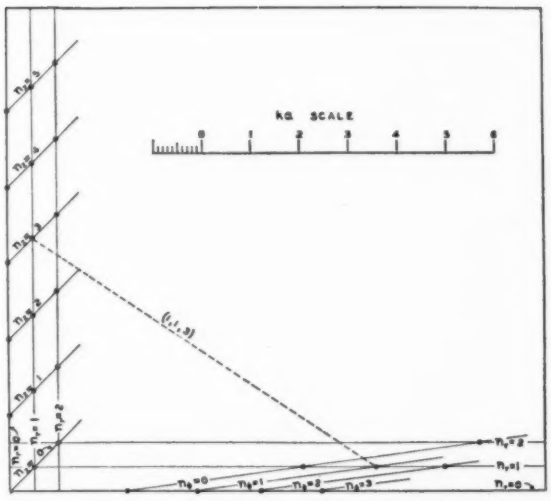

Fig. 8. Chart for finding the natural frequencies of a cylindrical resonator for any mode of oscillation with electric field of the type A_3. To find ka for the (n_r, n_ϕ, n_z) state enter the chart at the horizontal line marked n_r, find the point where this line intersects the n_ϕ line, then find the point where the vertical n_r line intersects the desired n_z line. The distance between these two points is then equal to ka. For example, the dotted line shows a ka of 8.45 for $(n_r, n_\phi, n_z)=(1, 1, 3)$. $k=2\pi/\lambda$ and a equals the radius of the cylinder. We are greatly indebted to Mr. J. R. Woodyard for permission to exhibit this ingenious construction.

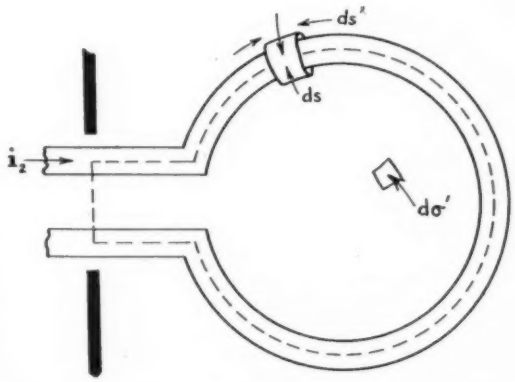

Fig. 7. Illustrating the notation used in Eq. (15). The original integration in Eq. (14) was to be over a tubular surface surrounding the wire of the loop. A short piece of this is shown. In doing the integration as in (15) one first integrates around the wire (using ds) and then along the wire using an element of length ds'. The integral is then transformed to a surface integral over the surface bounded by the dotted lines, the area element is called $d\sigma'$.

and it actually comes pretty close as may be verified in the case $n=4$ where the exact answer is available. There the exact answer is $\lambda=2.83a$ and Eq. (20) gives $\lambda=2.78a$, an error of 2 percent.

A question of some interest is that of the frequencies corresponding to the higher modes of oscillation. For cylindrical resonators oscillating in a way analogous to that of Fig. 3 these are determined by

$$(ka)^2=\left(\frac{n_z\pi}{2}\frac{a}{z_0}\right)^2+x^2, \qquad (21)$$

where x is any root of a Bessel function of integral order. The form of this equation suggests the geometry of the right triangle and Mr. J. R. Woodyard has devised a very ingenious graphical method based on this observation for finding the possible values of ka. This is shown in Fig. 8.

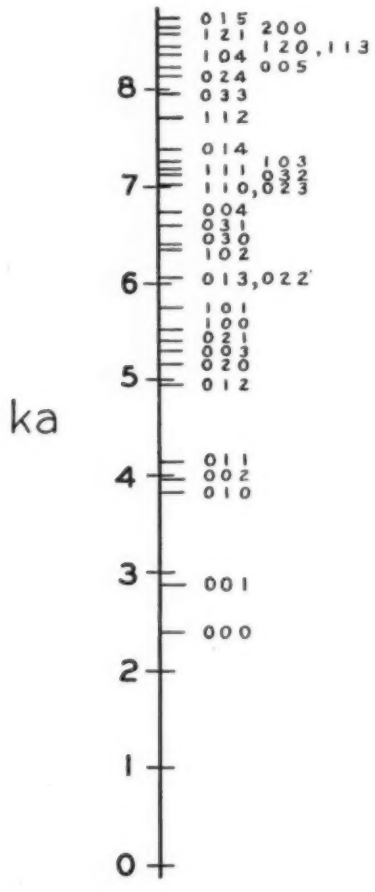

FIG. 9. Chart showing the allowed frequencies up to $ka=8.58$ for a cylindrical resonator with $z_0=a$. Only oscillations analogous to those of Fig. 3 are considered.

TABLE II. *Values of equivalent inductance, capacity, etc., for a cylindrical resonator working in a state like that of Fig. 3 but with radial nodes specified by the number n. The value n=1 corresponds to the lowest mode as in Fig. 3 and Table I. The values in this table are only approximate as they depend on an asymptotic formula for Bessel function roots. Note particularly that the quantity δ which appears in some of the formulae is itself a function of frequency and so of n.*

$$\lambda=2\pi c(LC)^{\frac{1}{2}}=\frac{2a}{n-1/4}$$

$$\left(\frac{L}{C}\right)^{\frac{1}{2}}=2\pi(n-1/4)\frac{z_0}{a}c$$

$$Q=1.414\,\frac{a}{\delta}\,\frac{1}{1+\frac{1}{2}(a/z_0)}$$

$$L=4\pi 0.159 z_0$$

$$C=\frac{1}{4\pi c^2}\,\frac{0.637}{(n-1/4)^2}\,\frac{a^2}{z_0}$$

$$\text{Series } R=\frac{1}{Q}\left(\frac{L}{C}\right)^{\frac{1}{2}}=0.450\frac{z_0\rho}{a\delta}\left[1+\frac{1}{2}\frac{a}{z_0}\right]$$

$$\text{Shunt } R=Q\left(\frac{L}{C}\right)^{\frac{1}{2}}=8.88\frac{z_0}{\delta}(n-\tfrac{1}{4})\frac{1}{1+\frac{1}{2}(a/z_0)}c$$

The states are ordered by "quantum numbers" n_r, n_ϕ, n_z, which give the number of r, ϕ, and z nodes. To show how rapidly the number of possible states increases with increasing numbers of nodes we have prepared Fig. 9 which shows all the states up to $ka=8.58$ for a cylindrical resonator with $z_0=a$.

There are so many of these higher states that it is hopeless to try to compute $(L/C)^{\frac{1}{2}}$ and Q values for them all. However, we have had some use for the states in which there are no φ nodes and also no z nodes. Because of the fortunate existence of a good asymptotic formula for the roots of J_0 approximate results for this case are easily obtained.[14] Since they show in a general way what can be expected of the higher states these results are reproduced in Table II.

A practical question that often comes up is how much energy is lost through holes that may be put in the resonator, for example holes for leads from a coupling loop. This question may be answered by using some calculations due to Lord Rayleigh. He found an expression for the energy passing through a small circular hole in an infinite plane conductor illuminated on one side by plane waves.[15] Using his expression and

[14] The formula used is due to Stokes and though it is an asymptotic formula, valid for $n\to\infty$, it actually works to about 2 percent for $n=1$. See Watson, *Theory of Bessel Functions*, p. 505.

[15] Lord Rayleigh, Phil. Mag. **44**, 28 (1897).

considering the field inside the resonator as built up of a superposition of plane waves we find the following expression which is a measure of the losses due to radiation through a hole of area $\Sigma \ll a^2$ in the side of a square resonator.

$$\pi \frac{\text{Energy stored}}{\text{Energy lost per half-cycle}} = Q' = \frac{27\pi^3}{16\sqrt{2}} \left(\frac{a^2}{\Sigma}\right)^3 \frac{z_0}{a}. \quad (22)$$

It will be seen that it is easy to make such losses negligible.

V. Experimental Confirmation

The present paper deals entirely with the theory of these resonators and it is not proposed to enter into any of the experiments that have been done. Nevertheless we may mention that a large fraction of the theory here developed has been examined experimentally with the result that the theory is verified at all points tested. In particular a number of measurements of wavelengths have been made, the formula for M has been tested very roughly, and measurements of Q have been made for one resonator. In the latter measurement Q was experimentally found[16] to be 49,400±5 percent for a particular resonator; the computed value was 53,000. This value of Q corresponds to a greater frequency stability than that usually obtained from a quartz crystal.

[16] We are greatly indebted to Mr. J. R. Woodyard, who made this measurement for Q, for allowing us to state this provisional result in advance of publication. He hopes to improve the accuracy somewhat and publish a description of the measurements and the methods used.

Electrical Conduction in Quartz, Periclase, and Corundum at Low Field Strength

E. G. Rochow
General Electric Company, Schenectady, N. Y.
(Received June 20, 1938)

1. A method has been devised for measuring the electrical conductivity of single crystals at elevated temperatures and at field strengths below 3 volts per mm. 2. The conductivities of single crystals of quartz, periclase, and corundum have been measured by this method over a temperature range of 600° to 1400°C, in equilibrium with air. 3. The increase of conductivity with temperature follows a single exponential relation in all cases, throughout the temperature range covered. Experimental curves and a table of interpolated values are given.

MUCH of our knowledge of conduction in silica, magnesia, and similar oxides is confused and contradictory. The extent of conduction, its variation with temperature, and even the manner in which the current is carried, are not known with any degree of assurance. Indeed, a "specific conductance" for quartz, in the sense of a material constant for the pure substance, would be difficult to assign within several decades,[1] despite the fact that the electrical properties of quartz have been studied for half a century.

Recent advances in the general study of conduction in solids have revealed some of the reasons for this state of confusion. For one thing, the term "pure" has acquired a more rigid meaning; extremely minute amounts of a foreign substance may markedly alter the conductance of a solid.[2] There is a growing number of compounds known to be excess or deficiency semiconductors[3] and these are sensitive to very small excesses of one of the normal components of the solid. Hence "pure" compounds, with strictly stoichiometric proportions, have seldom been used in investigations; in some cases they are likely to remain but a hypothetical possibility.

In addition to the question of purity, it is known that conduction in nonmetallic solids also is influenced by particle size,[4] by field strength,[5] by phase changes,[6] and sometimes by unique properties of the substance itself. Again taking quartz for an example, the anomalous charge and discharge currents offer a serious obstacle to the determination of the steady-state d.c. conductivity. At room temperature the conduction current is very small and is obscured by the slow charging current which decreases according to the relation

$$\kappa = aZ^{-n},$$

where Z is the time, and a and n are constants for a given temperature.[7] There is a normal charging current which is instantaneous, but this anomalous charging current will persist for very long periods.[8]

Obviously any measurement of conductance under such conditions is purely arbitrary, for the magnitude of the current will depend more upon the operator's patience than upon the conduction characteristics of the crystal. As the temperature is increased, however, the conductivity rises exponentially while the charging current is but little affected. Hence at sufficiently elevated temperatures the charging current becomes insignificant, and the conductivity may be measured directly. Surface leakage is eliminated at the same time. For these reasons, an extrapolation to room temperature of the conductivity curve is likely to give a more reliable indication of the true conductivity than direct measurement.

[1] Sosman, *The Properties of Silica* (Chemical Catalog Co. 1927), Chapter 27.
[2] Ebert and Tubandt, *Handbuch der Experimentalphysik, Teil* 1, p. 419 *et seq.*
[3] Ebert and Tubandt, reference 2, p. 446.
[4] Reference 2, p. 420.
[5] Reference 2, p. 422.
[6] Reference 2, p. 431.
[7] Curie, Comptes rendus Acad. Paris **103**, 928 (1886); Ann. Chim. et Phys. **18**, 203 (1889).
[8] Likewise, the slow discharge current will continue to come out of the crystal long after the normal discharge has ceased. H. H. Race reports currents still obtainable from a quartz crystal after the electrodes had been short circuited for a month (see J. A. I. E. E. **788**, 1 (1928)).

In the matter of field strength, the experimenter faces an arbitrary choice. It has been reported repeatedly that oxides like silica increase in conductivity as the potential rises, in a manner approximating Poole's equation [9]

$$\kappa = ae^{bx} \text{ where } x \text{ is the field strength.}$$

If a galvanometer or electrometer method be used to measure resistance, in order to attain the level of sensitivity of the instrument at low temperatures the potential must be increased many fold. A bridge circuit imposes the same requirement. Thus any variable-potential technique superimposes Poole's law on the temperature-conductivity characteristic, giving the latter a false slope.

It seems probable that "specific conductance," as a material constant, is a term without meaning for such oxides. Comparative measurements may be informative, however, if made on single crystals over a wide range of elevated temperatures, in equilibrium with air,[10] and at a constant low potential. The experiments described in this paper represent an approach of this nature.

Experimental

The experimental conditions which were chosen were: a temperature range of 200 to 1200°C; an isothermal arrangement of crystal, electrodes, and leads; and a circuit permitting a constant potential sufficiently low to prevent avalanche effects or breakdown at the elevated temperatures.

The electrode supports shown in Fig. 1 were designed to fit within a large platinum-wound furnace. They were shaped from talc blocks, the upper one being in one piece and having a projecting area 1 cm square, ground flat, on its under surface. This flat area was covered with thin platinum sheet, the platinum lead coming out through the block as shown.

The lower block had a small hemispherical depression cut in the center of its upper surface, and a separate talc piece was shaped with one side flat and square, the other side bearing a hemispherical projection. This projection fitted into the depression of the lower block to form a ball-and-socket joint that would automatically align the electrodes parallel to the crystal faces. This movable lower electrode had its surface covered with thin platinum sheet, and a coil of thin platinum wire allowed flexible connection with the lead emerging from the block.[11]

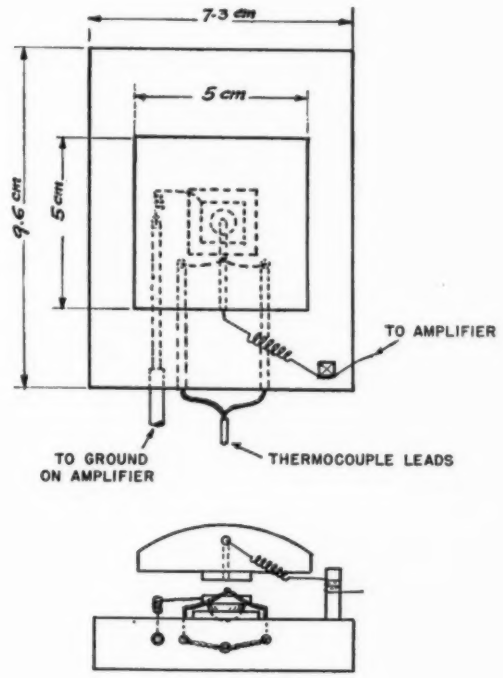

Fig. 1. Electrode blocks.

These talc electrode blocks were fired to characteristic hardness at 1300°C, without any considerable change in dimensions. In use, a thin plate obtained from a crystal of the substance to be studied was placed on the lower platinum electrode, and the upper electrode was then centered on the crystal so that its weight was borne entirely by the crystal, and the talc blocks were nowhere in contact.[12]

[9] H. H. Poole, Phil. Mag. **32**, 112 (1916); **34**, 195 (1917); **42**, 488 (1921).

[10] Measurements in vacuum are excluded because MgO and similar oxides are known to be excess semiconductors under such conditions. See Podszus, Zeits. f. Elektrochem. **39**, 75 (1933).

[11] A guard ring electrode system was considered, but was discarded because of the impossibility of separating guard and test electrodes with insulating material superior to the substances to be measured. The necessity for a guard is minimized by the absence of surface moisture under test conditions.

[12] Some crystals were coated on two sides with metal by the usual method of brushing on an oil suspension of Pt and Au compounds and firing to 800°. It was found that such crystals gave temperature-conductivity curves of

This assembly was then inserted in an alundum muffle furnace having an interior 36 in. long, 3½ in. wide, and 2½ in. high, with a uniform hot region 18 in. long. In order to measure the temperature of the specimen, a thermocouple was supported by the lower block adjacent to the crystal electrodes as shown. The insulated leads were brought to the mouth of the furnace and connected to a precision potentiometer capable of measuring the e.m.f. within 0.01 mv.

Leads for the electrodes were thin Pt wires. The lower lead was insulated from the thermocouple wires and was grounded. The upper lead was a bare wire, supported in the furnace by a long, slender crystal of periclase fastened in the lower block, and emerging from the hot region of the furnace without other supports. Outside the furnace this lead passed through an earthed shield directly to the input terminal of the amplifier circuit. The metal furnace case was grounded, and the heating current was shut off during measurements.

Since maximum fields of about 10 volts per cm were desired, the corresponding currents to be measured were known to be as low as 10^{-14} amp. In order to measure such currents, the d.c. amplifier circuit shown in Fig. 2 was set up. An FP 54 vacuum tube is used with a variety

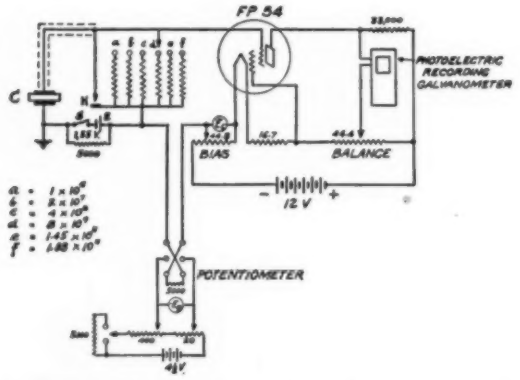

FIG. 2. D.C. amplifier for conductivity measurements.

of shunt resistors in the grid circuit so that a million-fold range in currents may be covered with not more than 1 volt impressed on the sample. A photoelectric recording galvanometer in the plate circuit provides a record of every measurement.

To operate the amplifier, the grid bias is set at −3.0 volts with switch S open and an appropriate grid resistor in place. The galvanometer is then adjusted to its zero point, and the switch S is closed. The resulting current through the sample and grid shunt resistor causes a net change of potential of the control grid which results in a deflection of the recording galvanometer. By appropriate adjustment of the potentiometer circuit this change in grid potential is balanced out and the galvanometer brought back to zero. The potentiometer voltmeter then reads $-Eg$, where Eg is the change in grid potential caused by closing the switch S. Knowing $E(=1.55$ v), Eg, and the value of the grid resistor, the current through the sample and its resistance were calculated.

When used in this manner, the amplifier is a null-point device that is simple to operate and requires no previous determination of the mutual conductance curves.

Results for quartz

Data are plotted in Fig. 3 for a plate of quartz $1.45\times1.45\times0.0394$ cm, cut parallel to the C axis of a crystal and parallel to one of the prism faces.[13] Data for two runs are indicated by squares and circles, in order to show the degree of reproducibility.

Sample records of the measurements on quartz are shown in Fig. 4. At 30° the charging current falls off exponentially with time, as found by previous investigators. At 282° the charge and discharge curves assume a different form, but a steady state is still difficult to define. At 513° the d.c. conduction has almost obscured the polarization effect. The temperature at which the polarization became too small to show on the record of d.c. conduction was taken as the lowest temperature for reliable observa-

slope greater than those of the uncoated crystals. When an attempt was made to coat crystals of NaCl in the same manner, the coating seemed to be absorbed by the crystal; in crystals of KI blue color centers were produced by such absorption. It seems evident that crystals are altered internally by the platinizing process, and therefore only measurements on unplatinized crystals are reported herein. The flat surfaces of crystal and electrode with soft Pt foil between them were considered to provide adequate contact under the load of about 100 g per cm.[2]

[13] This orientation permits measurement of the conductivity in a direction perpendicular to the C axis, designated as "equatorial conductivity" by Sosman (*Properties of Silica*, Chap. 27).

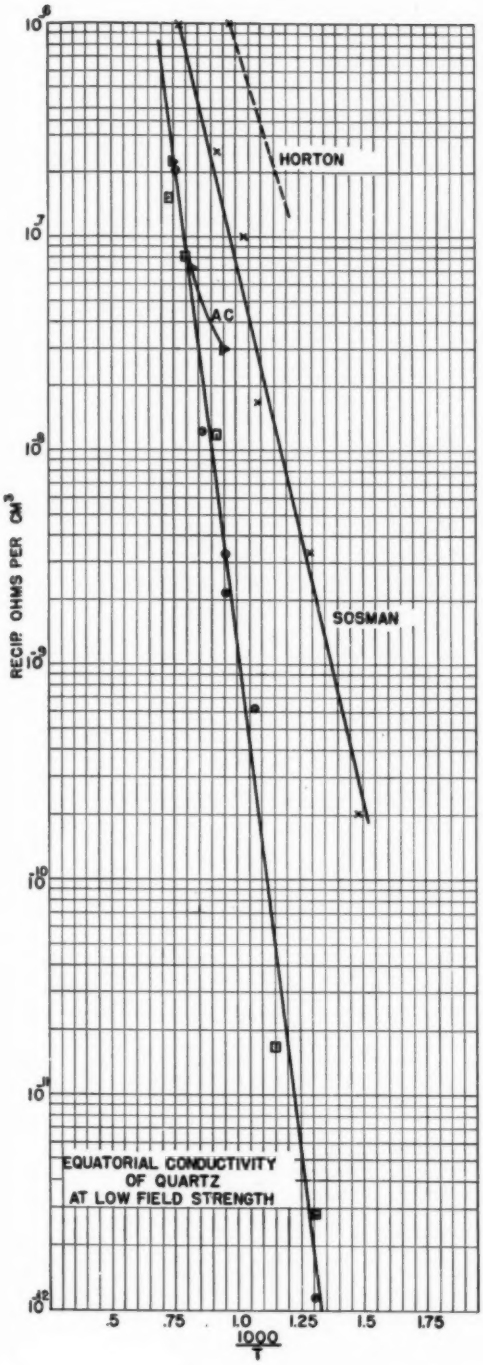

FIG. 3. Equatorial conductivity of quartz at low field strength.

tions. For quartz, this temperature was about 550°

Above 1100° the conductivity became too large to measure with the d.c. amplifier, and

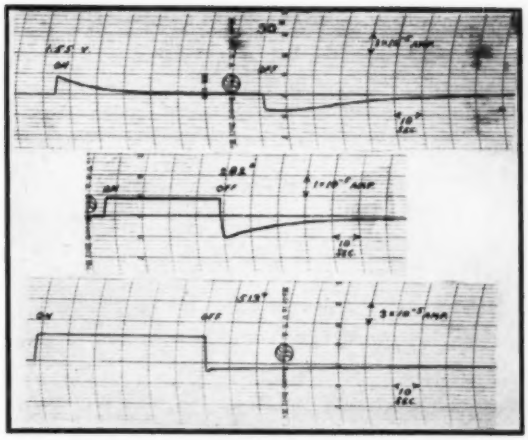

FIG. 4. Sample records of the measurements on quartz.

several measurements therefore were made with an a.c. bridge that passed 1 ma through the sample at a variable potential of 10 to 800 volts. These data are plotted on Fig. 3, together with values taken from Sosman[14] and an extrapolation of Horton's curve.[15] Table I gives interpolated values of conductivity taken from the curve of Fig. 3. It will be noticed that at the lower conductivities (high potential applied to sample) the a.c. curve departs from the low potential d.c. curve and assumes a slope comparable to that of the Horton curve, which was obtained with relatively high and increasing potential.

TABLE I. *Interpolated values of conductivity for quartz and periclase.*

TEMPERATURE, °C	COND. QUARTZ	COND. PERICLASE
500	2.1×10^{-12}	7.7×10^{-12}
600	4.6×10^{-11}	7.4×10^{-11}
700	6.4×10^{-10}	4.9×10^{-10}
800	5.2×10^{-9}	2.2×10^{-9}
900	3.0×10^{-8}	7.8×10^{-9}
1000	1.2×10^{-7}	2.2×10^{-8}
1100	4.0×10^{-7}	5.6×10^{-8}
1200	1.1×10^{-6}	1.2×10^{-7}
1300	—	2.3×10^{-7}
1400	—	4.0×10^{-7}

Results for periclase (MgO)

While crystals of periclase obtained by the fusion of calcined magnesite are available,[16] such

[14] *The Properties of Silica*, p. 528.
[15] Horton, Phil. Mag. **11**, 505 (1906).
[16] Strong and Brice, J. Opt. Soc. Am. **25**, 207 (1935).

crystals contain appreciable quantities of CaO and other oxides, and therefore are unsuitable for conductivity measurements.

In order to grow crystals of pure periclase for this investigation, MgO was first obtained by hydrating bars of metallic Mg (of the highest grade commercially available) and calcining the hydroxide at 800°. This oxide was then fused in a 70 kw a.c. arc with graphite electrodes, producing a polycrystalline ingot of periclase. Crystals were selected from the crushed ingot and placed on a layer of powdered periclase at the base of the arc furnace. The furnace was started again and MgO was added continuously at the top, so that a deepening pool of liquid collected above the selected crystals, which were to act as seeds. As the arc current was gradually reduced over a period of several hours, columnar crystals grew into the liquid at various orientations. After cooling slowly, irregular crystals as large as $1.5\times1.5\times3$ cm were broken from the mass, and plates of clear periclase larger than 1 cm square could be cleaved from these crystals. Spectrographic analysis of the crystals revealed minute traces of Cu and Mn, but no other impurity. Since periclase exhibits perfect cubic cleavage, the plates which were obtained required no grinding.

Conductivities were measured by the procedure previously described, and the results for a sample 0.0814 cm thick are shown in Fig. 5. Two sets of data are indicated by squares and circles. The results obtained by Goodwin and Mailey[17] with rods of fused MgO are shown for comparison. Table I contains interpolated values taken from Fig. 5.

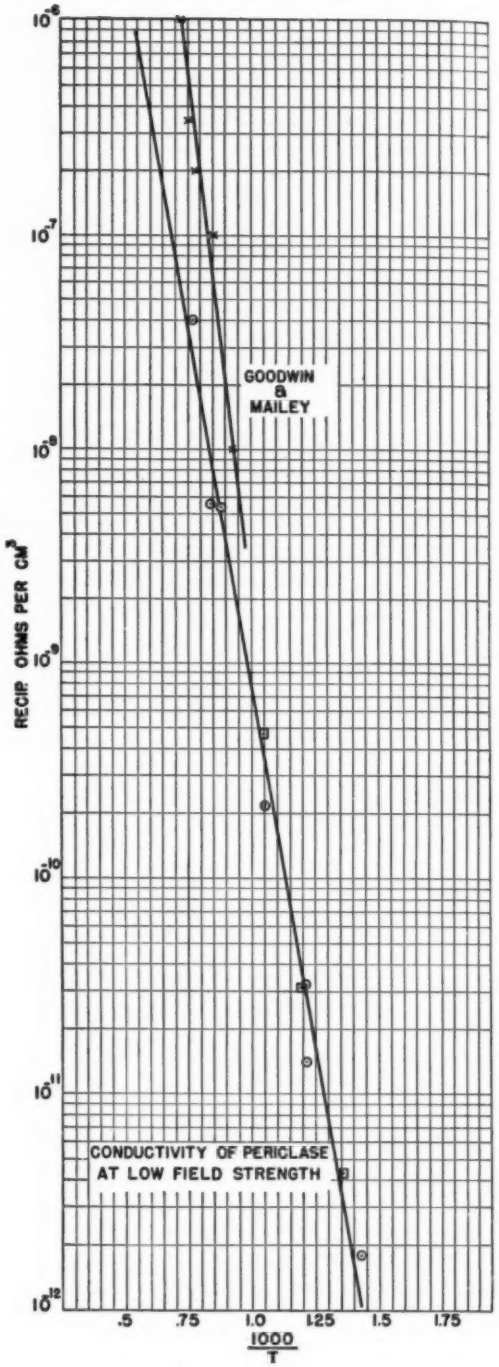

FIG. 5. Conductivity of periclase at low field strength.

Results for corundum (Al_2O_3)

A semicircular section cut from a colorless boule of artificial sapphire (fused Al_2O_3) was measured with the same apparatus employed for quartz and periclase. The first results gave a plot of log κ *vs.* $1/T$ which had a small but constant curvature. Subsequent measurements did not reproduce this curve, but gave a more linear result. After holding at 1200° for several hours, a third set of data was taken, and this gave a linear plot. Because the reasons for the change in behavior with heating are not known, it cannot be said that the latter data represent the true conductivity. It seems probable, however, that they are the most reliable. Experi-

[17] Goodwin and Mailey, Phys. Rev. **23**, 22 (1906). See also Rousseau, Chim. et Ind. 755–8, April (1934).

mental points from the linear curve are as follows:

t°C	$1/T\times10^{3}$	Spec. Cond.
565	11.9	2.74×10^{-12}
846	9.0	2.06×10^{-9}
1155	7.0	1.02×10^{-7}
1234	6.6	1.96×10^{-6}

Discussion

The measurements which are described in this paper indicate that the equatorial conductivity of quartz at very low potentials is considerably less than the published values obtained at high potentials, and that the difference manifests itself as a greater slope of the temperature-conductivity curve. This suggests the existence of an exponential relation between conductivity and field strength. For the fields used in this work, the slope of the temperature characteristic corresponds to an activation energy of 41.2 Kcal.

The temperature-conductivity curve for periclase indicates an activation energy of 30 Kcal. Because of the different slopes of the quartz and periclase curves, they cross at a point corresponding to 650°C. Below this temperature the quartz is a better insulator than the periclase; above this temperature the periclase is superior.

While the potentials used in this study varied by only a few tenths of a volt, in no case was there a sudden increase in conductivity within this range, indicating no discharge of ions. Within these narrow limits, the conduction appeared to be ohmic. It seems probable that the mechanism in these oxides is electronic in nature, and resembles that in semiconductors.

The curves for both quartz and periclase show no discontinuities, and therefore conform to a simple conductivity relation

$$\kappa = ae^{-E/RT},$$

where E has the values previously given. There is no evidence of an ionic component entering in the conduction at the higher temperatures.

The author wishes to thank Drs. Louis Navias and Frederick Seitz for many helpful suggestions.

The Effect of Pressure on the Viscosity of Boric Anhydride Glass*

Ernest B. Dane, Jr., and Francis Birch
Harvard University, Cambridge, Massachusetts

(Received June 6, 1938)

The effect of pressure on the viscosity of B_2O_3 glass has been determined by a high pressure capillary flow method up to about 2000 kg/cm², at two temperatures, 516° and 359°C. The results are satisfactorily represented by the expression $\eta=\eta_0 e^{\alpha p}$, with $\alpha=4.6\cdot10^{-4}$ cm²/kg at 516°, $\alpha=15\cdot10^{-4}$ cm²/kg at 359°. The ratio of the viscosity at 1000 kg/cm² to the viscosity at 1 atmosphere is therefore 1.58 at 516°, 4.48 at 359°. The results are briefly compared with those for organic liquids.

1. Introduction

NUMEROUS studies have been made of the viscosity of glass as a function of temperature and composition, which is evidently a subject of fundamental importance for the glass manufacturer. Other factors influencing the viscosity of glass, which are of interest primarily to the geological sciences, are the pressure and the presence of volatile components in solution. The effect of these factors does not appear to have been investigated for glass-forming materials. The magnitude of the effect of pressure

* Paper No. 46, published under the auspices of the Committee on Geophysical Research and the Division of Geological Sciences at Harvard University.

upon the viscosity of a large number of liquids of initially low viscosity has, however, been measured by Bridgman,[1] and correlated with the complexity of the molecular structure. Similarly, the effect of temperature upon viscosity has been related by Sheppard[2] to the effective molecular weight in the liquid state. Wolarowitsch and Leontjewa[3] have used Sheppard's theory to calculate the number of associated molecules in glasses of SiO_2 and B_2O_3; they find that the effective molecular weight corresponds, in B_2O_3 glass, to 53 molecules at 500°C, to 73 at 350°. These considerations lead us to anticipate an important effect of pressure upon the viscosity of glasses of even the simplest chemical composition.

In order to reduce the viscosity of most glasses, especially of silicate glasses, to an order of magnitude such that many of the more reliable methods of measuring viscosity can be applied, the temperature must be raised to from 400° to 1000°; there are evident difficulties in combining these temperatures with enough pressure to give measurable effects. There is the further serious difficulty that the dependence of viscosity upon temperature is so great that extremely close control of the temperature is essential. With these two factors in mind, we have chosen for an initial study a material of no geological importance, but one which is characterized by a low viscosity and also by an unusually low temperature coefficient of viscosity. This material is anhydrous boric trioxide, B_2O_3; an additional advantage in using this glass is that it has recently been the subject of a number of studies of its density, viscosity and other properties, as functions of temperature at ordinary pressure.[4] The reasonably good agreement between the results of different investigators for the viscosity-temperature curve indicates the reliability of B_2O_3 for the present purpose. Studies with the rotating-cylinder viscometer have demonstrated, moreover, the absence of a "yield point," or of any departure from purely viscous behavior, for temperatures above approximately 300°.

The method which we have adopted was originally used by Barus;[5] with refinements of technique and of theory, it has been employed by Hersey and Snyder[6] for a study of the effect of pressure on the viscosity of oils. The material under investigation is forced from a high pressure cylinder in which a constant pressure is maintained, through a capillary tube into the open air, where it is collected and weighed after a measured time interval. The rate of flow is found as a function of the pressure at the inner end of the capillary and from this relation may be derived the dependence of the viscosity upon pressure.

2. Apparatus and Procedure

With this method, the parts in which the high pressure is established, including the capillary, must all be maintained at the required high temperature. We have used one variety of stainless steel (Allegheny 44), for the pressure cylinder, and another (Allegheny metal), for the capillary and connecting pipe. The arrangement of the principal parts is shown in Fig. 1. The cylinder (A) is surrounded by a heavy copper cylinder (B), which in turn is placed centrally in a much longer tubular, wire-wound resistance furnace. Pressure is generated in a hydraulic press, of the type used by Bridgman, and measured by the change of resistance of a 200-ohm manganin coil, mounted in a cylinder at room temperature. The pipe (F) leads from the high temperature cylinder (A) to a block with two valves outside the furnace; from this block runs another pipe to the hydraulic press. The two valves are arranged to permit the sudden application or release of the pressure in the cylinder (A). The glass is extruded from the capillary (E) at the bottom, where it is collected by appropriate methods.

The pressure medium was nitrogen; originally the gas was allowed to act directly upon the glass

[1] P. W. Bridgman, *The Physics of High Pressure* (Macmillan, New York).
[2] S. E. Sheppard, Nature **125**, 489 (1930). S. E. Sheppard and R. C. Houk, J. Rheology **1**, 349 (1930).
[3] M. P. Wolarowitsch and A. A. Leontjewa, Acta Phys. U. S. S. R. **7**, 357 (1937).
[4] G. S. Parks and M. E. Spaght, Physics **6**, 67 (1935). M. P. Volarovich and D. M. Tolstoi, Trans. Soc. Glass Tech. **18**, 209 (1934). K. Arndt, Zeits. f. Elektrochem. **13**, 578 (1907). M. P. Wolarowitsch, Acta. Phys. U. S. S. R. **2**, 695 (1935). S. B. Thomas and G. S. Parks, J. Phys. Chem. **35**, 2091 (1931).
[5] C. Barus, Am. J. Sci. **45**, 87 (1893).
[6] M. D. Hersey and G. H. S. Snyder, J. Rheology **3**, 298 (1932).

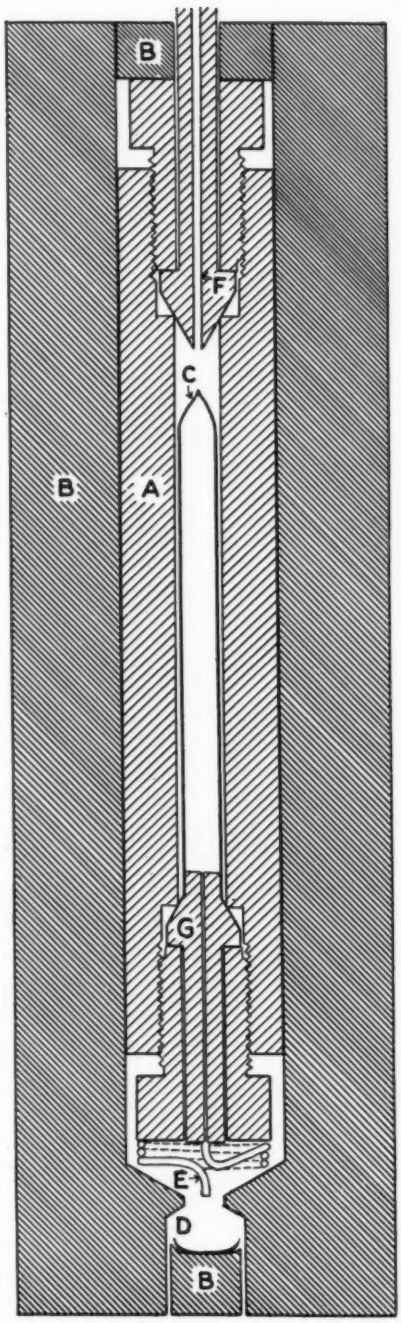

FIG. 1. Arrangement of high temperature cylinder and capillary.

in cylinder (A), but it was soon found that enough gas dissolved in the glass to produce frothing when the pressure was released, and to carry glass into the cool part of tube (F), which became plugged after a few runs. A seal of molten tin used in an effort to separate the glass from the nitrogen apparently contaminated the glass. The final arrangement, which proved convenient as well as satisfactory, was to draw the molten glass by gentle suction into a thin-walled drawn copper tube (C), silver-soldered to the plug (G) which connects the capillary to the cylinder (A). When filled, the copper tube was closed and soldered at the top, and mounted as indicated in Fig. 1. Under pressure, this tube readily collapsed upon the glass, forcing it out through the capillary, with no direct contact between glass and nitrogen. A pressure difference of less than one atmosphere was required to flatten the copper tubing.

Constancy of temperature, essential for the success of this work, was assured by a thyratron control circuit and a resistance thermometer, described by Benedict,[7] with certain improvements for which we are indebted to Mr. Dennison Bancroft. The temperature remained constant to within about 0.1°C, as measured by a chromel-alumel thermocouple inserted in the wall of the copper block near the capillary; runs were not started until the thermocouple had indicated the desired temperature for several hours.

Measurements were made successfully at two temperatures, around 500° and around 350°. The viscosity of the glass is so different at these two temperatures that very different methods of collecting samples were necessary. Near 500°, where the viscosity is about 10^4 poises, the glass issuing from the end of the capillary spread over the end of the tube until enough accumulated to form a drop; when this drop fell, it carried with it a thread, which continued to spin out from the mass on the end of the capillary until the pressure was released. After a time the thread would part somewhere in the middle. At this temperature, the glass was caught in a small platinum cup (D), placed near the end of (E), which could be removed for weighing after the flow had stopped. The amount of glass remaining on the end of the tube was somewhat variable and could not be measured; a large part of the irregularity of the results at this temperature is probably to be ascribed to this cause. All attempts to wipe or cut off the last drop were defeated by the

[7] Manson Benedict, Rev. Sci. Inst. **8**, 252 (1937).

tendency of the glass to stick to everything it touches at this temperature. The effect of the last drop could be decreased by taking larger samples but this procedure, involving longer runs, increased the danger of temperature drift. At 500°, the viscosity changes by more than 2 percent per degree temperature change; the maximum change due to pressure was about 150 percent.

At 359°, where the viscosity is nearly 10^8, the glass was extruded as a straight rod slightly larger in diameter than the bore of the capillary, with no tendency to spread over the end of the tube. As this rod showed no inclination to drop off even if left overnight, it was easy to get accurate samples by cutting off the rod at the end of the tube with a special pair of nippers. As a result, more regular results were obtained at this temperature in spite of the fact that the viscosity changes here by 8 percent per degree.

Several sizes of capillary were used, with inside diameters of 0.041 and 0.063 cm at 500°, and of 0.159 cm at 359°, with lengths varying from 7 to 40 cm. The outside diameters were, respectively, 0.15, 0.23 and 0.80 cm. The shorter ones were almost entirely enclosed in the end of the pressure cylinder; the longer ones were coiled between this cylinder and the bottom of the copper block. Although the latter arrangement left the capillary somewhat more exposed to temperature fluctuations, with care equally smooth results could be secured in either case. The diameters of the capillaries were not measured accurately, since only relative values were needed, No great precision can be expected for the absolute viscosity, which agrees roughly, however, with the values of other observers.

The glass was prepared from Merck's "reagent" grade anhydrous B_2O_3 by fusing at 1100° in a platinum crucible, holding at this temperature overnight, with about an equal time at 900° under a water-aspirator vacuum. At the end of this time, the glass had been quiet and free from bubbles for several hours. The viscosity at 900° is of the order of 100 poises.

A total of about 3.5 g of glass could be extruded from the collapsible tubes. The times for the individual runs were regulated to yield about 0.2 g in each sample, so that 15 or more points, at different inlet pressures, could be obtained from a single charge. Since the duration of the runs was from 20 minutes to 10 hours, errors in the measurement of the time were negligible. The required pressure was built up in the press before the valve leading to the cylinder (A) was opened; the run was begun by suddenly opening this valve, and terminated by closing this valve and opening the release valve. Variation of inlet pressure during a run could be held within narrow limits by occasional pumping. At very low pressures, small changes of the zero of the manganin pressure gauge occasionally introduced uncertainties of as much as several percent. The chief sources of irregularity were temperature changes and variable retention of glass at the outside end of the capillary.

There is, however, a possibility of systematic error due to the heating effect of forcing the glass through the capillary. The mechanical energy lost in transporting a given quantity of glass from the upper pressure to the lower pressure is transformed into heat; if this heat were not dissipated, the rise of temperature of the glass in passage might be as great as 70° for a pressure difference of 1000 kg/cm². We wish to realize as nearly as possible an isothermal flow. This may be approached by diminishing the velocity for a given pressure drop, that is, by using longer or finer capillaries. The effect of the heating is evidently to reduce the viscosity, whereas the effect of pressure alone, for isothermal flow, is to increase the viscosity. If the flow were too rapid, the heating effects might completely mask the true pressure effect.

The temperature difference which can exist between the axis and the wall of the capillary even when equilibrium conditions are reached has been calculated by Hersey[8] and is negligibly small. The computation is more difficult when neither equilibrium nor adiabatic conditions exist; this case, which embraces all real experimental conditions, has been attacked by Hersey and Zimmer[9] with some success. Experimentally, the natural approach appears to be to decrease the velocity of flow for a given pressure drop, by using successively longer or finer capillaries. As the velocity is decreased, equilibrium is ap-

[8] M. D. Hersey, Physics **7**, 406 (1936).
[9] M. D. Hersey and J. C. Zimmer, J. App. Phys. **8**, 359 (1937).

proached and the apparent effect of pressure in increasing the viscosity increases toward a limiting value. Thus, when at 500° the mean velocity was reduced from 0.5 cm/sec. to 0.1 cm/sec., the apparent pressure coefficient was raised about 25 percent. A further reduction of the velocity to 0.06 cm/sec. gave no perceptible change in the pressure coefficient, within the rather large probable error, amounting to several percent. It seems unlikely that the value of the pressure coefficient for infinitely slow flow will be very much greater than is found with our finest capillary (40 cm long, 0.041 cm diameter). At 360°, the heating effect is certainly negligible.

No corrections have been applied for the compressibility of the glass, which is not known, nor for the elastic stretch of the capillary. These corrections are much smaller than the probable error due to the other causes which have been discussed. The absence of any appreciable creep or permanent stretch of the capillary was verified by taking measurements alternately at high and at low pressures. It is hardly necessary to add that these velocities of flow are far below the Reynolds critical velocity, by a factor of about 10^9 at 500°. The shearing stress in the glass, at the wall of the capillary where it is greatest, is about 250 g/cm² for the longest capillary, and about 3100 g/cm² for the shortest and widest, with an inlet pressure of 1000 kg/cm².

3. Results

With this type of viscometer, the pressure to which the glass is subjected decreases from a high value P at the inner end of the capillary to one atmosphere, which we take as zero, at the outer end. If the viscosity varies with the pressure, and is given by $\eta(p)$, the rate of flow Q, in cm³/sec., will be given by the integral

$$Q = C\int_{p=0}^{p=P} dp/\eta(p),$$

where C is a constant for a given capillary. The viscosity as a function of pressure may be obtained by taking the slope of a plot of Q as function of the inner pressure P, as shown by Hersey and Snyder. Another way of treating the results has been adopted here. If the viscosity were independent of the pressure, a plot of the quantity Q/P against P would be a straight horizontal line. On the other hand, if η increases with pressure, the values of Q/P will decrease as P increases, and the form of variation of η with the pressure may be derived from such a curve.

In Fig. 2 is shown a representative set of

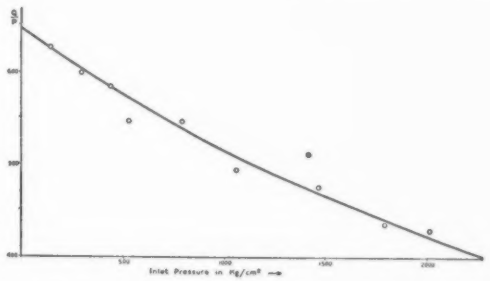

Fig. 2. Experimental results at 516° C. Q/P in arbitrary units. The smooth curve is calculated from the expression, $\eta = \eta_0 e^{0.00046p}$.

points at 516°. This set in which the greatest inlet pressure, about 2000 kg/cm², was attained, is typical of a number of runs at this temperature, with regard to the average slope and to the consistency of the results. The average deviation of the points from any one of several smooth curves is about 2 percent of the ordinate. On the basis of these measurements alone, it is not possible to distinguish among the several simple analytical expressions for the variation of viscosity with pressure which suggest themselves. In the case of the results for 359°, shown in Fig. 3, the measured effect is much greater, the scattering is less, and the choice of expressions is consequently more restricted.

In Table I are given several simple expressions

Table I.

T °C	η/η_0	Q/P	Value of Coefficient in cm²/kg	η_{1000}/η_0
516°	$1/(1-\beta p)$	$A(1-\beta P/2)$	$\beta = 0.00035$	1.54
	$(1+ap)$	$A\ln(1+aP)/aP$	$a = 0.00053$	1.53
	$e^{\alpha p}$	$A(1-e^{-\alpha P})$	$\alpha = 0.00046$	1.58
359°	$e^{\alpha p}$		$\alpha = 0.0015$	4.48

with numerical values for the coefficients to fit the data for 516°, and one expression for the data at 359°. In addition to the formula for $\eta(p)$ we give the integrated expression for Q/P, and the ratio η_{1000}/η_0 of the viscosity at 1000

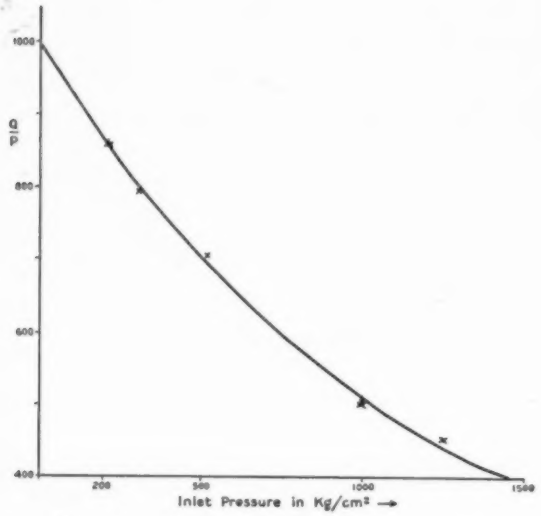

FIG. 3. Experimental results at 359 C. Q/P in arbitrary units. The smooth curve is calculated from the expression, $\eta = \eta_0 e^{0.0015p}$.

kg/cm² to that at 1 kg/cm², at the same temperature. The most suitable expression appears to be $\eta = \eta_0 e^{\alpha p}$; this is consistent with the results at both temperatures and has received a certain amount of theoretical justification in Andrade's theory of viscosity.[10] Of the other expressions which are consistent with the high temperature results, the straight line interpretation of Q/P *versus* P, leads to an infinite viscosity at 2860 kg/cm²; this is certainly incorrect. The linear increase of viscosity with pressure gives a satisfactory fit at 516°, but not at 359°.

It is of some interest to compare these results with those of Bridgman and others for organic liquids. At 516°, the initial rate of increase of viscosity of B_2O_3 is about the same as that of methyl alcohol at 30°; at 359°, the initial rate of increase of viscosity of the glass is greater than that of eugenol or of oleic acid, the pure liquids which showed the greatest effects among Bridgman's materials, and even greater than that of castor oil, studied by Hersey and Snyder. The viscosity of castor oil could also be represented approximately by an exponential expression up to 3000 kg/cm². Several lubricating oils studied by Dow[11] showed increases of viscosity by factors of ten or more in the first thousand kg/cm². In Bridgman's work, the rate of increase with pressure of the *logarithm* of the viscosity generally fell off appreciably in the first few thousands of kg/cm², remaining relatively constant thereafter to 12,000 kg/cm². Caution is therefore recommended in applying the present results to pressures higher than 2000 kg/cm².

No general law for the effect of temperature upon the pressure coefficient can be derived from Bridgman's measurements at 30° and 75°; in some cases the increase of viscosity with pressure was greater at 30°, in others, at 75°. Dow's results for lubricating oils showed marked decreases of the pressure effect as the temperature increased, from about 40° to 100°. For B_2O_3 glass, the pressure coefficient α is about three times as great at 359° as at 516°. This is very much greater than might be anticipated on the basis of Andrade's theory, which gives a pressure coefficient roughly inversely proportional to the absolute temperature. The "reaction rate" theory of viscosity, recently reviewed by Ewell,[12] which gives a very satisfactory account of the initial effect of pressure on the viscosity of pure liquids, may prove adequate to deal also with the more complicated case of vitreous materials, although, for the moment, data for a quantitative application to glasses are lacking.

[10] E. N. da C. Andrade, Nature, Mar. 1 and Apr. 12 (1930); Phil. Mag. **17**, 497 and 698 (1934).

[11] R. B. Dow, J. App. Phys. **8**, 367 (1937).

[12] R. H. Ewell, J. App. Phys. **9**, 252 (1938).